Response to the comments of Referee #1 on "Influence of anthropogenic pollution on the molecular composition of organic aerosols over a forest site in the Qinling Mountains region of central China"

by Xin Zhang and Yuemei Han

We greatly appreciate the valuable comments and suggestions from Referee #1 on our manuscript (ID: egusphere-2025-519). We have carefully revised the manuscript by taking into account of all the concerns raised by the referee. Please find our detailed point-to-point responses to these comments below. A copy of the manuscript and supplement with all the changes and other minor corrections tracked is also attached for reference.

(*The blue bold, green, and black fonts represent the Referee's comments, the related text in the manuscript, and the authors' responses, respectively.*)

In this study, Zhang* et al. *report an extensive molecular characterisation of organic aerosol in particulate matter (PM$_{2.5}$) from a forest site in the Qinling mountains, China, and investigated the influence of anthropogenic pollution on the aerosol composition. For this they sampled 33 filter samples in summer and wintertime, used liquid extraction and measured the extracts with an ultrahigh-performance liquid chromatography coupled to high-resolution Orbitrap mass spectrometry. With a non-target analysis known and unknown compounds were detected and identified. The combination of molecular fingerprints, air quality measurements, meteorological data as well as back-trajectories enables detailed interpretation of origin and transformation pathways of the sampled aerosol. Tracer species confirm the interpretation of more influence from biogenic precursors in summer and a more diverse and largely anthropogenic influenced composition in winter.
The authors have combined their comprehensive results and have produced a detailed characterization of the molecular composition of organic aerosol. The manuscript has a

good structure, meaningful illustrations and is written clear and precise. The work is worth to be published in "Atmospheric Chemistry and Physics" with some minor comments.

Response: We gratefully thank Referee #1 for the insightful and positive evaluation on our manuscript. We have seriously addressed all the concerns and revised the manuscript accordingly. Our detailed responses to these comments are as follows.

Comments

1. L84: Delete "city" in "[…] 50 km southwest of the megacity city Xi'an, as shown […]".
Related sentence: "This site is situated in the northern foothill of the Qinling Mountains and approximately 50 km southwest of the megacity **city** Xi'an, as shown in Fig. 1."

Response: Yes, it has been deleted in the revised manuscript, as follows:

"This site is situated in the northern foothill of the Qinling Mountains and approximately 50 km southwest of the **megacity Xi'an**, as shown in Fig. 1." (Lines 83–84)

2. L102: Have the authors considered that ultrasonication can influence the chemical composition due to free radical production? (Miljevic et al., 2014)
Related sentence: "A quarter of each sample in 12.56 cm^2 area was ultrasonically extracted using 9 g acetonitrile and water mixture in 9:1 volume for 30 min (3 g for 10 min, repeated three times)."

Response: Yes, we definitely agree with the referee that the ultrasonication of filter samples can degrade the chemical composition due to OH radical production under certain conditions. The chemical effects of ultrasonic irradiation mainly resulted from the high local temperature and pressures within the collapsing cavitation bubbles by the energy of ultrasonic waves (Miljevic et al., 2014). However, given that we performed the ultrasonic extraction of filter samples in a water–ice bath and the procedure lasted 10 min for each time in this study, the chemical effects should be limited under the low temperatures.
Moreover, the effects of ultrasonication on aerosol chemical composition were turned out to depend largely on the extraction solvents. As demonstrated by Hettiyadura et al. (2015), for

higher percentage of organic solvents (that is, acetonitrile and ultra-pure water in 95 : 5 by volume in their study), there were no degradation effects and only minor chemical differences between the ultrasonication and rotary shaking procedures for sample treatment. In fact, the ultrasonication was determined to be a better method due to its higher precision compared with rotary shaking (Hettiyadura et al., 2015). Similarly, we used the solvent of acetonitrile and pure water mixture in 9 : 1 volume in our current study, thereby the chemical effects should be at least not significant.

Taken the above two aspects together, we believe that the chemical composition should be insignificantly affected by the ultrasonication procedure in this study. We have highlighted this point in the revised manuscript, as follows:

"The extraction system was placed in a water–ice bath to **eliminate potential evaporation or chemical reactions** of aerosol components." (Lines 103–104).

Two references cited above are listed below:

Miljevic, B., Hedayat, F., Stevanovic, S., Fairfull-Smith, K. E., Bottle, S. E., and Ristovski, Z. D.: To sonicate or not to sonicate PM filters: Reactive oxygen species generation upon ultrasonic irradiation, Aerosol Sci. Technol., 48, 1276–1284, 2014.

Hettiyadura, A. P. S., Stone, E. A., Kundu, S., Baker, Z., Geddes, E., Richards, K., and Humphry, T.: Determination of atmospheric organosulfates using HILIC chromatography with MS detection, Atmos. Meas. Tech., 8, 2347–2358, 2015.

3. L142: Calculating HYSPLIT trajectories at 34.06° N, 108.34° E, 500 m height above ground level result in a height of 1885 m above sea level, since the height of the cell grid is already 1385 m. Can the authors comment on why they used 500 m height above ground level?

Related sentence: "In addition, the backward trajectories of air masses **(500 m height above ground level** and 72 h duration) arrived at the sampling site were calculated hourly across the study periods using the Hybrid Single Particle Lagrangian Integrated Trajectory model (v5.2.1) (Stein et al., 2015)."

Response: The altitude of our sampling site is around 530 m above the sea level, as described in the manuscript, "Atmospheric $PM_{2.5}$ was sampled at a forest site (34.06° N, 108.34° E,

around 530 m above sea level) in the Qinling Mountains region of central China during summer and winter seasons of 2021/2022." This is somewhat different from the height of the cell grid (that is, 1385 m) suggested by the referee, which was possibly obtained from a different method. We used the 500 m height above ground level for calculating the back trajectories of air masses, mainly considering the requirement of HYSPLIT model and the height of planetary boundary layer in our studied area. On the one hand, it is not recommended to start the model at the height too close to the ground, because the trajectory can easily hit the ground and lose accuracy, as demonstrated by the HYSPLIT Cheat Sheet (https://www.ready.noaa.gov/documents/ppts/Cheat_Sheet_2020.pdf). On the other hand, the 500 m height is mostly situated within the planetary boundary layer and close to the height of mixed layer in our studied area, according to the results reported in previous literature (e.g., Xin et al., 2024; Wang et al., 2023). This height thus could reflect the average concentrations of air pollutants in the well-mixed boundary layer, which is suitable for investigating the transport of near-surface pollution from the surrounding urban and rural areas to the studied location. Therefore, we used the 500 m above ground level to calculate the back trajectories of air masses in our current study.

Two references cited above include:
Xin, J., Peng, K., Zhu, X., Pan, X., Wang, Q., Cao, J., Wang, Z., Cao, X., Ren, X., Yang, S., Wei, Y., Zhao, D., and Ma, Y.: AI model to improve the mountain boundary layer height of ERA5, Atmos. Res., 304, 2024.
Wang, Y., Xu, T., Shi, G., Yang, F., Tang, X., Zhao, X., Wan, C., and Liu, S.: Climatology of the planetary boundary layer height over China and its characteristics during periods of extremely temperature, Atmos. Res., 294, 2023.

4. L205: Can the compounds also have different transmission efficiencies in the mass spectrometer? And is therefore not just an effect of different ionization efficiencies?

Related sentence: "This result can be attributed to either the large abundance of these species in this forest atmosphere or their high **ionization efficiency** under ESI− mode, despite that quantitative analyses were not available herein due to the technical limitation."

Response: The referee raised a good point here. We agree that organic compounds with different chemical properties (e.g., molecular size, structure, and polarity) would have varied transmission efficiencies in the mass spectrometer. Therefore, both the ionization and transmission efficiencies could affect the observed peak area intensity of organic species. We have added this information in the revised manuscript, as follows:

"This result can be attributed to either the large abundance of these species in this forest atmosphere or their high **ionization and transmission efficiencies** under ESI− mode, despite that quantitative analyses of the highly complex composition of organic aerosols remain challenging due to the lack of authentic standards (Evans et al., 2024; Ma et al., 2022; Noziere et al., 2015)." (Lines 204–207)

5. L206: Can the authors clarify what they mean with "technical limitations"?
The lack of authentic standards (and the fact that many compounds in ambient PM are not even precisely characterized) does not allow a quantitative approach on such a highly complex composition, independent of the analytical devices used. For example, Ma et al. (2022) and Evans et al. (2024) showed that semi-quantification is possible but with great uncertainties.

Related sentence: "This result can be attributed to either the large abundance of these species in this forest atmosphere or their high ionization efficiency under ESI− mode, despite that quantitative analyses were not available herein due to the **technical limitation**."

Response: As suggested by the referee, we have clarified the meaning of "technical limitations" in the revised manuscript, as follows:

"This result can be attributed to either the large abundance of these species in this forest atmosphere or their high ionization and transmission efficiencies under ESI− mode, despite that quantitative analyses **of the highly complex composition of organic aerosols remain challenging due to the lack of authentic standards (Evans et al., 2024; Ma et al., 2022; Noziere et al., 2015)**." (Lines 204–207)

The following two references have been also added in the revised manuscript:

"**Evans, R. L., Bryant, D. J., Voliotis, A., Hu, D., Wu, H., Syafira, S. A., Oghama, O. E.,**

McFiggans, G., Hamilton, J. F., and Rickard, A. R.: A Semi-Quantitative Approach to Nontarget Compositional Analysis of Complex Samples, Anal. Chem., 96, 18349–18358, https://doi.org/10.1021/acs.analchem.4c00819, 2024." (Lines 582–584)

"Ma, J., Ungeheuer, F., Zheng, F., Du, W., Wang, Y., Cai, J., Zhou, Y., Yan, C., Liu, Y., Kulmala, M., Daellenbach, K. R., and Vogel, A. L.: Nontarget Screening Exhibits a Seasonal Cycle of PM2.5 Organic Aerosol Composition in Beijing, Environ. Sci. Technol., 56, 7017–7028, https://doi.org/10.1021/acs.est.1c06905, 2022." (Lines 693–695)

6. Figure 3: The legend is not optimally visible in panel b. Since the legends applies to all panels, maybe a central positioning above would be easier to see (compare with the legend of Fig. 4).

Response: Yes, we agree. The legend of Figure 3 has been placed at the top central in the revised manuscript. Now it is clearly visible for all panels, as follows:
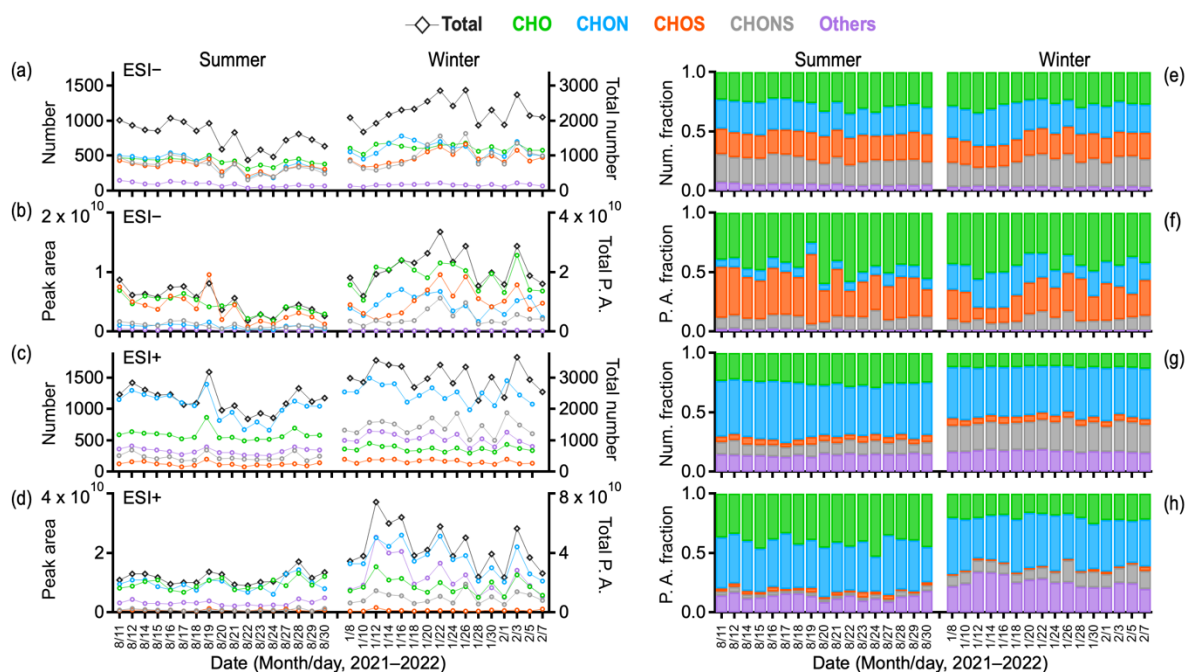

Figure 3.

7.1 Figure 5: In the caption the authors explain " […] dashed lines inside boxes […]", but the lines are solid.

Related sentence: "In the box plots, the bottom and top whiskers represent the 10th and 90th percentiles, respectively, the floating boxes represent the 25th–75th percentiles, and the **dashed lines** inside boxes represent the medians."

Response: Here we meant the "short lines" indeed. Therefore, we have made the following correction in the revised manuscript:

"In the box plots, the bottom and top whiskers represent the 10th and 90th percentiles, respectively, the floating boxes represent the 25th–75th percentiles, and the **short lines** inside boxes represent the medians." (Lines 267–269)

7.2 Can the authors explain why they show box plots and violin plots? Since the data is not bimodal distributed, the reader can hardly get any additional information from both plots.

Response: The purpose of showing both box plots and violin plots in Figure 5 is because of the following reasons. The box plots provided the key statistic summaries of data, including the values of mean, median, maximum, minimum, and percentiles. In contrast, the violin plots presented a more intuitive depiction of the data distribution from probability density across different values. Combining these two together can provide more comprehensive illustrations of the key statistics and overall distributional profiles of the data. Therefore, we have highlighted this point in the revised manuscript, as follows:

"The **key statistics and overall distribution profiles** of these parameters were presented using the box (left) and violin plots (right), respectively." (Lines 266–267)

8. L311: The comparison of tracer species was only made based on the sum formula? Have the authors considered fragmentation spectra to identify compounds with databases to get a higher level of confidence (e.g. aerosolomics (Thoma et al. (2022)) or the mzCloud database)?

Related sentence: "A variety of organic tracer species of anthropogenic and biogenic origins reported by previous laboratory and field studies have been found in this forest atmosphere, the details of which are summarized in Table S1–S5 of the Supplement."

Response: Since we performed the UHPLC–HRMS analysis in the full scan mode, there were no fragmentation spectra available in this current study. Also, for most of these hundreds of organic tracer species, we could not find their fragmentation spectra in the original literature. Therefore, a parallel comparison of these species with other studies was primarily based on

the sum formula. The scan mode information of our study has been added in the revised manuscript as: "The mass range was set at *m*/*z* 50–750 **in full MS scan mode**, with the mass resolution of approximately 140,000 at *m*/*z* 200." (Lines 114–115).

Nevertheless, we definitely agree with the referee that identifying compounds with the support of available fragmentation spectra from existing databases can get a higher level of confidence. To analyze organic tracer species and other specific compounds using HRMS, it would be more accurate to perform a full MS scan followed by MS/MS fragmentation scans of all ions at a wide isolation range. This should be an important topic in our future study. As a result, we have proposed this research topic in the Summary and Implications section of the revised manuscript, as follows:

"**The current work focuses primarily on the non-target characterization of organic species in aerosol particles over the Qinling Mountains region based on the HRMS analysis. To further identify organic tracers and other specific substances with the aid of fragmentation spectra in existing MS databases would achieve even higher reliability. Future studies** on the quantification and source apportionment of organic molecular composition **will be also valuable** to elucidate the complex anthropogenic–biogenic interactions and to incorporate the results into atmospheric chemistry model for improved prediction of organic aerosol burden and impacts in similar regions worldwide." (Lines 507–512)

9. L336: Have fragmentation experiments carried out to validate the assignment of the compound classes? The functional groups of organosulfates (m/z 96.9601 (HSO_4^-) and m/z 79.9573 (SO_3^-)) as well as nitrate groups (m/z 61.9883 (NO_3^-)) are very strongly represented in the fragmentation spectra and a clear indicator for organosulfates and nitrooxy organosulfates.

Related sentence: "Among these, organosulfate and nitrooxy-organosulfate compounds (abbreviated as OSs hereafter), defined as those with sufficient oxygen atoms to assign the −OSO_3H and −ONO_2 groups in the molecules (Brüggemann et al., 2020; Lin et al., 2012b), were important components in both seasons."

Response: As described in the response to comment #8, the HRMS analysis was performed only in the full MS scan mode, and thereby no fragmentation spectra are available for this study. In fact, it was a commonly used method in previous literature to identify organosulfate and nitrooxy-organosulfate compounds based on the assignment of $-OSO_3H$ and $-ONO_2$ groups from HRMS analysis, although we did not carry out fragmentation experiments to validate the assignment of these classes herein. Nevertheless, we agree that this method would result in an upper limit of the predicted numbers. Therefore, we have revised/added the following statement regarding this uncertainty in the revised manuscript:

"Among these, organosulfate and nitrooxy-organosulfate compounds (abbreviated as OSs hereafter), **roughly** defined as those with sufficient oxygen atoms to assign the $-OSO_3H$ and $-ONO_2$ groups in the molecules (Brüggemann et al., 2020; Lin et al., 2012b), were important components in both seasons. **Note that the designated OSs here would correspond to those at the upper limit, since no further fragmentation spectra available.**" (Lines 336–339)

Response to the comments of Referee #2 on "Influence of anthropogenic pollution on the molecular composition of organic aerosols over a forest site in the Qinling Mountains region of central China"

by Xin Zhang and Yuemei Han

We greatly thank Referee #2 for the helpful comments and suggestions on our manuscript (ID: egusphere-2025-519). We have seriously addressed all the issues raised by the referee and made relevant revisions on the manuscript. Please find below for the details of our responses to these comments. A copy of the manuscript and supplement with all the changes and other minor corrections tracked is also attached for reference.

(*The blue bold, green, and black fonts represent the Referee's comments, the related text in the manuscript, and the authors' responses, respectively.*)

This manuscript presents observational evidence of the seasonal variability in organic aerosol composition. However, the research approach—combining seasonal sampling with high-resolution mass spectrometry—has been widely reported in previous studies. The study does not clearly provide novel mechanistic insights or substantial advancements in the understanding of anthropogenic–biogenic interactions. As such, the conclusions drawn lack originality and scientific novelty. I regret to conclude that the manuscript, in its current form, does not meet the publication standards of the journal. My main concerns are as follows:

Response: We really appreciate the referee for providing these comments on our manuscript. We believe that it might be to some extent true that "combining seasonal sampling with high-resolution mass spectrometry has been widely reported in previous studies" in certain areas of the world. However, this is definitely not the case in the Qinling Mountains region of central China, despite its significant roles of serving as natural geographical and climatic boundary between the northern and southern China. Actually, based on our latest literature survey, the

molecular composition of organic aerosols in the Qinling Mountains region has rarely been investigated to date, especially utilizing the advanced HRMS techniques. This point has been stated in the manuscript as follows: "So far to our knowledge, this study **for the first time reports** the overall molecular characteristics of organic aerosols between contrasting seasons in the Qinling Mountains region based on high-resolution Orbitrap mass spectrometry." (Lines 76–78)

Moreover, the research approach of HRMS analysis remains to be one of the most advanced technologies in the field of atmospheric aerosol research currently. In this study, we focused primarily on the application of HRMS technique in the Qinling Mountains region for organic molecular characterization, rather than the development of this research approach itself. Therefore, the originality and novelty of this study should not be only judged by the research approach used herein, but more importantly by the research objectives and scientific findings. We acknowledge that it is somewhat challenging to directly elucidate mechanistic insights from aerosol sampling and offline HRMS analysis under complex atmospheric conditions, compared with those using real-time measurement techniques in laboratory studies that have the capability of capturing rapid changes in specific aerosol reaction chemistry. For this sake, we have included more mechanistic insights from previous literature to strengthen our conclusions, as addressed in detail in the response to the referee's comment #4.

Taken these facts together, the originality and scientific novelty of this current study include the following main aspects: 1) it first provided a comprehensive insight on the chemical characteristics of organic aerosols at the molecular level in the Qinling Mountains region, which has unique and significant geographical and climatic features; 2) it first demonstrated the substantial influence of anthropogenic pollution on the organic molecular composition in this region; 3) it advanced our knowledge on the anthropogenic and biogenic interactions as well as elucidated its seasonal variabilities and underlying influencing factors. As a result, we believe that this study would initiate and promote more atmospheric aerosol researches to further understand the anthropogenic perturbations on air quality, atmospheric chemistry, and associated environmental and climate impacts in the Qinling Mountains region, and also provide important references for similar regions worldwide.

1. Line 305: this interpretation lacks strong causal linkage, as biogenic emissions—particularly monoterpene-derived secondary organic aerosols (SOA)—also predominantly fall within the C_6–C_{11} range. Therefore, the contribution from biogenic precursors should not be overlooked when interpreting the molecular composition in this carbon number range.

Related sentence: "In contrast, the CHO and CHON species in ESI+ mode and CHONS species in both modes had increased number fractions at approximately C_{6-11} in winter, possibly resulted from the enhanced influence of anthropogenic pollution."

Response: The referee's viewpoint here is slightly different from what we intended to express from this statement. In fact, we did not mean to rule out the contribution from biogenic precursors at the C_6–C_{11} range, as addressed in the context of the same paragraph: "Among them, the number and peak area fractions of organic species were particularly dominated by the C_5–C_{11} compounds, which can be derived from both biogenic and anthropogenic sources." (Lines 299–301). Rather, the key point here is that the increased number fractions of those species in winter were contributed by the enhanced influence of anthropogenic pollution from the surrounding areas. It is likely that the original expression was not clear enough to be understood. Therefore, we have highlighted this point for clarity in the revised manuscript, as follows:

"In contrast, **prominent increases were observed for the number fractions of CHO and CHON species in ESI+ mode and CHONS species in both modes at approximately C_{6-11} range during the winter period, probably resulted mainly from the enhanced influence of anthropogenic pollution from the surrounding areas, compared with those of the summer period**." (Lines 306–309)

2. Lines 365-370: here only discuss the seasonal variation of molecules identified under the ESI− mode using VK diagrams, while omitting the analysis of VK characteristics of compounds detected in the ESI+ mode. This incomplete treatment results in a weak logical connection between the data presented and the conclusions drawn, leading to a lack of coherence in the overall interpretation. Given that ESI+ typically captures a distinct subset

of organic compounds—often including important nitrogen- and sulfur-containing species—its exclusion leaves a significant gap in the discussion. I recommend the authors include a comparative analysis of VK diagrams under both ionization modes to ensure a more comprehensive and balanced understanding of the seasonal dynamics of organic aerosol composition.

Related sentence: "The anthropogenic and biogenic organic tracer species identified in ESI− mode were further analyzed in the van Krevelen diagram based on their elemental ratios of O/C and H/C, as shown in Fig. 8a. Except for those derived from glyoxal, isoprene, and some anthropogenic precursors with O/C > 0.5, other tracer species were primarily distributed in the regime with O/C ≤ 0.5. In addition, the anthropogenic tracer species widely dispersed at the regime with H/C from approximately 0.5 to 2.5, whereas the biogenic ones were mainly situated at the H/C ≥ 1.5 regime."

Response: Since the VK diagrams for organic tracer species in ESI+ mode showed quite similar seasonal variation trends as those in ESI− mode, together with that organic tracer species from more precursors were identified in the ESI− mode, we therefore only discussed the results of negative mode in the original manuscript. As suggested by the referee, we have provided the results of VK diagrams for both ESI− and ESI+ modes in order to gain a more comprehensive understanding on the seasonal dynamics of organic aerosol composition. Specifically, we have revised the original Figure 8 by including the VK diagram results and seasonal variation of organic species in both ESI− and ESI+ modes (see the revised Figure 8 below). We have also modified and added the relevant discussions in the revised manuscript, as follows:

"The anthropogenic and biogenic organic tracer species identified in **the ESI− and ESI+ modes** were further analyzed in the van Krevelen diagram based on their elemental ratios of O/C and H/C, as shown in Fig. 8a. **Similar variation patterns were generally observed between the two modes. Specifically,** except for those derived from glyoxal, isoprene, and some anthropogenic precursors with O/C > 0.5, other tracer species were primarily distributed in the regime with O/C ≤ 0.5." (Lines 365–368)

"Figure 8b presents the example results on two different days **(that is, August 30 and January 26) obtained in the ESI− mode.**" (Lines 375–376)

"**Similar tendencies were also found for those in the two modes** across the entire study periods in summer and winter (Fig. 8c)." (Lines 380–381)

"**In ESI− mode,** the number fraction of organic species in the aromatic regime was on average $21 \pm 2\%$ on individual days in winter, which was higher than those of $17 \pm 2\%$ in summer." (Lines 381–382)

"**Likewise, in ESI+ mode, the number and peak area fractions of aromatic species were slightly higher in winter than in summer, while those of aliphatic species were higher in summer.**" (Lines 384–386)
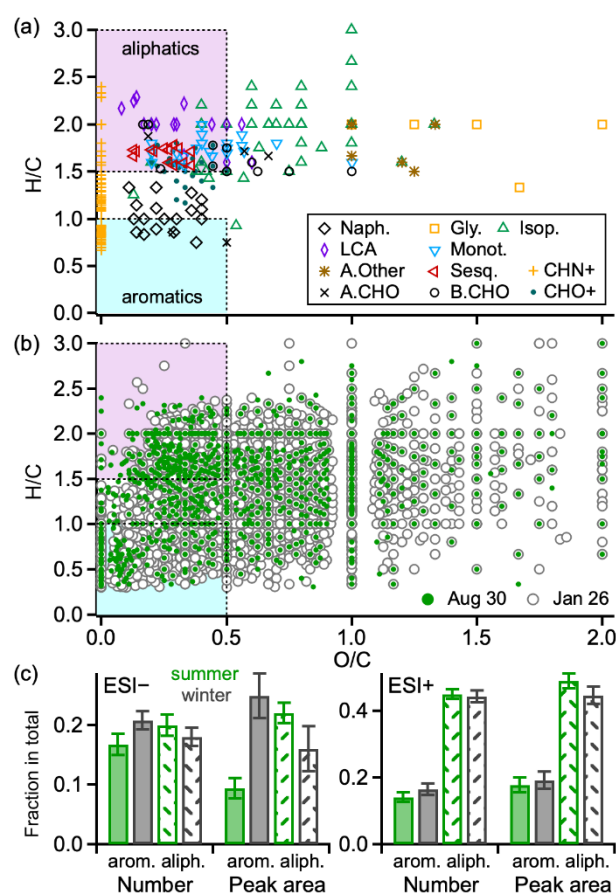

Figure 8. van Krevelen diagrams plotting of (a) organic tracer species derived from anthropogenic and biogenic precursors **in both modes (as listed in Table S1–S5)**, and (b) organic species identified on a summer day (August 30) and a winter day (January 26) in ESI− mode. (c) Averaged number and peak area fractions of organic species in aromatic and

aliphatic molecular structures for summer and winter samples **in ESI− and ESI+ modes**. In panels (a, b), the shaded pink (H/C ≥ 1.5, O/C ≤ 0.5) and cyan (H/C ≤ 1.0, O/C ≤ 0.5) areas represent aliphatic and aromatic regimes, respectively. The O/C was replaced by (O−3S)/C or (O−3S−2N)/C in the case of organosulfates or nitrooxy-organosulfates. The error bars in panel (c) represent 1σ standard deviations for all the samples in each season.

3. Lines 395-410: The conclusions regarding the influence of relative humidity on the molecular characteristics of organic species are solely based on compounds identified under the ESI− mode. This raises concerns about the completeness of the analysis, as ESI− and ESI+ modes often detect different classes of organic compounds with distinct physicochemical properties. Relying only on ESI− data may lead to a biased or incomplete understanding of humidity-driven processes. A more balanced interpretation should incorporate results from both ionization modes to better capture the full range of organic species affected by relative humidity.

Response: As suggested by the referee, we have performed further analysis with regard to the influence of relative humidity on the molecular characteristics of organic species in the ESI+ mode during the study periods. The results eventually showed that the overall variation trends of the number of organic species under different RH conditions were to some extent similar between the two ionization modes (see Figure S2 below and also in the revised Supplement), although the RH influence on organic species in the ESI+ mode were not as strong as those in the ESI− mode. This is most likely associated with the distinct physicochemical properties of organic species in these two ionization modes, that is, basic organic substances were readily protonated and thus detected in the positive mode, while acidic substances were easily deprotonated and more sensitive in the negative mode. As a result, we have added the relevant discussions regarding the influence of RH on organic species in the ESI+ mode in the revised manuscript, as follows:

"**In contrast, the similar but weaker dependence on RH was found for organic species in the ESI+ mode (Fig. S2 in the Supplement), probably associated in part with their distinct physicochemical properties compared with those in the ESI− mode. This result**

" (Lines 416–419)

The following literature also has been added in the References section of the revised manuscript:

Laskin, J., Laskin, A., and Nizkorodov, S. A.: Mass spectrometry analysis in atmospheric chemistry, Anal. Chem., 90, 166–189, https://doi.org/10.1021/acs.analchem.7b04249, 2018. (Lines 647–648)
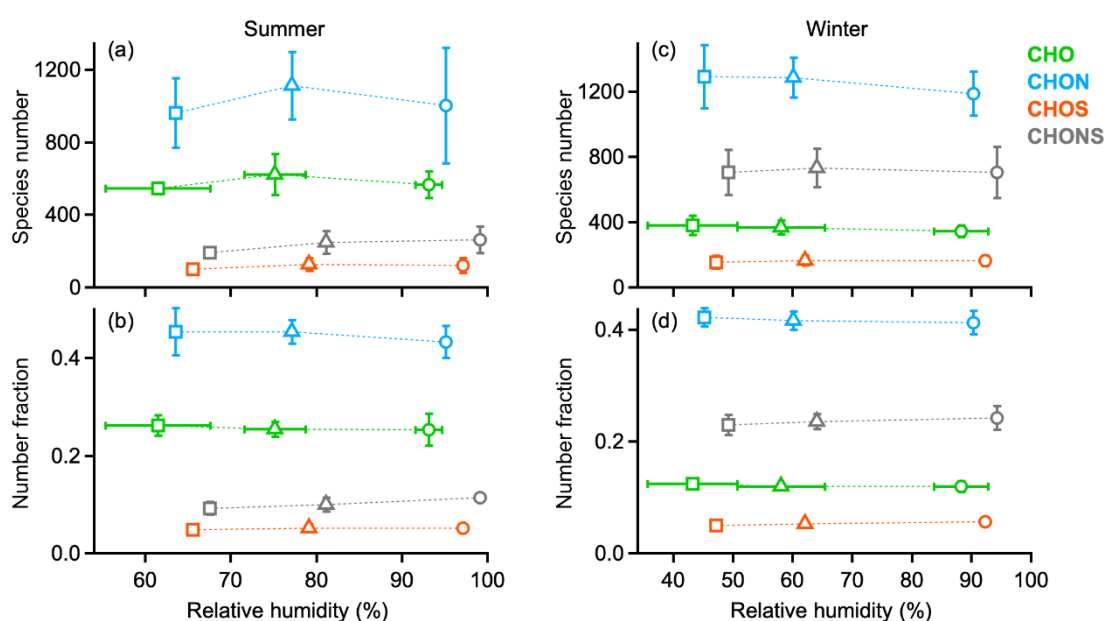

Figure S2. Species number and the relative fractions of organic molecular subgroups in positive ESI mode under varied relative humidity conditions in (a, b) summer and (c, d) winter periods. The symbols of each type shared the same RH values (that is, 62 ± 6%, 75 ± 4%, 93 ± 2% in summer and 43 ± 8%, 58 ± 7%, 88 ± 5% in winter) but were offset horizontally for a clear vision. The horizontal error bars in the CHO species represent 1σ standard deviations of RH values. The vertical error bars represent 1σ standard deviations for all the samples in each RH condition.

In addition, we have also added the following result (Figure S4) and relevant discussions regarding the influence of temperature on organic species in ESI+ mode into the Supplement, for a more comprehensive understanding on the influence of meteorological factors.

"The species numbers of all organic subgroups **in ESI− mode** were almost comparable at the mean temperatures of 21.5 ± 0.8 and 24.5 ± 0.8 °C in summer, while they were largely increased at the highest temperature level of 27.6 ± 1.0 °C **(Fig. S3 in the Supplement**)." (Lines 430–432)

"**The species number and fraction of organic subgroups in ESI+ mode varied insignificantly with temperature as well (Fig. S4 in the Supplement).**" (Lines 433–434)
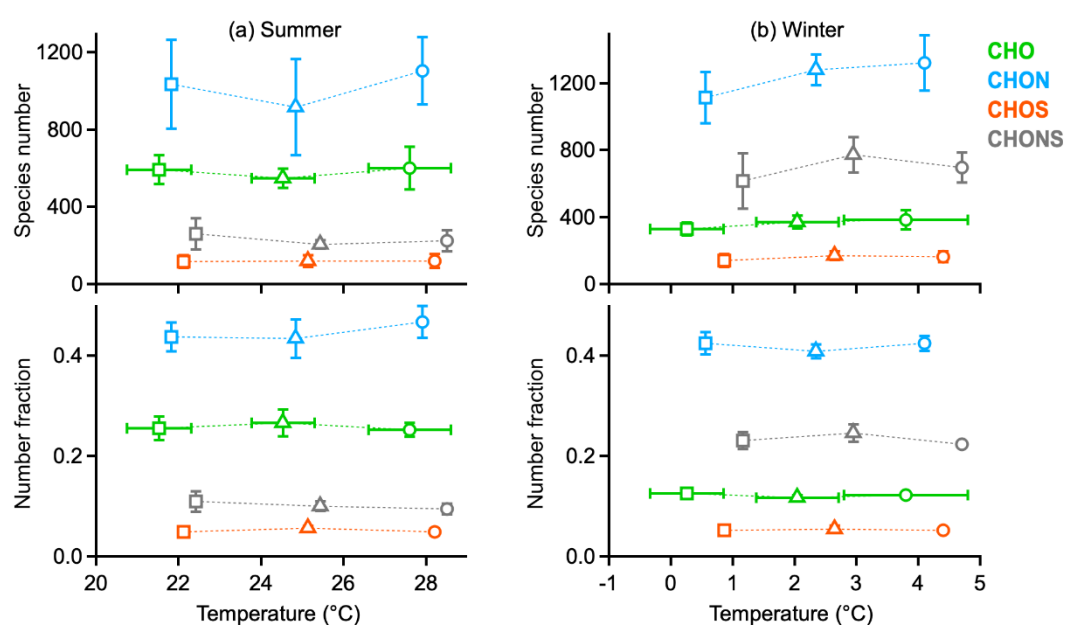

Figure S4. Species number and the relative fractions of organic molecular subgroups in positive ESI mode under varied temperature conditions in (a) summer and (b) winter periods. The symbols of each type shared the same temperature values (that is, 21.5 ± 0.8, 24.5 ± 0.8, 27.6 ± 1.0 °C in summer and 0.3 ± 0.6, 2.0 ± 0.7, 3.8 ± 1.0 °C in winter) but were offset horizontally for a clear vision. The horizontal error bars in the CHO species represent 1σ standard deviations of temperature values. The vertical error bars represent 1σ standard deviations for all the samples under each temperature condition.

4. Lines 450-475: The authors primarily rely on positive and negative correlations with gaseous and particulate pollutants, as well as SOR, NOR, and Ox, to infer their influence on the chemical composition of organic aerosols. However, the correlation-based analysis lacks mechanistic support, making the conclusions less convincing. Furthermore, the discussion remains rather superficial and does not adequately elucidate the underlying interactions between pollutants and organic aerosol formation. It is recommended that the authors incorporate mechanistic insights from previous literature to strengthen the scientific basis and credibility of their conclusions.

Response: We hope the referee could understand that the dataset of this study was mainly derived from HRMS measurement of aerosol filter samples, thereby the correlation-based analysis of organic species with air pollutants was one of the efficient methods to explore the underlying interactions. We acknowledge that although the offline HRMS analysis had advantages in determining organic molecular composition and identifying reaction products, it remains challenging to directly elucidate specific reaction mechanisms, especially under atmospheric conditions with complex influences of multiple environmental factors. Actually, the conclusions drawn from the correlation-based analysis in our current study are highly consistent with some previous laboratory studies. Therefore, as recommended by the referee, we have incorporated the following mechanistic insights to strengthen the scientific basis and credibility of our conclusions in the revised manuscript:

"This phenomenon **could partly** result from the chemical transformation of these species into **other chemically diverse substances (e.g., CHON and CHONS) through acid-catalyzed heterogeneous reactions and/or aqueous phase chemistry in the presence of anthropogenic air pollutants (Darer et al., 2011; Fan et al., 2022; Kwong et al., 2018; Lam et al., 2019).**" (Lines 466–469)

"**Another proposed explanation is that the productions of CHO and CHOS species were to some extent governed by the consumption of anthropogenic pollutants at the low concentration levels in summer (Fig. 2c), as those reported in some other ambient atmospheres (Lin et al., 2022; Riva et al., 2019; Wang et al., 2020).**" (Lines 469–472)

"**Possible reaction pathways include such as biogenic isoprene and monoterpene**

precursors being oxidized by nitrate radicals to form condensable organic nitrates and nitrooxy-organosulfates (Hamilton et al., 2021; Ng et al., 2017)." (Lines 473–475)

"**These species might be partly associated with primary emissions (Song et al., 2018; Zhong et al., 2023), such as those of biomass burning and fossil fuel combustion from the surrounding rural and urban areas.**" (Lines 479–480)

"**This is consistent with previous studies that oxidant levels were one of the most important governing factors for the production of organosulfur species by limiting the oxidation of organic precursors (Bryant et al., 2021; Wang et al., 2021f).**" (Lines 487–489)

The following literatures have been added in the References section to support our conclusions in the revised manuscript:

"**Darer, A. I., Cole-Filipiak, N. C., O'Connor, A. E., and Elrod, M. J.: Formation and stability of atmospherically relevant Isoprene-derived organosulfates and organonitrates, Environ. Sci. Technol., 45, 1895–1902, https://doi.org/10.1021/es103797z, 2011.**" (Lines 564–566)

"**Kwong, K. C., Chim, M. M., Davies, J. F., Wilson, K. R., and Chan, M. N.: Importance of sulfate radical anion formation and chemistry in heterogeneous OH oxidation of sodium methyl sulfate, the smallest organosulfate, Atmos. Chem. Phys., 18, 2809–2820, https://doi.org/10.5194/acp-18-2809-2018, 2018.**" (Lines 641–643)

"**Lam, H. K., Kwong, K. C., Poon, H. Y., Davies, J. F., Zhang, Z., Gold, A., Surratt, J. D., and Chan, M. N.: Heterogeneous OH oxidation of isoprene-epoxydiol-derived organosulfates: kinetics, chemistry and formation of inorganic sulfate, Atmos. Chem. Phys., 19, 2433–2440, https://doi.org/10.5194/acp-19-2433-2019, 2019**" (Lines 644–646)

"**Riva, M., Chen, Y., Zhang, Y., Lei, Z., Olson, N. E., Boyer, H. C., Narayan, S., Yee, L. D., Green, H. S., Cui, T., Zhang, Z., Baumann, K., Fort, M., Edgerton, E., Budisulistiorini, S. H., Rose, C. A., Ribeiro, I. O., Oliveira, R. L. E., Dos Santos, E. O., Machado, C. M. D., Szopa, S., Zhao, Y., Alves, E. G., De Sá, S. S., Hu, W., Knipping, E. M., Shaw, S. L., Duvoisin Junior, S., De Souza, R. A. F., Palm, B. B., Jimenez, J. L., Glasius, M., Goldstein, A. H., Pye, H. O. T., Gold, A., Turpin, B. J., Vizuete, W., Martin,**

S. T., Thornton, J. A., Dutcher, C. S., Ault, A. P., and Surratt, J. D.: Increasing isoprene epoxydiol-to-inorganic sulfate aerosol ratio results in extensive conversion of inorganic sulfate to organosulfur forms: Implications for aerosol physicochemical properties, Environ. Sci. Technol., 53, 8682–8694, https://doi.org/10.1021/acs.est.9b01019, 2019." (Lines 736–743)

"Wang, Y., Hu, M., Wang, Y.-C., Li, X., Fang, X., Tang, R., Lu, S., Wu, Y., Guo, S., Wu, Z., Hallquist, M., and Yu, J. Z.: Comparative study of particulate organosulfates in contrasting atmospheric environments: Field evidence for the significant influence of anthropogenic sulfate and NOx, Environ. Sci. Technol. Lett., 7, 787–794, https://doi.org/10.1021/acs.estlett.0c00550, 2020." (Lines 806–809)

"Hamilton, J. F., Bryant, D. J., Edwards, P. M., Ouyang, B., Bannan, T. J., Mehra, A., Mayhew, A. W., Hopkins, J. R., Dunmore, R. E., Squires, F. A., Lee, J. D., Newland, M. J., Worrall, S. D., Bacak, A., Coe, H., Percival, C., Whalley, L. K., Heard, D. E., Slater, E. J., Jones, R. L., Cui, T., Surratt, J. D., Reeves, C. E., Mills, G. P., Grimmond, S., Sun, Y., Xu, W., Shi, Z., and Rickard, A. R.: Key role of NO(3) radicals in the production of isoprene nitrates and nitrooxyorganosulfates in Beijing, Environ. Sci. Technol., 55, 842–853, https://doi.org/10.1021/acs.est.0c05689, 2021." (Lines 595–599)

"Song, J., Li, M., Jiang, B., Wei, S., Fan, X., and Peng, P.: Molecular characterization of water-soluble humic like substances in smoke particles emitted from combustion of biomass materials and coal using ultrahigh-resolution electrospray ionization Fourier Transform Ion Cyclotron Resonance Mass Spectrometry, Environ. Sci. Technol., 52, 2575–2585, https://doi.org/10.1021/acs.est.7b06126, 2018." (Lines 761–764)

"Zhong, S., Chen, S., Deng, J., Fan, Y., Zhang, Q., Xie, Q., Qi, Y., Hu, W., Wu, L., Li, X., Pavuluri, C. M., Zhu, J., Wang, X., Liu, D., Pan, X., Sun, Y., Wang, Z., Xu, Y., Tong, H., Su, H., Cheng, Y., Kawamura, K., and Fu, P.: Impact of biogenic secondary organic aerosol (SOA) loading on the molecular composition of wintertime PM2.5 in urban Tianjin: an insight from Fourier transform ion cyclotron resonance mass spectrometry, Atmos. Chem. Phys., 23, 2061–2077, https://doi.org/10.5194/acp-23-2061-2023, 2023." (Lines 803–805)

"Bryant, D. J., Elzein, A., Newland, M., White, E., Swift, S., Watkins, A., Deng, W., Song, W., Wang, S., Zhang, Y., Wang, X., Rickard, A. R., and Hamilton, J. F.: Importance of oxidants and temperature in the formation of biogenic organosulfates and nitrooxy organosulfates, ACS Earth Space Chem., 5, 2291–2306, https://doi.org/10.1021/acsearthspacechem.1c00204, 2021." (Lines 541–544)

"Wang, Y., Zhao, Y., Wang, Y., Yu, J.-Z., Shao, J., Liu, P., Zhu, W., Cheng, Z., Li, Z., Yan, N., and Xiao, H.: Organosulfates in atmospheric aerosols in Shanghai, China: Seasonal and interannual variability, origin, and formation mechanisms, Atmos. Chem. Phys., 21, 2959–2980, https://doi.org/10.5194/acp-21-2959-2021, 2021f." (Lines 803–805)

Influence of anthropogenic pollution on the molecular composition of organic aerosols over a forest site in the Qinling Mountains region of central China

Xin Zhang[1,2], Lijuan Li[2], Jianjun Li[2], Yue Lin[2], Yan Cheng[1], Rui Wang[2], Shuyan Xing[2], Chongshu Zhu[2], Junji Cao[2,3,*], and Yuemei Han[2,4,*]

[1]School of Human Settlements and Civil Engineering, Xi'an Jiaotong University, Xi'an 710049, China

[2]Key Laboratory of Aerosol Chemistry and Physics, State Key Laboratory of Loess and Quaternary Geology, Institute of Earth Environment, Chinese Academy of Sciences, Xi'an 710061, China

[3]Institute of Atmospheric Physics, Chinese Academy of Sciences, Beijing 100029, China

[4]National Observation and Research Station of Regional Ecological Environment Change and Comprehensive Management in the Guanzhong Plain, Xi'an 710061, China

Correspondence to: Yuemei Han (yuemei.han@ieecas.cn), Junji Cao (jjcao@mail.iap.ac.cn)

Abstract. Biogenic organic aerosols interacting with anthropogenic pollutants lead to large uncertainties in aerosol properties and impacts, yet the underlying mechanisms remain to be fully elucidated. To explore the anthropogenic–biogenic interactions in the Qinling Mountains region of central China, we investigated the molecular composition of organic aerosols in atmospheric $PM_{2.5}$ at a forest site in summer and winter of 2021/2022, using ultrahigh performance liquid chromatography coupled with Orbitrap mass spectrometry. Organic species were more abundant and chemically diverse in winter compared with those in summer, as revealed by their higher numbers and peak area intensities. The molecular characteristics of organic species exhibited distinct seasonal variabilities, with higher peak-area-weighted mean values of molecular weight and oxidation state but lower unsaturation degree in summer, possibly associated with more biogenic emissions and intense photochemical processes. A variety of organic tracer species were identified in the two seasons, among which the biogenic ones were relatively more abundant in summer, contrasting with the substantial increase of anthropogenic ones in winter. A higher ambient relative humidity, except for heavy precipitation, usually promoted the production of nitrogen- and sulfur-containing organic species by involving more anthropogenic pollutants. The synergistic effects of meteorology and anthropogenic pollution greatly affected the organic aerosol production in this forest atmosphere, thereby altering their molecular composition and related properties under different environmental conditions. The combined set of results herein provides direct evidence for the anthropogenic perturbations on air quality, atmospheric chemistry, and associated climate impacts in the Qinling Mountains region.

1 Introduction

Atmospheric aerosol particles generated from various natural and anthropogenic sources have substantial impacts on Earth's climate, regional air quality, and human health (Liu et al., 2019; McNeill, 2017). Biogenic organic aerosols comprise an important component of aerosol particles globally (Mahilang et al., 2021; Shrivastava et al., 2017). Terrestrial vegetation emits huge amounts of volatile organic species and primary biological particles into the atmosphere, which constitute the main sources of biogenic organic aerosols (Després et al., 2012; Rap et al., 2018; Wang et al., 2024a). A number of laboratory and field studies have demonstrated that the presence of anthropogenic pollutants (e.g., NO_x, SO_2, NH_3, sulfate, and etc.) may alter the physicochemical properties and production yields of biogenic organic aerosols (Carlton et al., 2018; Hoyle et al., 2011; Zhao et al., 2016). However, the interactions of anthropogenic pollution with biogenic organic aerosols vary considerably across spatial and temporal scales, which lead to large uncertainties in assessing their environmental and climate related

impacts (Dong et al., 2022; Matsui et al., 2014; Xu et al., 2021a). Therefore, despite the enormous efforts of existing studies, the underlying mechanisms of anthropogenic–biogenic interactions remain to be fully elucidated.

40   Anthropogenic pollution can affect biogenic organic aerosol through various atmospheric chemical and physical processes, as previously proposed in the literature. They could promote the oxidation of biogenic volatile species for more organic aerosol production by increasing the levels of atmospheric oxidants (e.g., hydroxyl, ozone, and nitrate radicals) (Ng et al., 2017; Wu et al., 2020; Xu et al., 2015). The reaction chemistry of biogenic precursors would be changed under different NO_x levels, leading to complex chemical composition and yields of the secondary products (Han et al., 2016; Xu et al., 2014; Yan et al.,

45   2020; Zhao et al., 2018). Meanwhile, anthropogenic particulate matter provides important surface for gas–particle partitioning and particle-phase reactions of biogenic organic products, whereas these processes were to a large extent governed by the particle properties such as acidity and physical state (Pye et al., 2020; Reid et al., 2018). In addition, acidic pollutants (e.g., SO_2, NO_x, and sulfate) may involve in formation of organosulfur and organonitrogen compounds by reacting with biogenic aerosol in various ambient environments (Brüggemann et al., 2020; Fan et al., 2022). Nevertheless, previous relevant studies

50   are primarily focused on the characterization of bulk organic matter or fragments using traditional techniques such as online aerosol mass spectrometry (Noziere et al., 2015; Wang et al., 2021a). A thorough investigation of anthropogenic–biogenic interactions at the molecular level is crucial to gain deep insights into the mechanisms and impacts.

The Qinling Mountains region is primarily situated in the southern part of Shaanxi Province in central China (Fig. 1). It serves as an important natural geographical and climatic boundary between the northern and southern China (Yang et al., 2015; Yao

55   et al., 2020). This region also lies on the edge of the Asian monsoon region and is quite sensitive to climate change (Cai et al., 2010). The unique geographical features of this region have attracted great interests for ecological and environmental research (Wang et al., 2021b; Zhang et al., 2022). The Qinling Mountains are enriched in a huge variety of forested vegetation (Wang et al., 2021c; Zhao et al., 2014), such as *Quercus*, *Betula*, conifer, and subalpine meadows, contributing large amounts of biogenic primary emissions and secondary oxidation products into the atmosphere (Cao et al., 2022; Li and Xie, 2014; Xu et

60   al., 2020). Also, this region is often affected by anthropogenic air pollutants from the surrounding rural and urban areas in the Guanzhong Plain of northwest China (Cao and Cui, 2021; Zhao et al., 2015). Previous studies on atmospheric aerosols in this region were primarily focused on the remote environments at high altitudes, such as Mountains Hua and Taibai (Li et al., 2013; Meng et al., 2014; Shen et al., 2023; Li et al., 2023). From those work, the characteristics of inorganic species and the formation and evolution processes of organic aerosols are gradually being understood (Li et al., 2020; Niu et al., 2016). However, the

65   interactions of anthropogenic pollution with biogenic organic aerosols and the potential impacts are still rarely reported at the lower altitudes of this region to date, especially at the anthropogenic–biogenic intersection zones.

The present study investigates the influence of anthropogenic pollution on molecular characteristics of atmospheric organic aerosols in the Qinling Mountains region, in order to advance our current knowledge on the complex interactions between anthropogenic pollutants and biogenic emissions. The molecular composition of organic aerosols in ambient $PM_{2.5}$ was

70   characterized at a forest site in the northern foothills of this region during contrasting summer and winter seasons of 2021–2022, using ultrahigh-performance liquid chromatography coupled with electrospray ionization and Orbitrap mass spectrometry. The chemical compositional and structural variability of organic aerosols were presented and discussed thoroughly to understand the underlying causes across the two seasons. The anthropogenic and biogenic contributions to organic molecular composition were further examined based on a variety of organic tracer species. Finally, the effects of

75   meteorological parameters and anthropogenic pollutants were explored to gain insights into the potential pathways of organic aerosol production in this forest atmosphere. So far to our knowledge, this study for the first time reports the overall molecular characteristics of organic aerosols between contrasting seasons in the Qinling Mountains region based on high-resolution Orbitrap mass spectrometry.

2 Methodology

2.1 Site and aerosol sampling

Atmospheric PM2.5 was sampled at a forest site (34.06° N, 108.34° E, around 530 m above sea level) in the Qinling Mountains region of central China during summer and winter seasons of 2021/2022. This site is situated in the northern foothill of the Qinling Mountains and approximately 50 km southwest of the megacity ~~city~~ Xi'an, as shown in Fig. 1. It belongs to the
85 National Observation and Research Station of Regional Ecological Environment Change and Comprehensive Management in the Guanzhong Plain. A medium-flow air sampler (HC-1010, Qindao Hecheng Ltd., China) was operated at 100 L min^{-1} for collecting PM2.5 samples on precombusted quartz fiber filters (90 mm in diameter, Whatman Inc., USA). The sampling height was approximately 3.5 m above the ground. Each sample collection lasted around 23 h from 10:00 am to 9:00 am of the next day in local time. A total of 33 aerosol samples were collected during the entire study period, including 17 and 16 samples in
90 summer and winter, respectively. Four field blanks were also collected using the same approach but with the sampler pump turned off. All the samples were stored in a freezer at −20 °C for further chemical analysis.
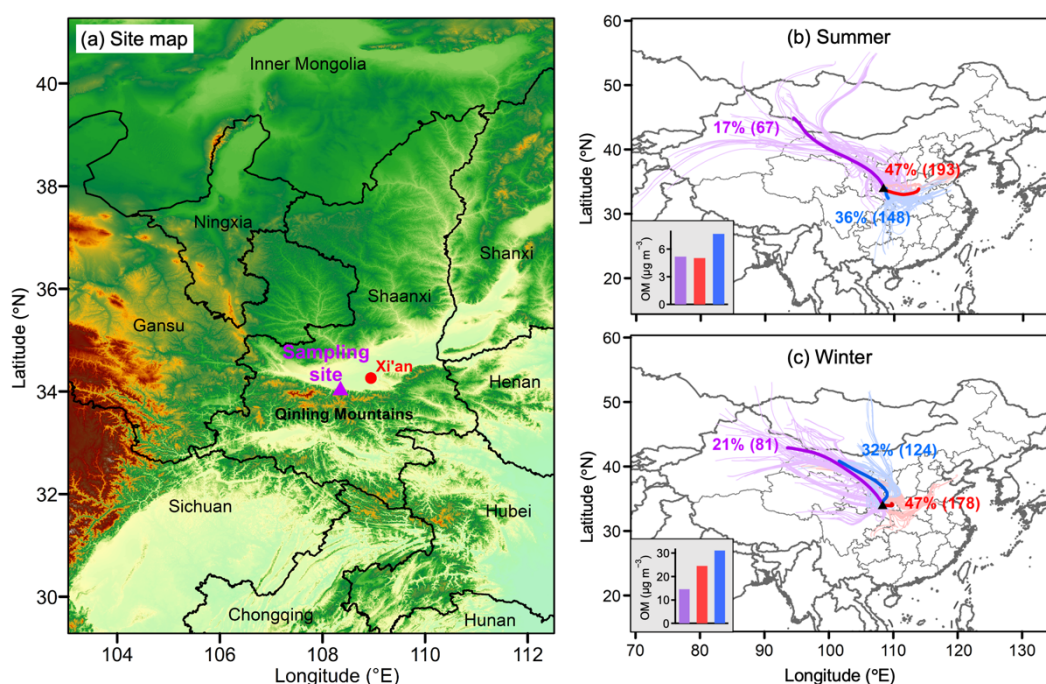

95 **Figure 1. (a) A map showing the sampling site at northern foothill of the Qinling Mountains region in central China. (b, c) Back trajectories of air masses arrived at 500 m above the ground level over the sampling site and their cluster analysis (represented by the thick solid lines with percentages and numbers) during the summer and winter periods. The bottom left panels in panels (b, c) present the mass concentrations of organic matter in the corresponding air mass directions.**

100

2.2 UHPLC–HRMS measurement and data processing

A quarter of each sample in 12.56 cm^2 area was ultrasonically extracted using 9 g acetonitrile and water mixture in 9:1 volume for 30 min (3 g for 10 min, repeated three times). The extraction system was placed in a water–ice bath to ~~avoid possible~~ eliminate potential evaporation or chemical reactions of aerosol components. The extracts were filtered through 0.2
105 μm pore-size polytetrafluoroethylene membranes (Pall Co., USA) and then concentrated to 500 μL under a gentle nitrogen stream. The organic molecular composition of individual samples was subsequently measured using a Vanquish Flex ultrahigh-performance liquid chromatograph coupled with a high-resolution Q-Exactive Orbitrap mass spectrometer (UHPLC–HRMS,

Thermo Scientific Inc., Germany). For each sample, a volume of 5 μL analyte was injected and separated using a Thermo Hypersil Gold C_{18} column (100 × 2.1 mm, 1.9 μm) with two mobile phases consisting of (A) 0.1% formic acid in ultrapure water and (B) acetonitrile. A gradient elution at a flow rate of 0.25 mL min^{-1} was performed for 25 min, including initially 5% B at 0–2.5 min, linearly increased to 50% B at 2.5–8 min with a 3-min hold, linearly increased to 95% B at 11–17.5 min with a 5.5-min hold, and then dropped to 5% B within 0.2 min and held for 1.8 min. The analyte was then introduced into a heated electrospray ionization source (ESI) and determined by the HRMS. Raw data were acquired in both negative and positive ESI modes (i.e., ESI− and ESI+) at the spray voltages of −3 and 4 kV, respectively. The mass ~~scanning~~ range was set at m/z 50– 750 in full MS scan mode, with the mass resolution of approximately 140,000 at m/z 200. The HRMS was externally calibrated using Thermo Scientific Pierce standard calibration solutions before the measurement.

The raw data from UHPLC–HRMS analysis was processed using an open-source software MZmine 2.53 (Pluskal et al., 2010). The main procedures were similar to our previous work (Li et al., 2024a; Lin et al., 2022). Briefly, the elemental composition of organic molecular species was constrained to $C_{1–40}H_{1–80}O_{0–50}N_{0–4}S_{0–2}$ in the two ionization modes, using a mass tolerance of 2 ppm. An additional Na atom was also applied for possible sodium adducts in ESI+ mode. The assigned molecular species were further screened using the elemental ratios of H/C (0.3–3.0), O/C (0–3), N/C (0–1.3), and S/C (0–0.8) to ensure their presence in nature. The formulas disobeying the nitrogen rule for even electron ions were excluded for further analysis (Zielinski et al., 2018). The oxidation state of carbon atoms ($\overline{OS}_c$) in a molecule was calculated as $2 \times O/C − H/C$ for individual organic species (Kroll et al., 2011). The number of rings and double bonds in organic molecules was characterized with ring and double-bond equivalent (DBE), which was calculated as $(2 + 2c + n − h)/2$ by assuming the trivalent nitrogen and divalent sulfur atoms (Kind and Fiehn, 2007; Yassine et al., 2014). All the analyses and discussions in this study refer to the neutral organic molecules.

2.3 Other analyses

Each filter sample was weighted using an electronic microbalance before and after sampling, the difference of which dividing by the sampled air volume was used for calculating $PM_{2.5}$ mass concentration. The organic and elemental carbons on the filter samples were measured with the interagency monitoring of protected visual environments protocol using a thermal/optical carbon analyzer (model 2001A, Desert Research Institute, USA) (Chow and Watson, 2002). The mass concentration of organic matter was then estimated by 2.1 times that of organic carbon for this forest site (Turpin and Lim, 2001). Water-soluble inorganic ionic species on the samples were determined using a Metrohm ion chromatograph (model 940 Professional IC Vario) with routine procedures of our group (Zhang et al., 2011).

The hourly air quality data of SO_2, NO_2, CO, and O_3 during the study periods were obtained from the National Environmental Monitoring Centre of China (http://www.cnemc.cn) at the nearest monitoring station. The sulfur and nitrogen oxidation ratios (SOR and NOR) in the atmosphere were calculated respectively as $nSO_4^{2−}/(nSO_4^{2−} + nSO_2)$ and $nNO_3^{−}/(nNO_3^{−} + nNO_2)$, in which n refers to the molar concentration (Kaneyasu et al., 1995). The odd oxygen ($O_x = NO_2 + O_3$) concentration was used to reflect atmospheric oxidation capacity (Herndon et al., 2008). The meteorological parameters of ambient temperature, relative humidity (RH), wind speed, and precipitation at three-hour intervals were downloaded from the Meteomanz database (http://www.meteomanz.com). In addition, the backward trajectories of air masses (500 m height above ground level and 72 h duration) arrived at the sampling site were calculated hourly across the study periods using the Hybrid Single Particle Lagrangian Integrated Trajectory model (v5.2.1) (Stein et al., 2015).

3 Results and discussion

3.1 Seasonal variability in molecular composition of organic aerosols

Figure 2 presents the temporal variations of chemical components in $PM_{2.5}$, gas pollutants, and meteorological conditions

during the entire study periods. The PM$_{2.5}$ mass concentration ranged at 12–56 (mean 29 ± 10) μg m^{-3} in summer, which was much lower than those in winter (49–164, mean 89 ± 31 μg m^{-3}) (Table 1). Among the quantified chemical species, organic matter was the most dominant component that accounted for on average 22% of PM$_{2.5}$ mass in summer and 25% in winter (Fig. 2a, b). The inorganic salts of sulfate, nitrate, and ammonium were also abundant in both seasons. The mean mass fractions of sulfate were relatively higher in summer (11% vs. 8% in winter), whereas those of nitrate and ammonium were much higher in winter (14% and 7% vs. 4% of both in summer). This result suggests that the typical atmospheric conditions in summer (e.g., strong solar radiation and high temperature) would facilitate the chemical conversion of SO$_2$ into sulfate, while nitrate and ammonium were more efficiently produced under winter conditions. The PM$_{2.5}$ mass also consisted of 16–86% other components, including some additional ionic species, mineral dust, crustal materials, and etc. Overall, the seasonal variation tendencies of PM$_{2.5}$ and its chemical components at this forest site to some extent resembled those reported in the nearby rural and urban areas of Guanzhong Plain (Cao and Cui, 2021; Han et al., 2023; Zhao et al., 2015), where coal and biomass combustion and unfavorable atmospheric dispersion conditions were highly prevalent during winter heating seasons.
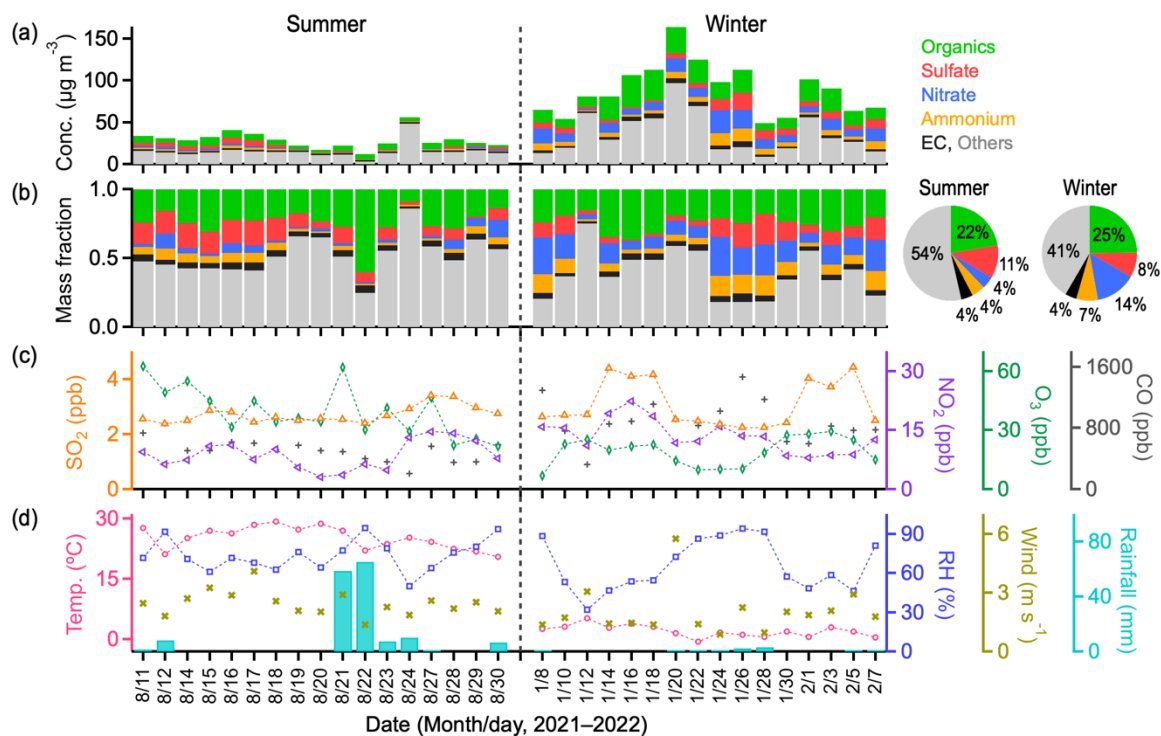

Figure 2. Temporal variations of the (a) mass concentrations and (b) mass fractions of chemical components in ambient PM$_{2.5}$, (c) gas pollutant concentrations, and (d) meteorological factors over the studied periods in 2021/2022. The two pie charts in panel (b) represent the averaged mass fractions of PM$_{2.5}$ components in summer and winter periods.

The distinct PM$_{2.5}$ mass concentration and chemical composition between summer and winter seasons over this forest atmosphere can be attributed to multiple factors such as emission sources, formation pathways, gaseous precursors, meteorological conditions, and air mass origins. The gas pollutants of SO$_2$, NO$_2$, and CO had higher concentration levels in winter (mean 3.1, 14, and 887 ppb) than those in summer (2.7, 9, and 511 ppb) (Fig. 2c and Table 1), suggesting the large contributions of combustion sources such as fossil fuel and biomass burning (Mallik and Lal, 2014; Wei et al., 2023). In contrast, the higher O$_3$ levels in summer (mean 39 ppb) would facilitate atmospheric oxidation processes to produce more secondary aerosols compared with those in winter (19 ppb). Moreover, the studied summer period was characterized by the higher values of temperature, RH, wind speed, and more precipitation (Fig. 2d and Table 1). These typical ambient conditions

in summer would promote the biogenic emissions (especially isoprene), aqueous phase chemistry, and disperse of air pollutants, respectively (Gu et al., 2023; Guo et al., 2016; Seco et al., 2022; Vettikkat et al., 2023). The air mass origins were also quite different in the two seasons (Fig. 1b, c). They primarily originated from the eastern (47%) and adjacent southern (36%) areas in summer, contrasting to those from the adjacent eastern (47%) and long-range northern (32%) areas in winter. The prevalent air masses with adjacent southern origins in summer at the studied site revealed the large biogenic emission contributions from the forested vegetation in the Qinling Mountains region. On the contrary, the long-range transported air masses from northwestern area (17% in summer and 21% in winter) were mostly clean ones with relatively lower levels of organic pollutants (see the small embedded panels in Fig. 1b, c).

Table 1. The ranges and mean values of PM$_{2.5}$ chemical components, gas pollutants, and meteorological factors over the studied summer and winter periods in 2021/2022.

	Summer	Winter
Particulate mass concentration (µg m^{-3})		
PM$_{2.5}$	12–56 (29 ± 10)	49–164 (89 ± 31)
Organics	3.1–9.9 (6.5 ± 1.9)	8.8–38.7 (22.1 ± 9.5)
Sulfate	0.1–7.0 (3.3 ± 2.2)	1.3–20.1 (7.5 ± 4.7)
Nitrate	0.2–3.3 (1.2 ± 1.0)	2.8–28.0 (12.4 ± 6.3)
Ammonium	0.1–2.8 (1.3 ± 0.9)	1.2–15.4 (6.6 ± 4.0)
EC	0.5–2.1 (1.2 ± 0.5)	1.3–6.8 (3.6 ± 1.7)
Others	3.1–48.2 (15.6 ± 9.0)	9.2–96.7 (37.0 ± 24.9)
Gas pollutants concentration (ppb)		
NO$_2$	3–15 (9 ± 4)	8–22 (14 ± 4)
SO$_2$	2.4–3.4 (2.7 ± 0.3)	2.2–4.4 (3.1 ± 0.9)
O$_3$	22–62 (39 ± 13)	7–29 (19 ± 7)
CO	204–855 (511 ± 154)	319–1468 (887 ± 281)
Meteorological factors		
Temp. (℃)	20.4–29.2 (25.1 ± 2.8)	−0.6–5.2 (2.0 ± 1.5)
RH (%)	50–94 (74 ± 12)	32–94 (66 ± 20)
Rainfall (mm)	0.2–65.4 (19.7 ± 26.4)	0.2–3.2 (1.2 ± 1.1)
Wind (m s^{-1})	1.4–4.1 (2.4 ± 0.6)	0.9–5.7 (2.0 ± 1.2)

Figure 3 presents the molecular compositions of organic aerosols detected in ESI− and ESI+ modes during the summer and winter periods. The total numbers of organic molecular species assigned in ESI− mode were 879–2073 in summer and 1674–2873 in winter (Fig. 3a), corresponding to those of 1684–3188 and 2263–3648 in ESI+ mode (Fig. 3c). The total peak area intensities of organic species in both modes exhibited similar variation trends as those of species numbers (Fig. 3b, d), that is, with relatively higher values (approximately two times) observed in winter than those in summer. They were also consistent with the absolute mass concentrations of organic matter and PM$_{2.5}$ in the two seasons (Fig. 2a). These results together revealed that organic aerosols in this forest atmosphere were more abundant and chemically diverse in winter compared with those in summer. In addition, both the number and peak area intensity of organic species were relatively higher in ESI+ mode, possibly resulting from the higher proton affinity and gas phase basicity of organic molecules that were readily ionized and detected than those in ESI− mode (Kiontke et al., 2016; Liigand et al., 2017).

The assigned organic species primarily consisted of those in CHO, CHON, CHOS, CHONS, and other oxygen-free groups based on the elemental composition in the molecules. Most of these groups in the ESI− and ESI+ modes had greater species number and peak area intensity in winter than those in summer (Fig. 3a–d), which is consistent with the higher levels of air

pollutants during the wintertime. In ESI− mode, the number fractions of organic species in both seasons were nearly comparable among the four primary groups of CHO, CHON, CHOS, and CHONS, ranging at 22–35%, 19–34%, 18–24%, and 15–28%, respectively (Fig. 3e). Nevertheless, the peak area intensity was predominated by the CHO species, followed by the CHOS species (Fig. 3f). This result can be attributed to either the large abundance of these species in this forest atmosphere or their high ionization ~~efficiency~~and transmission efficiencies under ESI− mode, despite that quantitative analyses ~~were not available herein~~of the highly complex composition of organic aerosols remain challenging due to the ~~technical limitation~~lack of authentic standards (Evans et al., 2024; Ma et al., 2022; Noziere et al., 2015). Moreover, the peak area fractions of CHON species increased on average 164% in winter compared with those in summer, which might be partly associated with the involvement of enhanced inorganic nitrogen species such as nitrate and NO_2 during the wintertime (Fig. 2b, c). More CHON species could also favorably partition into the particle phase under the low ambient temperature conditions in winter (Bejan et al., 2007; Li et al., 2024b).
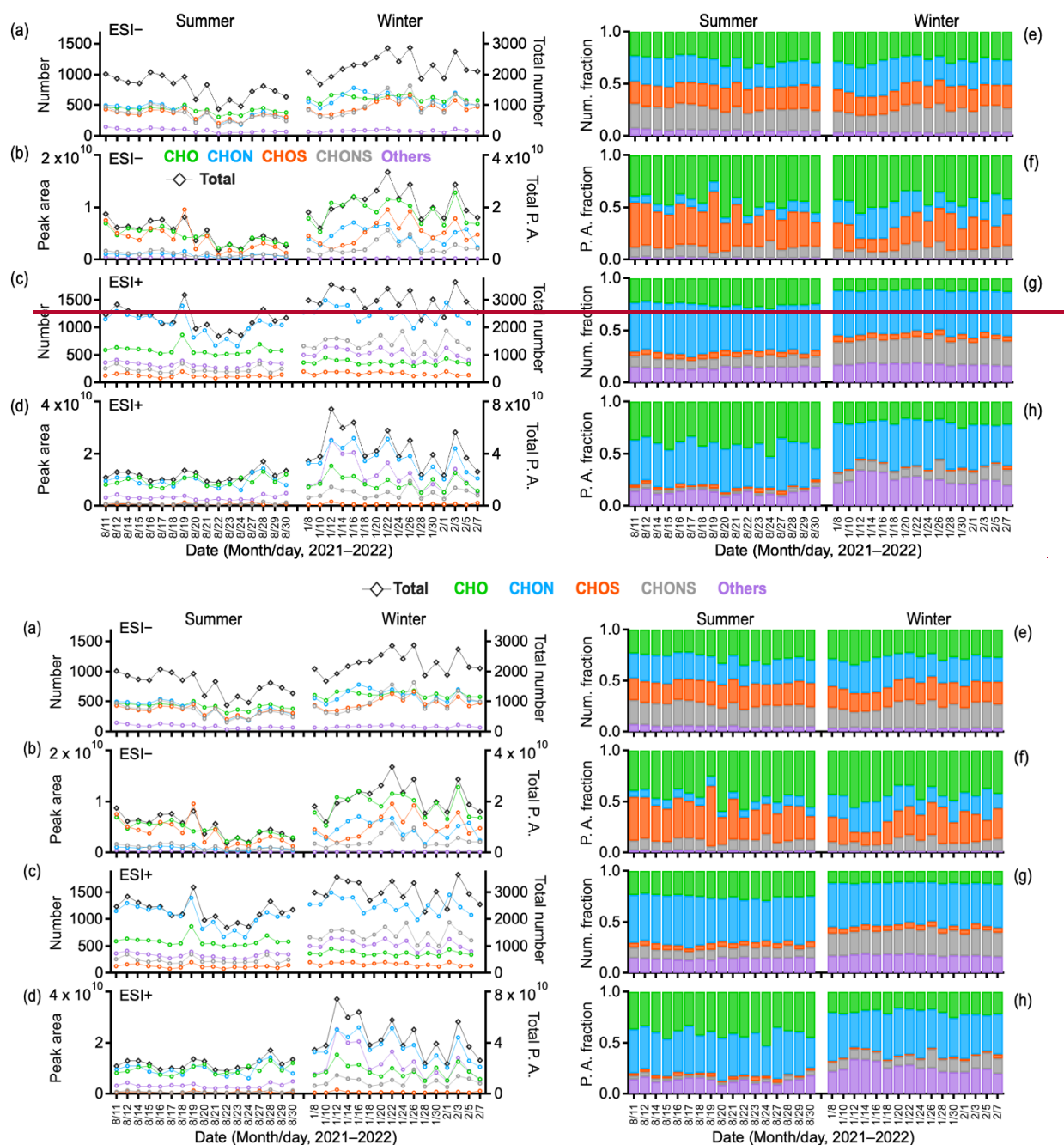

Figure 3. (a, c) Species number and (b, d) peak area intensity of organic molecular composition (including each

subgroup and total species), along with their corresponding number and peak area fractions (e–h), obtained from the UHPLC–HRMS analysis in negative and positive ESI modes over the study periods.

220   In contrast, the molecular composition of organic species had different variation patterns in the ESI+ mode. The CHON species were primarily dominant in terms of both number and peak area intensity, respectively accounting for 38−52% and 29−50% in those of total species across the entire period (Fig. 3g, h). Potential candidates for these CHON species included those with amino functional groups in the molecules (amines, amides, amino acids, and etc.), since protonated compounds were more sensitively detected in ESI+ mode. The CHOS species were very minor components in this mode, which can be primarily due

225 to their acidic nature (Lin et al., 2012a; Wang et al., 2017a). The number of CHONS species and the peak area intensity of other oxygen-free species (mainly CHN here) apparently increased in the winter period, while both the number and peak area intensity of CHO species inversely decreased. One proposed explanation is that the presence of high levels of anthropogenic air pollutants (e.g., SO_2, NO_2, sulfate, and nitrate; Fig. 2) during the wintertime facilitated the production of more chemically diverse organic species by reacting with organic precursors such as carbonyls, alcohols, and carboxyls (Fan et al., 2022; Xu et

230 al., 2021b).
     In addition to the observed seasonal variability of organic molecular composition, a number of organic species (286 in ESI− and 277 in ESI+ modes) were commonly found in both summer and winter samples (Fig. 4a, b), which could be originated from the same emission sources and/or reaction pathways. Nevertheless, these common species generally accounted for a small portion in the total number of assigned molecular formulas in individual samples, that is, 10–33% and 8–16% in ESI−

235 and ESI+ modes, respectively. Therefore, the large numbers of unique species between summer and winter indicate the large seasonal discrepancy in the sources and formation pathways of organic aerosols. Further details are discussed in Sections 3.3 and 3.4. Moreover, there were some common species identified in both ESI− and ESI+ modes during the study periods (33 in summer and 182 in winter, Fig. 4c), the numbers of which only accounted for 1–11% of total organic species in each mode for individual samples. Given that the detected organic molecular species were mostly distinct between the two ionization modes,

240 combining the results together would provide complementary insights into the molecular characteristics of organic aerosols and gain an overall profile.

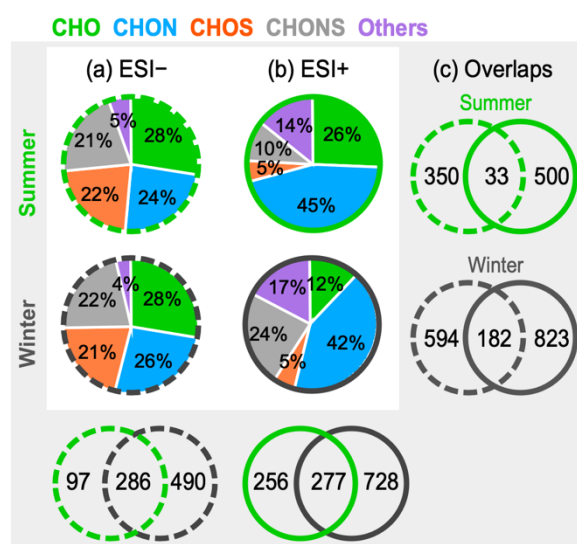245 **Figure 4. Number fractions of each subgroup in total organic species detected respectively in (a) negative and (b) positive ESI modes during the summer and winter periods. (c) Numbers of common and unique organic species found in the two modes (ESI−: dashed circles, ESI+: solid circles) and in the two seasons (summer: green circles, winter: black circles), as presented in the surrounding gray area.**

3.2 Chemical characteristics of organic molecular species

Figure 5 presents the bulk chemical characteristics of organic molecular species identified in ESI− and ESI+ modes during the summer and winter periods. These parameters for individual organic subgroups are summarized in Table 2. In ESI− mode, although the molecular weights of organic species were mostly abundant at the range of approximately m/z 168–424 for both seasons (as seen in the box and violin plots in Fig. 5a), the peak-area-weighted mean was higher in summer than those in winter (m/z 244 vs. 220), with a shift of 24 Da. This is mainly attributed to the increased molecular weights of CHON, CHOS, and CHONS species in summer (Table 2) that usually had lower volatilities (Li et al., 2016; Wang et al., 2024b). Similar variation patterns were also obtained in ESI+ mode, with a higher peak-area-weighted mean of molecular weight in summer than those in winter (m/z 247 vs. 208). Since air masses from the surrounding Qinling Mountains area in the south were more prevalent at the sampling site in summer season (Fig. 1b), biogenic emissions from forest vegetation (especially those with larger molecules such as monoterpenes and sesquiterpenes) and their oxidation products might be key factors resulting in the higher organic molecular weight. Other intensive processes such as thermal ablation of plant waxes in summer could also contribute to the higher molecular weight substances in the forest atmosphere (Deshmukh et al., 2019; Ehn et al., 2012).
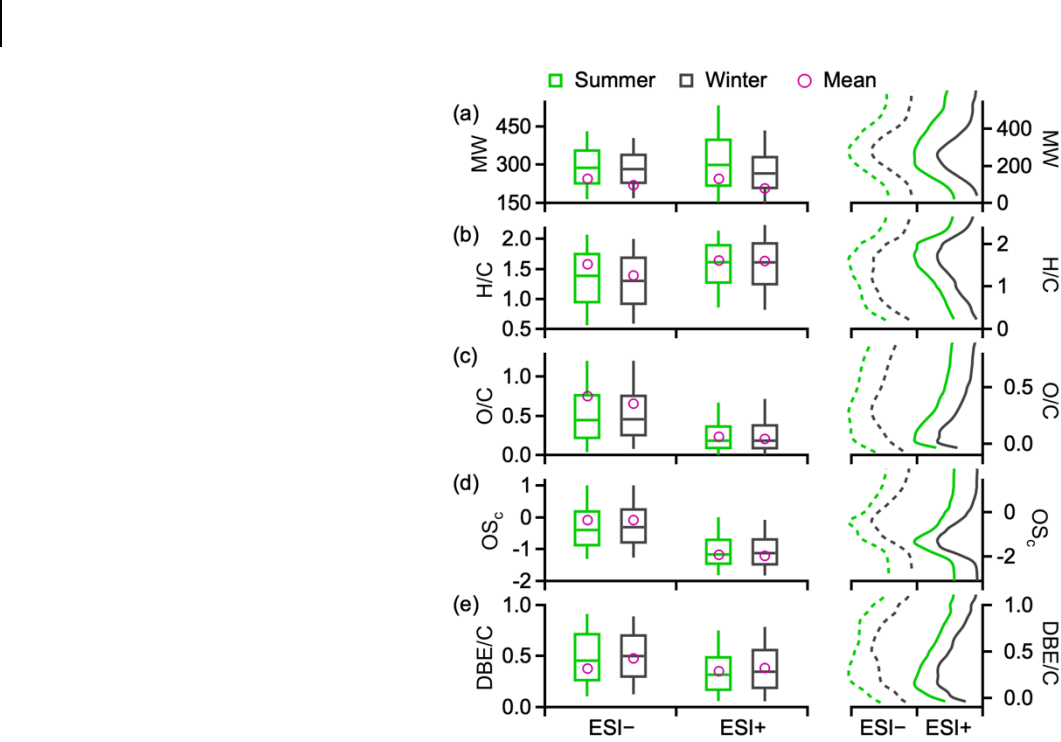
Figure 5. Statistical analyses on the molecular characteristics of all organic species identified in summer and winter samples: (a) molecular weight, (b) H/C ratio, (c) O/C ratio, (d) the oxidation state of carbon atoms, and (e) ring and double-bond equivalent per carbon atom. The combined dataset of organic species identified in at least one sample in each season were used for analysis here. The ~~ranges~~key statistics and ~~distributions~~overall distribution profiles of these parameters were presented using the box (left) and violin plots (right), respectively. In the box plots, the bottom and top whiskers represent the 10th and 90th percentiles, respectively, the floating boxes represent the 25th–75th percentiles, and the ~~dashed~~short lines inside boxes represent the medians.

Table 2. Averaged species number, peak area intensity, and peak-area-weighted molecular weight (M.W.), elemental ratios (H/C and O/C), oxidation state of carbon atoms ($\overline{OS}_c$), ring and double-bond equivalent per carbon (DBE/C) for

individual organic subgroups and total species assigned in negative and positive ESI modes over the studied summer and winter periods in 2021/2022.

Species	Summer							Winter						
	number	peak area (10⁹)	M.W.	H/C	O/C	$\overline{OS}_c$	DBE/C	number	peak area (10⁹)	M.W.	H/C	O/C	$\overline{OS}_c$	DBE/C
ESI−														
CHO	419 ± 51	4.4 ± 1.7	206	1.45	0.62	−0.20	0.41	617 ± 49	9.3 ± 2.3	211	1.28	0.50	−0.29	0.48
CHON	380 ± 117	0.8 ± 0.4	250	1.37	0.49	−0.38	0.51	592 ± 107	4.5 ± 1.7	192	1.03	0.54	0.04	0.71
CHOS	343 ± 76	3.8 ± 2.4	255	1.84	1.00	0.15	0.24	473 ± 93	5.2 ± 2.2	231	1.78	1.01	0.23	0.29
CHONS	340 ± 106	1.0 ± 0.4	302	1.63	0.84	0.06	0.44	503 ± 163	2.3 ± 1.3	265	1.67	0.78	−0.10	0.41
Others	87 ± 32	0.2 ± 0.1	323	0.72	n.a.	n.a.	0.81	80 ± 16	0.1 ± 0.04	263	0.93	n.a.	n.a.	0.74
Total	1568 ± 370	10.1 ± 4.3	244	1.58	0.75	−0.08	0.38	2266 ± 359	21.4 ± 5.8	220	1.39	0.65	−0.09	0.47
ESI+														
CHO	585 ± 88	9.4 ± 1.8	243	1.34	0.26	−0.83	0.42	362 ± 45	8.8 ± 2.8	195	1.26	0.27	−0.72	0.48
CHON	1040 ± 210	9.4 ± 2.2	234	1.87	0.27	−1.33	0.31	1249 ± 145	17.8 ± 5.3	209	1.64	0.24	−1.15	0.39
CHOS	118 ± 31	0.6 ± 0.2	406	1.68	0.23	−1.23	0.22	161 ± 32	0.6 ± 0.3	321	1.52	0.18	−1.17	0.32
CHONS	230 ± 58	0.7 ± 0.3	392	1.69	0.30	−1.09	0.31	715 ± 130	4.8 ± 2.0	280	1.98	0.39	−1.20	0.26
Others	325 ± 48	3.1 ± 0.9	177	1.58	n.a.	n.a.	0.42	525 ± 92	11.8 ± 6.0	175	1.71	n.a.	n.a.	0.36
Total	2298 ± 396	23.2 ± 4.1	247	1.64	0.23	−1.18	0.35	3011 ± 417	43.8 ± 15.0	208	1.63	0.20	−1.22	0.38

The carbon oxidation state $\overline{OS}_c$ and unsaturation degree (reflected by the DBE per carbon atom herein, DBE/C) derived from the H/C and O/C ratios of organic molecular species were further explored (Fig. 5b–e). The $\overline{OS}_c$ values of organic species in ESI− mode were mostly distributed at −0.9 to 0.3 range in the two seasons (Fig. 5d), which could result from various atmospheric oxidation processes such as photochemistry, heterogeneous reactions, and aqueous phase reactions (Bianchi et al., 2019; Kroll et al., 2011). In contrast, the $\overline{OS}_c$ values were much lower in ESI+ mode (−1.5 to −0.7 range), which were consistent with the more alkaline nature and/or reduced state of organic species detected in the positive mode (Lin et al., 2012a). The relatively higher H/C and O/C ratios eventually resulted in the slightly higher peak-area-weighted means of $\overline{OS}_c$ in summer than those in winter, that is, −0.08 vs. −0.09 in ESI− and −1.18 vs. −1.22 in ESI+ modes (Table 2). Moreover, the lower peak-area-weighted means and medians of DBE/C were obtained in summer for the two modes (Fig. 5e), indicating the more abundance of organic molecules with less unsaturated bonds or aromatic structures compared with those in winter. These results together revealed that organic species in this forest atmosphere were generally more oxidized and less unsaturated in summer than those in winter, which was possibly associated with the stronger photochemical processes as well as the less influence of anthropogenic pollutants, as evidenced by the higher O_3 while lower SO_2 and NO_2 concentrations in the summer period (Fig. 2c).
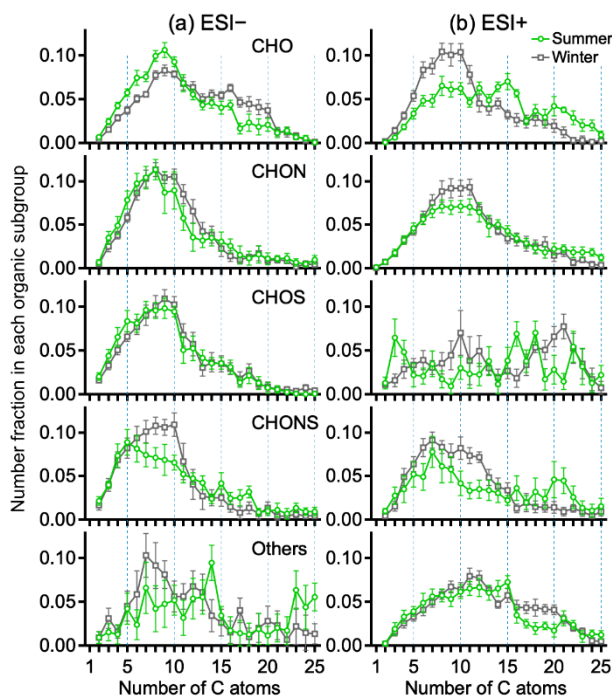
Figure 6. Number fractions of organic subgroups sorted by the carbon atoms number in molecular formulas assigned in (a) negative and (b) positive ESI modes for summer and winter samples. Only organic species with $C_{\leq 25}$ are shown here due to their higher abundance. The error bars represent 1σ standard deviations for all the samples in each season.

The observed changes in the molecular characteristics of organic species in the two seasons were as a result of the chemical variabilities of individual organic subgroups. Figure 6 presents the distributions of carbon atoms number in the molecular formulas of each subgroup during the study periods. The organic species with C_2–C_{25} composed 82–99% in number (or 94–99% in peak area, Fig. S1 in the Supplement) of total species for individual subgroups in the two modes. Among them, the number and peak area fractions of organic species were particularly dominated by the C_5–C_{11} compounds, which can be derived from both biogenic and anthropogenic sources. Moreover, the distributions of carbon atoms number for individual subgroups exhibited distinct seasonal variabilities. Specifically, the number fractions of CHO species with C_{3-10} in ESI− mode were slightly higher in summer, whereas those with C_{14-20} were apparently increased in winter. The abundance of different species in the two seasons could be closely associated with their origins and formation pathways (Wang et al., 2017a; Zhang et al., 2024). The distribution profiles of CHON and CHOS species in this mode were nearly comparable between summer and winter, indicating their similar sources and/or production pathways across the two seasons. In contrast, ~~the~~prominent increases were observed for the number fractions of CHO and CHON species in ESI+ mode and CHONS species in both modes ~~had increased number fractions~~ at approximately C_{6-11} ~~in~~ range during the winter~~, possibly~~ period, probably resulted mainly from the enhanced influence of anthropogenic pollution from the surrounding areas, compared with those of the summer period.

3.3 Contributions of anthropogenic and biogenic sources

A variety of organic tracer species of anthropogenic and biogenic origins reported by previous laboratory and field studies have been found in this forest atmosphere, the details of which are summarized in Table S1–S5 of the Supplement. They were primarily consisted of CHOS, CHONS, and CHO compounds in the ESI− mode, together with those of CHN and CHO compounds in the ESI+ mode. Figure 7 presents the temporal variations in the peak area intensities of these organic tracer species and their relative fractions over the study periods. Overall, distinct seasonal profiles were observed for the organic tracer species of different origins. The total peak area intensities of organic tracer species derived from biogenic precursors were almost comparable between the two seasons for both ESI− and ESI+ modes, whereas those derived from anthropogenic

11

precursors were substantially increased in winter period (Fig. 7a, d). The ratios between the total peak area intensities of anthropogenic to biogenic tracer species in ESI− mode were on average 0.3 ± 0.1 in summer and 1.1 ± 0.2 in winter, corresponding to those of 0.4 ± 0.3 and 3.5 ± 1.7 in ESI+ mode. The large seasonal discrepancy in peak area intensity ratios of anthropogenic to biogenic tracer species suggests that organic aerosols over this forest atmosphere were more strongly contributed by anthropogenic sources in winter, contrasting with the more prevailing contribution of biogenic sources in summer.
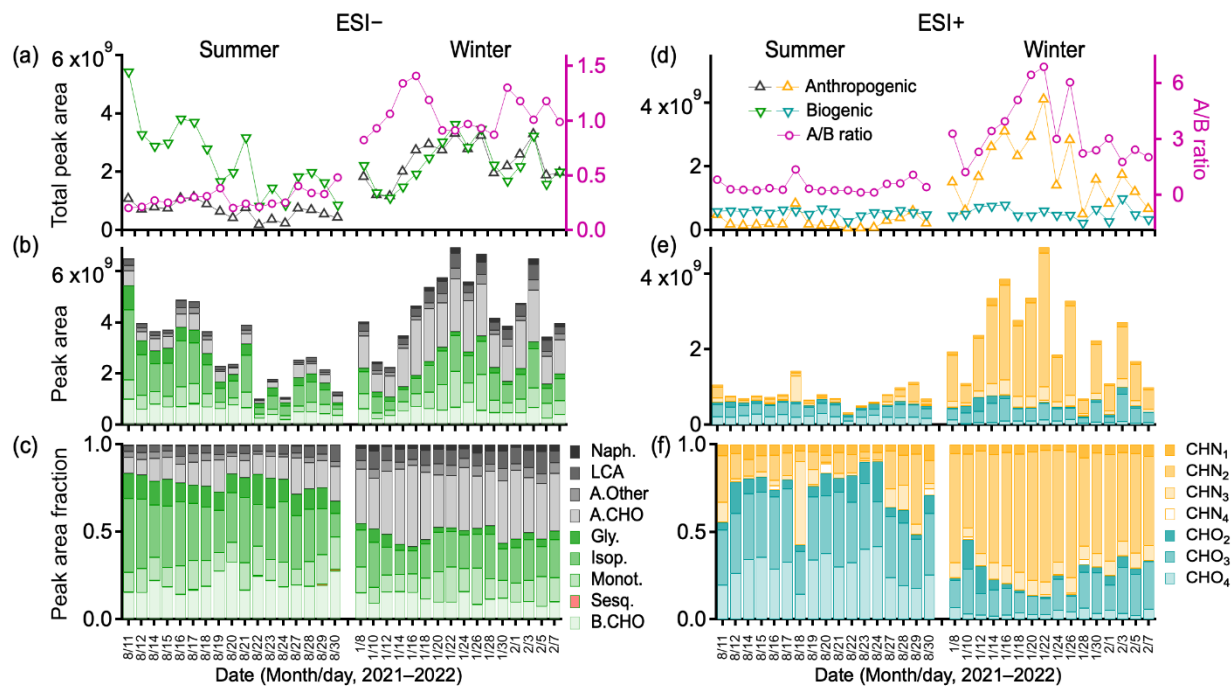

Figure 7. (a, d) Total peak area intensities of organic tracer species derived from anthropogenic and biogenic sources in negative and positive ESI modes, and the peak area ratios of anthropogenic to biogenic ones (A/B) over the study periods. (b, c) Peak area intensities of organic tracer species contributed by different types of precursors and (e, f) their relative fractions. In panels (b, c), the organic tracer species in ESI− mode consisted of various organosulfates, which were derived from anthropogenic (naphthalene, long-chain alkanes, and others) and biogenic (glyoxal, isoprene, monoterpenes, and sesquiterpene) precursors, and some other CHO compounds (Table S1–S3 in the Supplement). In panels (e, f), the organic tracer species in ESI+ mode consisted of CHN and CHO compounds derived from anthropogenic and biogenic sources, respectively (Table S4–S5).

The identified individual organic tracer species were mainly derived from biogenic precursors of glyoxal, isoprene, and monoterpenes along with anthropogenic precursors of naphthalene, long-chain alkanes, and others (Fig. 7b, e). In ESI− mode, the biogenic tracer species dominated the total peak area intensities in summer, accounting for 68–84% compared with those of 41–55% in winter (Fig. 7c). Among these, organosulfate and nitrooxy-organosulfate compounds (abbreviated as OSs hereafter), roughly defined as those with sufficient oxygen atoms to assign the −OSO₃H and −ONO₂ groups in the molecules (Brüggemann et al., 2020; Lin et al., 2012b), were important components in both seasons. Note that the designated OSs here would correspond to those at the upper limit, since no further fragmentation spectra available. The OSs derived from glyoxal and isoprene (mainly from biogenic sources) had higher peak area intensities and relative fractions in summer, which is consistent with the higher emissions and more intensive photochemical activities of these precursors than those in winter (Hu et al., 2017; Li et al., 2021; Vettikkat et al., 2023). On the contrary, the peak area intensities and fractions of monoterpenes derived OSs were on average slightly higher in winter than those in summer. Although the biogenic monoterpene emissions were likely higher in summer than in winter (Bai et al., 2017; Hakola et al., 2012), the highly abundance of anthropogenic pollutants (e.g., NOₓ, SO₂, and sulfate; Fig. 2) would more facilitate the production of these OSs in winter. In addition, biogenic CHO tracer species were also important components of organic aerosols in ESI− mode, with comparable peak area intensities

in the two seasons but higher fractions in summer (Fig. 7b, c). Similar trends were also observed for biogenic CHO tracer species in ESI+ mode, especially with the massive increase of $C_xH_yO_4$ fractions in summer (Fig. 7e, f). These CHO species were primarily associated with the oxidation products of isoprene and terpenes along with other biogenic species such as unsaturated fatty acids (Table S3 in the Supplement).

In contrast, the anthropogenic organic tracer species in both ESI− and ESI+ modes were relatively more abundant in winter, respectively accounting for 45–59% and 54–87% of total peak area intensities, compared with those of 16–32% and 10–57% in summer. Among these, the OSs derived from anthropogenic precursors in ESI− mode (Table S2) had much higher peak area intensities and relative fractions in winter than those in summer (Fig. 7b, c). This was most likely attributed to the enhanced contribution from anthropogenic sources (e.g., combustion of biomass and fossil fuels) in the surrounding rural and urban areas during the winter heating season, together with the unfavorable atmospheric dispersion conditions (Cao and Cui, 2021; Zhao et al., 2015). A number of aromatic CHO species (such as benzoic acid $C_7H_6O_2$ and phthalic acid $C_8H_6O_4$, Table S3) were also found in ESI− mode and relatively more abundant in winter, which might be contributed by primary combustion emissions and/or secondary products of anthropogenic aromatic precursors (Aggarwal and Kawamura, 2008; Vodička et al., 2023). Moreover, a variety of oxygen-free nitrogen-containing CHN species were identified as the major anthropogenic tracer species in ESI+ mode (Table S5). Their peak area intensities were dominated by the $C_xH_yN_2$ compounds such as $C_5H_8N_2$, $C_6H_{10}N_2$, $C_7H_{12}N_2$, $C_8H_8N_2$, and $C_9H_{10}N_2$ (Fig. 7f). These $C_4H_6N_2$-$(CH_2)_n$ and $C_6H_4N_2$-$(CH_2)_n$ homologs have been reported as heterocyclic alkaloids derived from coal combustion and biomass burning (Li et al., 2024c; Song et al., 2022; Wang et al., 2017b).

The anthropogenic and biogenic organic tracer species identified in the ESI− ~~mode~~ and ESI+ modes were further analyzed in the van Krevelen diagram based on their elemental ratios of O/C and H/C, as shown in Fig. 8a. ~~Except~~ Similar variation patterns were generally observed between the two modes. Specifically, except for those derived from glyoxal, isoprene, and some anthropogenic precursors with O/C > 0.5, other tracer species were primarily distributed in the regime with O/C ≤ 0.5. In addition, the anthropogenic tracer species widely dispersed at the regime with H/C from approximately 0.5 to 2.5, whereas the biogenic ones were mainly situated at the H/C ≥ 1.5 regime. This result is generally consistent with previous findings that the regime with H/C ≥ 1.5 and O/C ≤ 0.5 mainly consists of aliphatic species of anthropogenic and biogenic origins, while the regime with H/C ≤ 1 and O/C ≤ 0.5 are dominated by aromatic species of anthropogenic origins (Kourtchev et al., 2016a; Lin et al., 2022; Wang et al., 2017a). These two regimes are respectively represented as the pink and blue shaded areas in Fig. 8.

The organic molecular species assigned on individual days during the study periods were then compared in the aliphatic and aromatics regimes of the van Krevelen diagram. Figure 8b presents the example results on two different days~~,~~ (that is, August 30 and January 26) obtained in the ESI− mode. A larger number of organic species were present in the aliphatic regime than those in the aromatic regime (310 vs. 175) on August 30 in summer, whereas enhanced aromatic species (449 vs. those of 629 in the aliphatic regime) were observed on January 26 in winter. Also, more organic species were found in both aliphatic and aromatic regimes on the winter day compared with the summer day, suggesting the enhanced influence of anthropogenic pollution in winter over this forest atmosphere. ~~A similar tendency was~~ Similar tendencies were also ~~obtained~~ found for those in the two modes across the entire study periods in summer and winter (Fig. 8c). ~~The~~ In ESI− mode, the number fraction of organic species in the aromatic regime was on average 21 ± 2% on individual days in winter, which was higher than those of 17 ± 2% in summer. The peak area fractions of these aromatic species were even 2.7 times higher in winter than those in summer (25 ± 4% vs. 9 ± 2%). On the contrary, both the number and peak area fractions of aliphatic species were higher in summer than those in winter. Likewise, in ESI+ mode, the number and peak area fractions of aromatic species were slightly higher in winter than in summer, while those of aliphatic species were higher in summer. These results further confirmed the dominant roles of biogenic sources in summer but those of anthropogenic sources in winter in the production of organic aerosols over this forest atmosphere.

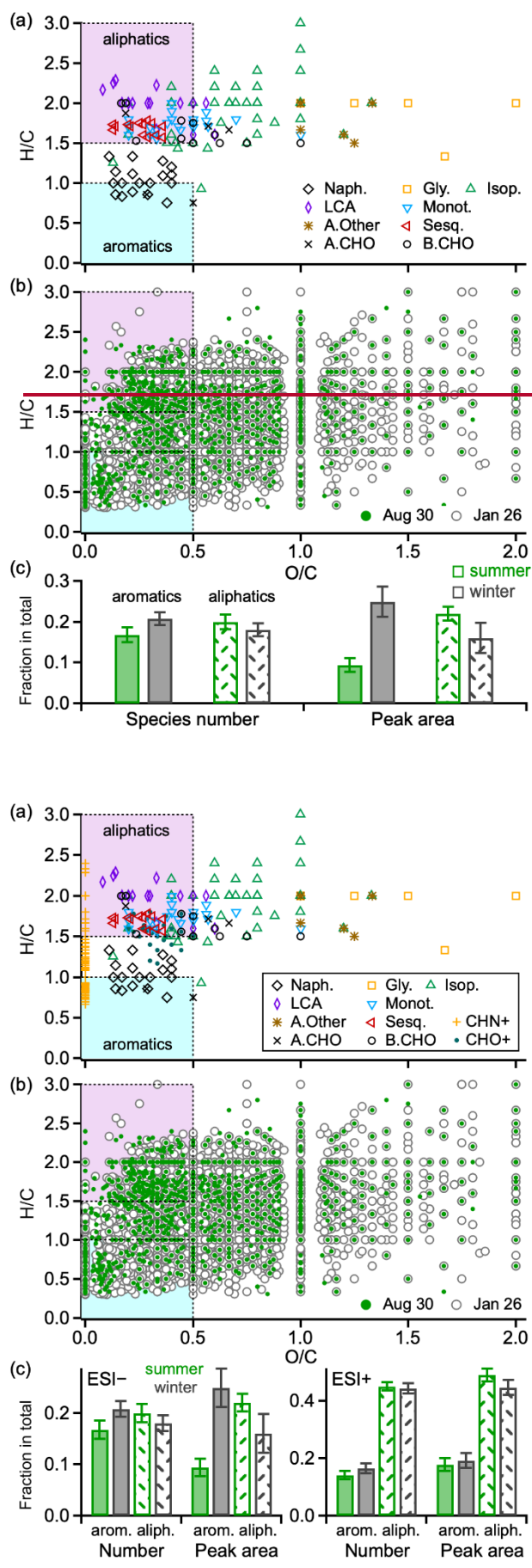**Figure 8.** van Krevelen diagrams plotting of (a) organic tracer species derived from anthropogenic and biogenic precursors **in both modes** (as listed in Table S1 ~~S3)~~**S5),** and (b) organic ~~molecular~~ species identified on a summer day

14

(August 30) and a winter day (January 26) in ~~negative~~ ESI_ mode. (c) Averaged number and peak area fractions of organic species in aromatic and aliphatic molecular structures for summer and winter samples~~.~~ in ESI− and ESI+ modes. In panels (a, b), the shaded pink (H/C ≥ 1.5, O/C ≤ 0.5) and cyan (H/C ≤ 1.0, O/C ≤ 0.5) areas represent aliphatic and aromatic regimes, respectively. The O/C was replaced by (O−3S)/C or (O−3S−2N)/C in the case of organosulfates or nitrooxy-organosulfates. The error bars in panel (c) represent 1σ standard deviations for all the samples in each season.

3.4 Synergistic effects of meteorology and anthropogenic pollutants

The production and molecular composition of organic aerosols can be affected by multiple environmental factors in this forest atmosphere. Among those, ambient RH turned out to be one of the key governing factors. Figure 9 presents the species number and fraction of individual organic subgroups in ESI− mode under varied RH conditions during the study periods. With the mean RH values increasing from $62 \pm 6\%$ to $75 \pm 4\%$ in summer, some evident increases (1.1–1.2 times, Fig. 9a) were observed in the numbers of CHO, CHON, CHOS, and CHONS species, possibly due to the enhanced heterogeneous and/or aqueous phase reactions of aerosol particles in semisolid or liquid physical state under higher RH conditions (Ervens et al., 2011; Reid et al., 2018; Wang et al., 2021d). Meanwhile, the number fractions of CHO species were decreased while those of other subgroups were increased (Fig. 9b). It was likely that more anthropogenic gas pollutants (SO_2, NO_x, and etc.) could absorb into aerosol liquid phase at the higher RH conditions, reacting with preexisting CHO species such as hydroperoxides, carbonyl/hydroxyl compounds, and unsaturated fatty acids to produce more nitrogen- and/or sulfur-containing species (Wang et al., 2021e; Xu et al., 2021c; Zhu et al., 2019). Nevertheless, all the species numbers were reversely decreased at the extremely high RH levels (mean $93 \pm 2\%$) in summer, during which heavy rainfalls occurred (Fig. 2d). Aerosol particles can be easily washed away under such heavy precipitation conditions. By comparison, the observed RH effect in winter was generally similar to those in summer, except without heavy precipitation. The numbers and relative fractions of organosulfur species CHOS and CHONS increased constantly for RH increased from $43 \pm 8\%$ to $88 \pm 5\%$ (Fig. 9c, d). The decreased number and fraction of CHON species at the highest RH level in winter could partly result from their hydrolysis reactions (Hu et al., 2011; Su et al., 2021). In contrast, the similar but weaker dependence on RH was found for organic species in the ESI+ mode (Fig. S2 in the Supplement), probably associated in part with their distinct physicochemical properties compared with those in the ESI− mode. This result also indicates that the influence of RH could be stronger for acidic organic substances, since these were more readily deprotonated and sensitive to be detected in negative mode than the basic ones (Laskin et al., 2018).
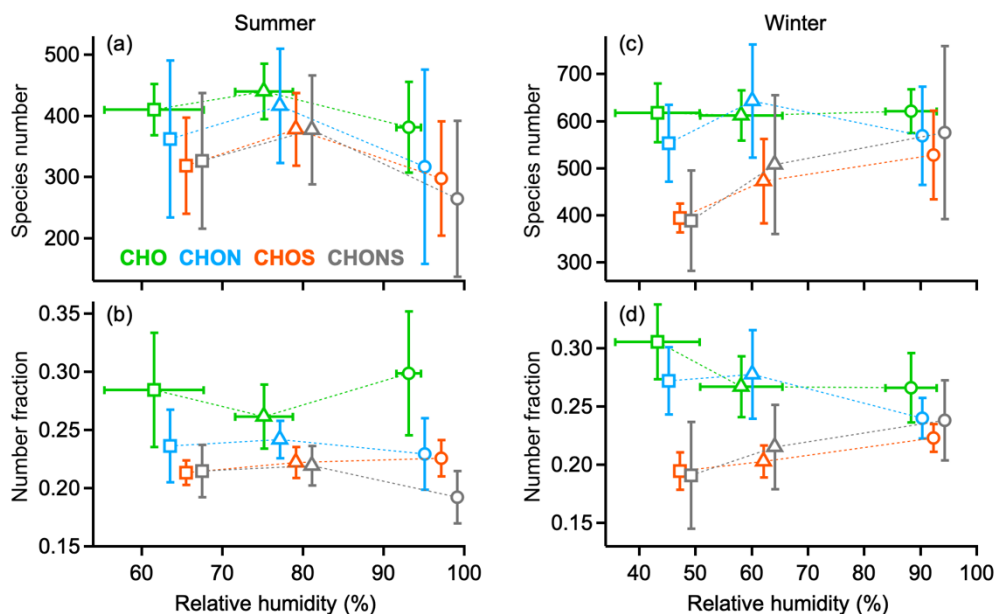
Figure 9. Species number and the relative fractions of organic molecular subgroups in negative ESI mode under varied relative humidity conditions in (a, b) summer and (c, d) winter periods. The symbols of each type shared the same RH values (that is, 62 ± 6%, 75 ± 4%, 93 ± 2% in summer and 43 ± 8%, 58 ± 7%, 88 ± 5% in winter) but were offset horizontally for a clear vision. The horizontal error bars in the CHO species represent 1σ standard deviations of RH values. The vertical error bars represent 1σ standard deviations for all the samples in each RH condition.

On the contrary, the effect of ambient temperature on organic molecular composition was more complex over the study periods. The species numbers of all organic subgroups in ESI− mode were almost comparable at the mean temperatures of 21.5 ± 0.8 and 24.5 ± 0.8 °C in summer, while they were largely increased at the highest temperature level of 27.6 ± 1.0 °C (Fig. ~~S2~~S3 in the Supplement). In contrast, all the species numbers were decreased at the highest temperature in winter (3.8 ± 1.0 °C). Their number fractions also had no obvious variation trends in the two seasons. The species number and fraction of organic subgroups in ESI+ mode varied insignificantly with temperature as well (Fig. S4 in the Supplement). Higher temperatures usually would promote biogenic volatile organic emissions from forest vegetation to form more secondary products, especially during summertime (Chang et al., 2014; Kourtchev et al., 2016b). The lack of a strong temperature dependence herein suggests that other influencing factors might be more dominant or the temperature variability in each season was too small to result in significant changes on the reaction chemistry of organic aerosols during the study periods.

A variety of anthropogenic pollutants also played crucial roles in affecting organic aerosol composition in this forest atmosphere. The winter period was primarily characterized by the higher loadings of anthropogenic pollutants NO_2, SO_2, sulfate, and nitrate compared with those in summer (Fig. 10a, b). The nitrogen and sulfur oxidation ratios (NOR and SOR) were also higher in winter, whereas the atmospheric oxidation capacity was stronger in summer (as indicated by the higher odd oxygen levels) (Fig. 10c). Some typical organic tracer species were identified under these different atmospheric conditions in each season. For instance, several organosulfates (e.g., $C_3H_6O_5S$, $C_3H_6O_6S$, and $C_4H_8O_6S$) were found to have the highest peak area intensities in winter samples, which were most likely derived from isoprene oxidation under high NO_x conditions (Schindelka et al., 2013; Shalamzari et al., 2013). In contrast, some isoprene oxidation products under low NO_x conditions, such as $C_5H_{12}O_7S$ and $C_5H_{10}O_7S$ (Surratt et al., 2008, 2010), were commonly found in summer samples. Moreover, a monoterpenes-derived organosulfate of $C_{10}H_{17}NO_7S$ was greatly abundant in both summer and winter samples. It can be generated either through the photooxidation of monoterpenes in the presence of NO_x and SO_2 or their nocturnal chemistry initiated by nitrate radicals (Iinuma et al., 2007; Surratt et al., 2008).
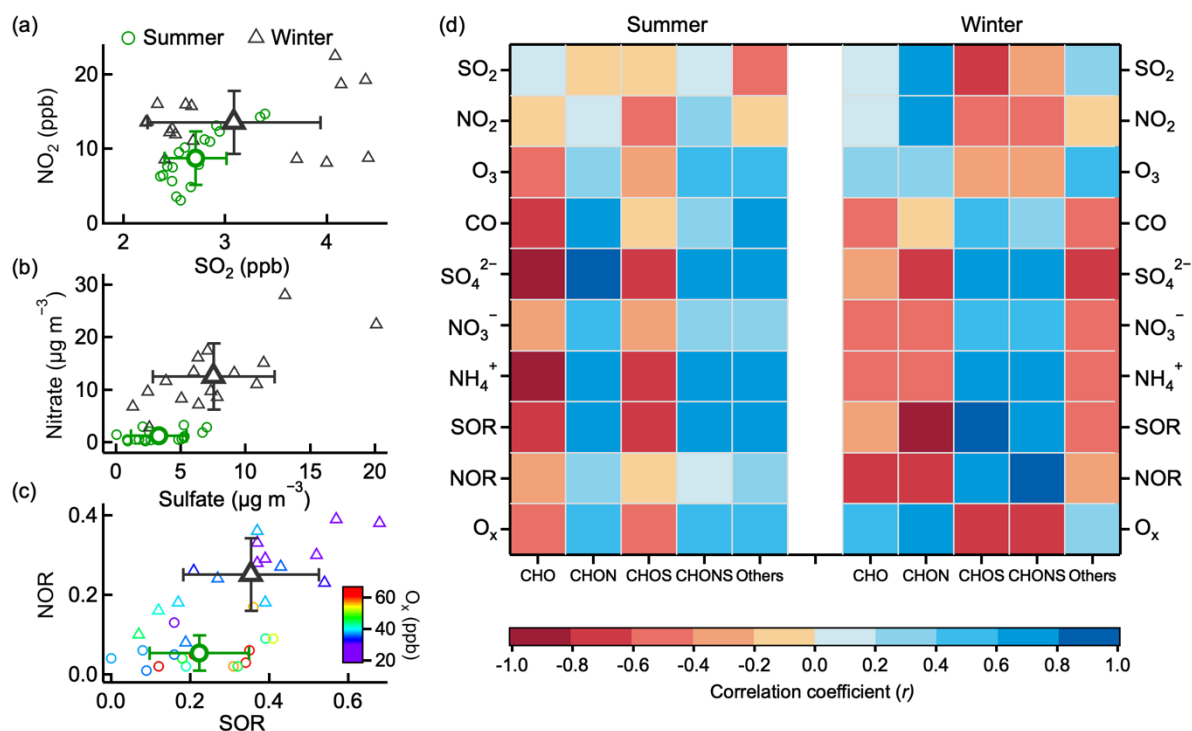
Figure 10. Typical atmospheric conditions of (a) NO₂ and SO₂, (b) nitrate and sulfate, and (c) nitrogen and sulfur oxidation ratios and oxidant levels in the studied summer and winter periods. (d) Correlations of gas and particulate pollutants with the number fractions of organic subgroups in negative ESI mode, which were all statistically highly significant at $p < 0.001$ level. In panels (a–c), the larger symbols with error bars represent the mean values and 1σ standard deviations of these parameters in each season.

The effects of anthropogenic pollution on the molecular composition of organic aerosols were further explored to understand their potential interactions. Figure 10d presents the correlations of gas and particulate pollutants, SOR, NOR, and O_x with the number fractions of individual organic subgroups in ESI− mode over the study periods. Distinct correlation patterns were obtained between summer and winter, partly attributed to the different production pathways of organic aerosols under the synergistic effects of anthropogenic pollutants and meteorology in the two seasons. In the summer period, the number fractions of CHO and CHOS species negatively correlated with all these parameters (correlation coefficients r: −0.07 to −0.82), except for a weak positive correlation of CHO species with SO₂ (r: 0.17). This phenomenon ~~can either~~could partly result from the chemical transformation of these species into other chemically diverse substances (e.g., CHON and CHONS) through acid-catalyzed heterogeneous reactions and/or aqueous phase chemistry in the presence of anthropogenic air pollutants~~, or their~~ (Darer et al., 2011; Fan et al., 2022; Kwong et al., 2018; Lam et al., 2019). Another proposed explanation is that the productions ~~were~~of CHO and CHOS species were to some extent governed by the consumption of anthropogenic pollutants ~~under~~at the low concentration levels in summer (Fig. ~~2c)~~2c), as those reported in some other ambient atmospheres (Lin et al., 2022; Riva et al., 2019; Wang et al., 2020). On the contrary, the CHON, CHONS, and other oxygen-free species (mainly CHNS herein) positively correlated with most of these parameters (r: 0.16–0.81; except for SO₂ and NO₂), suggesting their large anthropogenic contributions. Possible reaction pathways include such as biogenic isoprene and monoterpene precursors being oxidized by nitrate radicals to form condensable organic nitrates and nitrooxy-organosulfates (Hamilton et al., 2021; Ng et al., 2017). These results revealed that anthropogenic pollutants also played important roles in affecting the chemical composition of organic aerosols in summer period, despite their relatively low concentrations.

In winter period, however, the number fractions of CHO and CHON species correlated positively with SO₂, NO₂, O₃, and O_x

17

but negatively with other parameters. These species might be partly associated with primary emissions (Song et al., 2018; Zhong et al., 2023), such as those of biomass burning and fossil fuel combustion from the surrounding rural and urban areas. These correlation patterns were just opposite to those of organosulfur species (CHOS and CHONS). The strong positive correlations of organosulfur species with SOR and NOR (r: 0.60–0.86) suggest that secondary formation was important processes for their production. Indeed, several secondary reaction mechanisms have been previously proposed for organosulfur species formation, including acid-catalyzed ring-opening of epoxides, SO_2 reacting with unsaturated hydrocarbons, direct sulfate esterification, sulfate radical reactions in the aqueous phase, and so on (Brüggemann et al., 2020; Fan et al., 2022). Nevertheless, the atmospheric oxidants appeared to be a limiting factor for those reactions under the studied winter conditions, as indicated by the high negative correlations of O_x with the CHOS and CHONS species (r: –0.64 and –0.66). This is consistent with previous studies that oxidant levels were one of the most important governing factors for the production of organosulfur species by limiting the oxidation of organic precursors (Bryant et al., 2021; Wang et al., 2021f). Taken these observations together, the synergistic effects of meteorological factors and anthropogenic pollutants have played critical roles in affecting the production pathways and chemical transformation of organic aerosols, thereby altering their molecular composition and other related properties under different seasonal conditions in this forest atmosphere.

4 Summary and Implications

The molecular composition of organic aerosols in atmospheric $PM_{2.5}$ was characterized using UHPLC–HRMS at a forest site in the Qinling Mountains region of central China during contrasting summer and winter seasons of 2021/2022. Organic molecular species assigned in the negative and positive ESI modes had much higher numbers and peak area intensities in winter than those in summer, which were consistent with the mass concentration trends of total organic matter, suggesting that organic aerosols were more abundant and chemically diverse in this forest atmosphere during the wintertime. The higher peak-area-weighted mean values of molecular weight and oxidation state but the lower unsaturation degree of organic species were observed in summer, possibly resulted from the large biogenic emissions from forest vegetation and intense photochemical processes. The relative abundances of a variety of identified organic tracer species revealed that organic aerosols were substantially affected by anthropogenic sources in winter, whereas biogenic sources were more prevalent in summer. The increased organic species with aliphatic and aromatic molecular structures in the winter period were closely associated with the oxidation products of anthropogenic long-chain alkanes and aromatic hydrocarbons transported from the surrounding rural and urban areas. The production and transformation of organic aerosols in this region were largely influenced by the synergistic effects of meteorology and anthropogenic pollutants, which ultimately altered their molecular composition and other characteristics. Further The current work focuses primarily on the non-target characterization of organic species in aerosol particles over the Qinling Mountains region based on the HRMS analysis. To further identify organic tracers and other specific substances with the aid of fragmentation spectra in existing MS databases would achieve even higher reliability. Future studies on the quantification and source apportionment of organic molecular composition based on the HRMS analysis will be also valuable to elucidate the complex anthropogenic–biogenic interactions and to incorporate the results into atmospheric chemistry model for improved prediction of organic aerosol burden and impacts in similar regions worldwide.

Data Availability. The datasets used in this study are available upon request to the corresponding author.

Supplement. The supplement related to this article is available online at: https://doi.org.

Author contributions. YH and JC designed and conceptualized the study. XZ with support from JL, YC, CZ performed aerosol sampling and field measurements. XZ, LL, YL, RW, and SX contributed to the aerosol chemical analysis and data processing. XZ and YH wrote the original draft. All authors revised and approved the manuscript before submission.

References

Aggarwal, S. G. and Kawamura, K.: Molecular distributions and stable carbon isotopic compositions of dicarboxylic acids and related compounds in aerosols from Sapporo, Japan: Implications for photochemical aging during long-range atmospheric transport, J. Geophys. Res.-Atmos., 113, https://doi.org/10.1029/2007jd009365, 2008.

535 Bai, J., Guenther, A., Turnipseed, A., Duhl, T., and Greenberg, J.: Seasonal and interannual variations in whole-ecosystem BVOC emissions from a subtropical plantation in China, Atmos. Environ., 161, 176–190, https://doi.org/10.1016/j.atmosenv.2017.05.002, 2017.

Bejan, I., Barnes, I., Olariu, R., Zhou, S., Wiesen, P., and Benter, T.: Investigations on the gas-phase photolysis and OH radical kinetics of methyl-2-nitrophenols, Phys. Chem. Chem. Phys., 9, 5686–5692, https://doi.org/10.1039/b709464g, 2007.

540 Bianchi, F., Kurten, T., Riva, M., Mohr, C., Rissanen, M. P., Roldin, P., Berndt, T., Crounse, J. D., Wennberg, P. O., Mentel, T. F., Wildt, J., Junninen, H., Jokinen, T., Kulmala, M., Worsnop, D. R., Thornton, J. A., Donahue, N., Kjaergaard, H. G., and Ehn, M.: Highly oxygenated organic molecules (HOM) from gas-phase autoxidation involving peroxy radicals: A key contributor to atmospheric aerosol, Chem. Rev., 119, 3472–3509, https://doi.org/10.1021/acs.chemrev.8b00395, 2019.

545 Brüggemann, M., Xu, R., Tilgner, A., Kwong, K. C., Mutzel, A., Poon, H. Y., Otto, T., Schaefer, T., Poulain, L., Chan, M. N., and Herrmann, H.: Organosulfates in ambient aerosol: state of knowledge and future research directions on formation, abundance, fate, and importance, Environ. Sci. Technol., 54, 3767–3782, https://doi.org/10.1021/acs.est.9b06751, 2020.

Bryant, D. J., Elzein, A., Newland, M., White, E., Swift, S., Watkins, A., Deng, W., Song, W., Wang, S., Zhang, Y., Wang, X., Rickard, A. R., and Hamilton, J. F.: Importance of oxidants and temperature in the formation of biogenic
550 organosulfates and nitrooxy organosulfates, ACS Earth Space Chem., 5, 2291–2306, https://doi.org/10.1021/acsearthspacechem.1c00204, 2021.

Cai, Y., Tan, L., Cheng, H., An, Z., Edwards, R. L., Kelly, M. J., Kong, X., and Wang, X.: The variation of summer monsoon precipitation in central China since the last deglaciation, Earth Planet. Sci. Lett., 291, 21–31, https://doi.org/10.1016/j.epsl.2009.12.039, 2010.

555 Cao, J., Situ, S., Hao, Y., Xie, S., and Li, L.: Enhanced summertime ozone and SOA from biogenic volatile organic compound (BVOC) emissions due to vegetation biomass variability during 1981–2018 in China, Atmos. Chem. Phys., 22, 2351–2364, https://doi.org/10.5194/acp-22-2351-2022, 2022.

Cao, J. J. and Cui, L.: Current status, characteristics and causes of particulate air pollution in the fenwei plain, china: A review, J. Geophys. Res.-Atmos., 126, https://doi.org/10.1029/2020jd034472, 2021.

560 Cao, J. J., Lee, S. C., Ho, K. F., Zhang, X. Y., Zou, S. C., Fung, K., Chow, J. C., and Watson, J. G.: Characteristics of carbonaceous aerosol in Pearl River Delta Region, China during 2001 winter period, Atmos. Environ., 37, 1451–1460, https://doi.org/10.1016/s1352-2310(02)01002-6, 2003.

Carlton, A. G., Pye, H. O. T., Baker, K. R., and Hennigan, C. J.: Additional benefits of federal air-quality rules: model estimates of controllable biogenic secondary organic aerosol, Environ. Sci. Technol., 52, 9254–9265, https://doi.org/10.1021/acs.est.8b01869, 2018.

Chang, C.-C., Wang, J.-L., Candice Lung, S.-C., Chang, C.-Y., Lee, P.-J., Chew, C., Liao, W.-C., Chen, W.-N., and Ou-Yang, C.-F.: Seasonal characteristics of biogenic and anthropogenic isoprene in tropical–subtropical urban environments, Atmos. Environ., 99, 298–308, https://doi.org/10.1016/j.atmosenv.2014.09.019, 2014.

Chow, J. C. and Watson, J. G.: PM2.5 carbonate concentrations at regionally representative Interagency Monitoring of Protected Visual Environment sites, J. Geophys. Res.-Atmos., 107, https://doi.org/10.1029/2001jd000574, 2002.

Darer, A. I., Cole-Filipiak, N. C., O'Connor, A. E., and Elrod, M. J.: Formation and stability of atmospherically relevant Isoprene-derived organosulfates and organonitrates, Environ. Sci. Technol., 45, 1895–1902, https://doi.org/10.1021/es103797z, 2011.

Deshmukh, D. K., Haque, M. M., Kim, Y., and Kawamura, K.: Organic tracers of fine aerosol particles in central Alaska: summertime composition and sources, Atmos. Chem. Phys., 19, 14009–14029, https://doi.org/10.5194/acp-19-14009-2019, 2019.

Després, V., Huffman, J. A., Burrows, S. M., Hoose, C., Safatov, A., Buryak, G., Fröhlich-Nowoisky, J., Elbert, W., Andreae, M., Pöschl, U., and Jaenicke, R.: Primary biological aerosol particles in the atmosphere: A review, Tellus B Chem. Phys. Meteorol., 64, https://doi.org/10.3402/tellusb.v64i0.15598, 2012.

Dong, X., Liu, Y., Li, X., Yue, M., Liu, Y., Ma, Z., Zheng, H., Huang, R., and Wang, M.: Modeling analysis of biogenic secondary organic aerosol dependence on anthropogenic emissions in China, Environ. Sci. Technol. Lett., 9, 286–292, https://doi.org/10.1021/acs.estlett.2c00104, 2022.

Ehn, M., Kleist, E., Junninen, H., Petaja, T., Lonn, G., Schobesberger, S., Dal Maso, M., Trimborn, A., Kulmala, M., Worsnop, D. R., Wahner, A., Wildt, J., and Mentel, T. F.: Gas phase formation of extremely oxidized pinene reaction products in chamber and ambient air, Atmos. Chem. Phys., 12, 5113–5127, https://doi.org/10.5194/acp-12-5113-2012, 2012.

Ervens, B., Turpin, B. J., and Weber, R. J.: Secondary organic aerosol formation in cloud droplets and aqueous particles (aqSOA): A review of laboratory, field and model studies, Atmos. Chem. Phys., 11, 11069–11102, https://doi.org/10.5194/acp-11-11069-2011, 2011.

Evans, R. L., Bryant, D. J., Voliotis, A., Hu, D., Wu, H., Syafira, S. A., Oghama, O. E., McFiggans, G., Hamilton, J. F., and Rickard, A. R.: A semi-quantitative approach to nontarget compositional analysis of complex samples, Anal. Chem., 96, 18349–18358, https://doi.org/10.1021/acs.analchem.4c00819, 2024.

Fan, W., Chen, T., Zhu, Z., Zhang, H., Qiu, Y., and Yin, D.: A review of secondary organic aerosols formation focusing on organosulfates and organic nitrates, J. Hazard. Mater., 430, 128406, https://doi.org/10.1016/j.jhazmat.2022.128406, 2022.

Gu, Y., Huang, R.-J., Duan, J., Xu, W., Lin, C., Zhong, H., Wang, Y., Ni, H., Liu, Q., Xu, R., Wang, L., and Li, Y. J.: Multiple pathways for the formation of secondary organic aerosol in the North China Plain in summer, Atmos. Chem. Phys., 23, 5419–5433, https://doi.org/10.5194/acp-23-5419-2023, 2023.

Guo, J., Miao, Y., Zhang, Y., Liu, H., Li, Z., Zhang, W., He, J., Lou, M., Yan, Y., Bian, L., and Zhai, P.: The climatology of planetary boundary layer height in China derived from radiosonde and reanalysis data, Atmos. Chem. Phys., 16, 13309–13319, https://doi.org/10.5194/acp-16-13309-2016, 2016.

Hakola, H., Hellén, H., Hemmilä, M., Rinne, J., and Kulmala, M.: In situ measurements of volatile organic compounds in a boreal forest, Atmos. Chem. Phys., 12, 11665–11678, https://doi.org/10.5194/acp-12-11665-2012, 2012.

Hamilton, J. F., Bryant, D. J., Edwards, P. M., Ouyang, B., Bannan, T. J., Mehra, A., Mayhew, A. W., Hopkins, J. R., Dunmore, R. E., Squires, F. A., Lee, J. D., Newland, M. J., Worrall, S. D., Bacak, A., Coe, H., Percival, C., Whalley, L. K., Heard, D. E., Slater, E. J., Jones, R. L., Cui, T., Surratt, J. D., Reeves, C. E., Mills, G. P., Grimmond, S., Sun, Y., Xu, W., Shi,

605   Z., and Rickard, A. R.: Key role of NO(3) radicals in the production of isoprene nitrates and nitrooxyorganosulfates in Beijing, Environ. Sci. Technol., 55, 842–853, https://doi.org/10.1021/acs.est.0c05689, 2021.

Han, Y. M., Zhang, X., Li, L., Lin, Y., Zhu, C., Zhang, N., Wang, Q., and Cao, J.: Enhanced production of organosulfur species during a severe winter haze episode in the Guanzhong basin of northwest China, Environ. Sci. Technol., 57, 8708–8718, https://doi.org/10.1021/acs.est.3c02914, 2023.

610   Han, Y. M., Stroud, C. A., Liggio, J., and Li, S. M.: The effect of particle acidity on secondary organic aerosol formation from alpha-pinene photooxidation under atmospherically relevant conditions, Atmos. Chem. Phys., 16, 13929–13944, https://doi.org/10.5194/acp-16-13929-2016, 2016.

Herndon, S. C., Onasch, T. B., Wood, E. C., Kroll, J. H., Canagaratna, M. R., Jayne, J. T., Zavala, M. A., Knighton, W. B., Mazzoleni, C., Dubey, M. K., Ulbrich, I. M., Jimenez, J. L., Seila, R., de Gouw, J. A., de Foy, B., Fast, J., Molina, L. T.,
615   Kolb, C. E., and Worsnop, D. R.: Correlation of secondary organic aerosol with odd oxygen in Mexico City, Geophys. Res. Lett., 35, https://doi.org/10.1029/2008gl034058, 2008.

Hoyle, C. R., Boy, M., Donahue, N. M., Fry, J. L., Glasius, M., Guenther, A., Hallar, A. G., Hartz, K. H., Petters, M. D., Petaja, T., Rosenoern, T., and Sullivan, A. P.: A review of the anthropogenic influence on biogenic secondary organic aerosol, Atmos. Chem. Phys., 11, 321–343, https://doi.org/10.5194/acp-11-321-2011, 2011.

620   Hu, J. L., Wang, P., Ying, Q., Zhang, H. L., Chen, J. J., Ge, X. L., Li, X. H., Jiang, J. K., Wang, S. X., Zhang, J., Zhao, Y., and Zhang, Y. Y.: Modeling biogenic and anthropogenic secondary organic aerosol in China, Atmos. Chem. Phys., 17, 77–92, https://doi.org/10.5194/acp-17-77-2017, 2017.

Hu, K. S., Darer, A. I., and Elrod, M. J.: Thermodynamics and kinetics of the hydrolysis of atmospherically relevant organonitrates and organosulfates, Atmos. Chem. Phys., 11, 8307–8320, https://doi.org/10.5194/acp-11-8307-2011, 2011.

625   Iinuma, Y., Muller, C., Berndt, T., Boge, O., Claeys, M., and Herrmann, H.: Evidence for the existence of organosulfates from beta-pinene ozonolysis in ambient secondary organic aerosol, Environ. Sci. Technol., 41, 6678–6683, https://doi.org/10.1021/es070938t, 2007.

Kaneyasu, N., Ohta, S., and Murao, N.: Seasonal variation in the chemical composition of atmospheric aerosols and gaseous species in Sapporo, Japan, Atmos. Environ., 29, 1559–1568, https://doi.org/10.1016/1352-2310(94)00356-p, 1995.

630   Kind, T. and Fiehn, O.: Seven Golden Rules for heuristic filtering of molecular formulas obtained by accurate mass spectrometry, BMC Bioinf., 8, 105, https://doi.org/10.1186/1471-2105-8-105, 2007.

Kiontke, A., Oliveira-Birkmeier, A., Opitz, A., and Birkemeyer, C.: Electrospray ionization efficiency is dependent on different molecular descriptors with respect to solvent pH and instrumental configuration, PloS One, 11, e0167502, https://doi.org/10.1371/journal.pone.0167502, 2016.

635   Kourtchev, I., Godoi, R. H. M., Connors, S., Levine, J. G., Archibald, A. T., Godoi, A. F. L., Paralovo, S. L., Barbosa, C. G. G., Souza, R. A. F., Manzi, A. O., Seco, R., Sjostedt, S., Park, J.-H., Guenther, A., Kim, S., Smith, J., Martin, S. T., and Kalberer, M.: Molecular composition of organic aerosols in central Amazonia: An ultra-high-resolution mass spectrometry study, Atmos. Chem. Phys., 16, 11899–11913, https://doi.org/10.5194/acp-16-11899-2016, 2016a

Kourtchev, I., Giorio, C., Manninen, A., Wilson, E., Mahon, B., Aalto, J., Kajos, M., Venables, D., Ruuskanen, T., Levula, J.,
640   Loponen, M., Connors, S., Harris, N., Zhao, D., Kiendler-Scharr, A., Mentel, T., Rudich, Y., Hallquist, M., Doussin, J. F., Maenhaut, W., Back, J., Petaja, T., Wenger, J., Kulmala, M., and Kalberer, M.: Enhanced volatile organic compounds emissions and organic aerosol mass increase the oligomer content of atmospheric aerosols, Sci. Rep., 6, 35038, https://doi.org/10.1038/srep35038, 2016b.

Kroll, J. H., Donahue, N. M., Jimenez, J. L., Kessler, S. H., Canagaratna, M. R., Wilson, K. R., Altieri, K. E., Mazzoleni, L.
645   R., Wozniak, A. S., Bluhm, H., Mysak, E. R., Smith, J. D., Kolb, C. E., and Worsnop, D. R.: Carbon oxidation state as a metric for describing the chemistry of atmospheric organic aerosol, Nat. Chem, 3, 133–139, https://doi.org/10.1038/nchem.948, 2011.

Kwong, K. C., Chim, M. M., Davies, J. F., Wilson, K. R., and Chan, M. N.: Importance of sulfate radical anion formation and chemistry in heterogeneous OH oxidation of sodium methyl sulfate, the smallest organosulfate, Atmos. Chem. Phys., 18, 2809–2820, https://doi.org/10.5194/acp-18-2809-2018, 2018.

Lam, H. K., Kwong, K. C., Poon, H. Y., Davies, J. F., Zhang, Z., Gold, A., Surratt, J. D., and Chan, M. N.: Heterogeneous OH oxidation of isoprene-epoxydiol-derived organosulfates: kinetics, chemistry and formation of inorganic sulfate, Atmos. Chem. Phys., 19, 2433–2440, https://doi.org/10.5194/acp-19-2433-2019, 2019.

Laskin, J., Laskin, A., and Nizkorodov, S. A.: Mass spectrometry analysis in atmospheric chemistry, Anal. Chem., 90, 166–189, https://doi.org/10.1021/acs.analchem.7b04249, 2018.

Li, J., Zhang, Q., Wang, G., Li, J., Wu, C., Liu, L., Wang, J., Jiang, W., Li, L., Ho, K. F., and Cao, J.: Optical properties and molecular compositions of water-soluble and water-insoluble brown carbon (BrC) aerosols in northwest China, Atmos. Chem. Phys., 20, 4889–4904, https://doi.org/10.5194/acp-20-4889-2020, 2020.

Li, J., Cao, L., Gao, W., He, L., Yan, Y., He, Y., Pan, Y., Ji, D., Liu, Z., and Wang, Y.: Seasonal variations in the highly time-resolved aerosol composition, sources and chemical processes of background submicron particles in the North China Plain, Atmos. Chem. Phys., 21, 4521–4539, https://doi.org/10.5194/acp-21-4521-2021, 2021.

Li, J. J., Wang, G. H., Cao, J. J., Wang, X. M., and Zhang, R. J.: Observation of biogenic secondary organic aerosols in the atmosphere of a mountain site in central China: temperature and relative humidity effects, Atmos. Chem. Phys., 13, 11535–11549, https://doi.org/10.5194/acp-13-11535-2013, 2013.

Li, L., Li, J., Zhang, X., Lin, Y., Wang, R., Cao, J., and Han, Y.: Effects of relative humidity on atmospheric organosulfur species derived from photooxidation and nocturnal chemistry in a forest environment, Environ. Pollut., 363, 125253, https://doi.org/10.1016/j.envpol.2024.125253, 2024a.

Li, H., Duan, F., Ma, T., Ma, Y., Xu, Y., Wang, S., Zhang, Q., Jiang, J., Zhu, L., Li, F., Huang, T., Kimoto, T., and He, K.: Molecular characterization of organosulfur and organonitrogen compounds in summer and winter pm(2.5) via UHPLC-Q-Orbitrap MS/MS, Environ. Sci. Technol., 58, 21692–21701, https://doi.org/10.1021/acs.est.4c02727, 2024b.

Li, L., Han, Y., Li, J., Lin, Y., Zhang, X., Wang, Q., and Cao, J.: Effects of photochemical aging on the molecular composition of organic aerosols derived from agricultural biomass burning in whole combustion process, Sci. Total Environ., 946, https://doi.org/10.1016/j.scitotenv.2024.174152, 2024c.

Li, L. Y. and Xie, S. D.: Historical variations of biogenic volatile organic compound emission inventories in China, 1981-2003, Atmos. Environ., 95, 185–196, https://doi.org/10.1016/j.atmosenv.2014.06.033, 2014.

Li, X., Zhang, R., Tripathee, L., Yu, F., Guo, J., Yang, W., Guo, J., Kang, S., and Cao, J.: Characteristics, sources, and health risk assessment of atmospheric particulate mercury in Guanzhong Basin, Environ. Pollut., 342, 123071, https://doi.org/10.1016/j.envpol.2023.123071, 2023.

Li, Y., Pöschl, U., and Shiraiwa, M.: Molecular corridors and parameterizations of volatility in the chemical evolution of organic aerosols, Atmos. Chem. Phys., 16, 3327–3344, https://doi.org/10.5194/acp-16-3327-2016, 2016.

Liigand, P., Kaupmees, K., Haav, K., Liigand, J., Leito, I., Girod, M., Antoine, R., and Kruve, A.: Think negative: finding the best electrospray ionization/MS mode for your analyte, Anal. Chem., 89, 5665–5668, https://doi.org/10.1021/acs.analchem.7b00096, 2017

Lin, P., Rincon, A. G., Kalberer, M., and Yu, J. Z.: Elemental composition of HULIS in the Pearl River Delta Region, China: results inferred from positive and negative electrospray high resolution mass spectrometric data, Environ. Sci. Technol., 46, 7454–7462, https://doi.org/10.1021/es300285d, 2012a.

Lin, P., Yu, J. Z., Engling, G., and Kalberer, M.: Organosulfates in humic-like substance fraction isolated from aerosols at seven locations in East Asia: A study by ultra-high-resolution mass spectrometry, Environ. Sci. Technol., 46, 13118–13127, https://doi.org/10.1021/es303570v, 2012b.

690 Lin, Y., Han, Y., Li, G., Wang, Q., Zhang, X., Li, Z., Li, L., Prévôt, A. S. H., and Cao, J.: Molecular characteristics of atmospheric organosulfates during summer and winter seasons in two cities of southern and northern China, J. Geophys. Res.-Atmos., 127, https://doi.org/10.1029/2022jd036672, 2022.

Liu, C., Chen, R., Sera, F., Vicedo-Cabrera, A. M., Guo, Y., Tong, S., Coelho, M. S. Z. S., Saldiva, P. H. N., Lavigne, E., Matus, P., Valdes Ortega, N., Osorio Garcia, S., Pascal, M., Stafoggia, M., Scortichini, M., Hashizume, M., Honda, Y.,
695 Hurtado-Díaz, M., Cruz, J., Nunes, B., Teixeira, J. P., Kim, H., Tobias, A., Íñiguez, C., Forsberg, B., Åström, C., Ragettli, M. S., Guo, Y.-L., Chen, B.-Y., Bell, M. L., Wright, C. Y., Scovronick, N., Garland, R. M., Milojevic, A., Kyselý, J., Urban, A., Orru, H., Indermitte, E., Jaakkola, J. J. K., Ryti, N. R. I., Katsouyanni, K., Analitis, A., Zanobetti, A., Schwartz, J., Chen, J., Wu, T., Cohen, A., Gasparrini, A., and Kan, H.: Ambient particulate air pollution and daily mortality in 652 cities, N. Engl. J. Med., 381, 705–715, https://doi.org/10.1056/nejmoa1817364, 2019.

700 Ma, J., Ungeheuer, F., Zheng, F., Du, W., Wang, Y., Cai, J., Zhou, Y., Yan, C., Liu, Y., Kulmala, M., Daellenbach, K. R., and Vogel, A. L.: Nontarget screening exhibits a seasonal cycle of PM2.5 organic aerosol composition in Beijing, Environ. Sci. Technol., 56, 7017–7028, https://doi.org/10.1021/acs.est.1c06905, 2022.

Mahilang, M., Deb, M. K., and Pervez, S.: Biogenic secondary organic aerosols: A review on formation mechanism, analytical challenges and environmental impacts, Chemosphere, 262, https://doi.org/10.1016/j.chemosphere.2020.127771, 2021.

705 Mallik, C. and Lal, S.: Seasonal characteristics of SO$_2$, NO$_2$, and CO emissions in and around the Indo-Gangetic Plain, Environ. Monit. Assess., 186, 1295–1310, https://doi.org/10.1007/s10661-013-3458-y, 2014.

Matsui, H., Koike, M., Kondo, Y., Takami, A., Fast, J. D., Kanaya, Y., and Takigawa, M.: Volatility basis-set approach simulation of organic aerosol formation in East Asia: implications for anthropogenic-biogenic interaction and controllable amounts, Atmos. Chem. Phys., 14, 9513–9535, https://doi.org/10.5194/acp-14-9513-2014, 2014.

710 McNeill, V. F.: Atmospheric aerosols: clouds, chemistry, and climate, Annu. Rev. Chem. Biomol. Eng., 8, 427–444, https://doi.org/10.1146/annurev-chembioeng-060816-101538, 2017.

Meng, J., Wang, G., Li, J., Cheng, C., Ren, Y., Huang, Y., Cheng, Y., Cao, J., and Zhang, T.: Seasonal characteristics of oxalic acid and related SOA in the free troposphere of Mt. Hua, central China: Implications for sources and formation mechanisms, Sci. Total Environ., 493, 1088–1097, https://doi.org/10.1016/j.scitotenv.2014.04.086, 2014.

715 Ng, N. L., Brown, S. S., Archibald, A. T., Atlas, E., Cohen, R. C., Crowley, J. N., Day, D. A., Donahue, N. M., Fry, J. L., Fuchs, H., Griffin, R. J., Guzman, M. I., Herrmann, H., Hodzic, A., Iinuma, Y., Jimenez, J. L., Kiendler-Scharr, A., Lee, B. H., Luecken, D. J., Mao, J. Q., McLaren, R., Mutzel, A., Osthoff, H. D., Ouyang, B., Picquet-Varrault, B., Platt, U., Pye, H. O. T., Rudich, Y., Schwantes, R. H., Shiraiwa, M., Stutz, J., Thornton, J. A., Tilgner, A., Williams, B. J., and Zaveri, R. A.: Nitrate radicals and biogenic volatile organic compounds: oxidation, mechanisms, and organic aerosol,
720 Atmos. Chem. Phys., 17, 2103–2162, https://doi.org/10.5194/acp-17-2103-2017, 2017.

Niu, X. Y., Cao, J. J., Shen, Z. X., Ho, S. S. H., Tie, X. X., Zhao, S. Y., Xu, H. M., Zhang, B., and Huang, R. J.: PM$_{2.5}$ from the Guanzhong Plain: Chemical composition and implications for emission reductions, Atmos. Environ., 147, 458–469, https://doi.org/10.1016/j.atmosenv.2016.10.029, 2016.

Noziere, B., Kalberer, M., Claeys, M., Allan, J., D'Anna, B., Decesari, S., Finessi, E., Glasius, M., Grgic, I., Hamilton, J. F.,
725 Hoffmann, T., Iinuma, Yoshiteru., Jaoui, M., Kahno, A., Kampf, C. J., Kourtchev, I., Maenhaut, W., Marsden, N., Saarikoski, S., Schnelle-Kreis, J. J., Surratt, J. D., Szidat, S. S., Szmigielski, R., Wisthaler, A., Nozière, B., Kalberer, M., Claeys, M., Allan, J., D'Anna, B., Decesari, S., Finessi, E., Glasius, M., Grgić, I., Hamilton, J. F., Hoffmann, T., Iinuma, Yoshiteru., Jaoui, M., Kahnt, A., Kampf, C. J., Kourtchev, I., Maenhaut, W., Marsden, N., Saarikoski, S., Schnelle-Kreis, J. J., Surratt, J. D., Szidat, S. S., Szmigielski, R., and Wisthaler, A.: The Molecular identification of organic compounds
730 in the atmosphere: State of the art and challenges, Chem. Rev., 115, 3919–3983, https://doi.org/10.1021/cr5003485, 2015.

Pluskal, T., Castillo, S., Villar-Briones, A., and Oresic, M.: MZmine 2: Modular framework for processing, visualizing, and analyzing mass spectrometry-based molecular profile data, BMC Bioinf., 11, https://doi.org/10.1186/1471-2105-11-395, 2010.

Pye, H. O. T., Nenes, A., Alexander, B., Ault, A. P., Barth, M. C., Clegg, S. L., Collett Jr, J. L., Fahey, K. M., Hennigan, C. J., Herrmann, H., Kanakidou, M., Kelly, J. T., Ku, I. T., McNeill, V. F., Riemer, N., Schaefer, T., Shi, G., Tilgner, A., Walker, J. T., Wang, T., Weber, R., Xing, J., Zaveri, R. A., and Zuend, A.: The acidity of atmospheric particles and clouds, Atmos. Chem. Phys., 20, 4809–4888, https://doi.org/10.5194/acp-20-4809-2020, 2020.

Rap, A., Scott, C. E., Reddington, C. L., Mercado, L., Ellis, R. J., Garraway, S., Evans, M. J., Beerling, D. J., MacKenzie, A. R., Hewitt, C. N., and Spracklen, D. V: Enhanced global primary production by biogenic aerosol via diffuse radiation fertilization, Nat. Geosci., 11, 640–644, https://doi.org/10.1038/s41561-018-0208-3, 2018.

Reid, J. P., Bertram, A. K., Topping, D. O., Laskin, A., Martin, S. T., Petters, M. D., Pope, F. D., and Rovelli, G.: The viscosity of atmospherically relevant organic particles, Nat. Commun., 9, 956, https://doi.org/10.1038/s41467-018-03027-z, 2018.

Riva, M., Chen, Y., Zhang, Y., Lei, Z., Olson, N. E., Boyer, H. C., Narayan, S., Yee, L. D., Green, H. S., Cui, T., Zhang, Z., Baumann, K., Fort, M., Edgerton, E., Budisulistiorini, S. H., Rose, C. A., Ribeiro, I. O., Oliveira, R. L. E., Dos Santos, E. O., Machado, C. M. D., Szopa, S., Zhao, Y., Alves, E. G., De Sá, S. S., Hu, W., Knipping, E. M., Shaw, S. L., Duvoisin Junior, S., De Souza, R. A. F., Palm, B. B., Jimenez, J. L., Glasius, M., Goldstein, A. H., Pye, H. O. T., Gold, A., Turpin, B. J., Vizuete, W., Martin, S. T., Thornton, J. A., Dutcher, C. S., Ault, A. P., and Surratt, J. D.: Increasing isoprene epoxydiol-to-inorganic sulfate aerosol ratio results in extensive conversion of inorganic sulfate to organosulfur forms: Implications for aerosol physicochemical properties, Environ. Sci. Technol., 53, 8682–8694, https://doi.org/10.1021/acs.est.9b01019, 2019.

Schindelka, J., Iinuma, Y., Hoffmann, D., and Herrmann, H.: Sulfate radical-initiated formation of isoprene-derived organosulfates in atmospheric aerosols, Faraday Discuss., 165, https://doi.org/10.1039/c3fd00042g, 2013.

Seco, R., Holst, T., Davie-Martin, C. L., Simin, T., Guenther, A., Pirk, N., Rinne, J., and Rinnan, R.: Strong isoprene emission response to temperature in tundra vegetation, Proc. Natl. Acad. Sci. U.S.A., 119, e2118014119, https://doi.org/10.1073/pnas.2118014119, 2022.

Shalamzari, M. S., Ryabtsova, O., Kahnt, A., Vermeylen, R., Hérent, M., Quetin-Leclercq, J., Van der Veken, P., Maenhaut, W., and Claeys, M.: Mass spectrometric characterization of organosulfates related to secondary organic aerosol from isoprene, Rapid Commun. Mass Spectrom., 27, 784–794, https://doi.org/10.1002/rcm.6511, 2013.

Shen, M., Qi, W., Guo, X., Dai, W., Wang, Q., Liu, Y., Zhang, Y., Cao, Y., Chen, Y., Li, L., Liu, H., Cao, J., and Li, J.: Influence of vertical transport on chemical evolution of dicarboxylic acids and related secondary organic aerosol from surface emission to the top of Mount Hua, Northwest China, Sci. Total Environ., 858, https://doi.org/10.1016/j.scitotenv.2022.159892, 2023.

Shrivastava, M., Cappa, C. D., Fan, J., Goldstein, A. H., Guenther, A. B., Jimenez, J. L., Kuang, C., Laskin, A., Martin, S. T., Ng, N. L., Petaja, T., Pierce, J. R., Rasch, P. J., Roldin, P., Seinfeld, J. H., Shilling, J., Smith, J. N., Thornton, J. A., Volkamer, R., Wang, J., Worsnop, D. R., Zaveri, R. A., Zelenyuk, A., and Zhang, Q.: Recent advances in understanding secondary organic aerosol: Implications for global climate forcing, Rev. Geophys., 55, 509–559, https://doi.org/10.1002/2016RG000540, 2017.

Song, J., Li, M., Jiang, B., Wei, S., Fan, X., and Peng, P.: Molecular characterization of water-soluble humic like substances in smoke particles emitted from combustion of biomass materials and coal using ultrahigh-resolution electrospray ionization Fourier Transform Ion Cyclotron Resonance Mass Spectrometry, Environ. Sci. Technol., 52, 2575–2585, https://doi.org/10.1021/acs.est.7b06126, 2018.

Song, J., Li, M., Zou, C., Cao, T., Fan, X., Jiang, B., Yu, Z., Jia, W., and Peng, P.: Molecular characterization of nitrogen-containing compounds in humic-like substances emitted from biomass burning and coal combustion, Environ. Sci. Technol., 56, 119–130, https://doi.org/10.1021/acs.est.1c04451, 2022.

Stein, A. F., Draxler, R. R., Rolph, G. D., Stunder, B. J. B., Cohen, M. D., and Ngan, F.: Noaa's hysplit atmospheric transport and dispersion modeling system, Bull. Am. Meteorol. Soc., 96, 2059–2077, https://doi.org/10.1175/BAMS-D-14-00110.1, 2015.

Su, S., Xie, Q., Lang, Y., Cao, D., Xu, Y., Chen, J., Chen, S., Hu, W., Qi, Y., Pan, X., Sun, Y., Wang, Z., Liu, C. Q., Jiang, G., and Fu, P.: High molecular diversity of organic nitrogen in urban snow in north China, Environ. Sci. Technol., 55, 4344–4356, https://doi.org/10.1021/acs.est.0c06851, 2021.

Surratt, J. D., Gomez-Gonzalez, Y., Chan, A. W. H., Vermeylen, R., Shahgholi, M., Kleindienst, T. E., Edney, E. O., Offenberg, J. H., Lewandowski, M., Jaoui, M., Maenhaut, W., Claeys, M., Flagan, R. C., and Seinfeld, J. H.: Organosulfate formation in biogenic secondary organic aerosol, J. Phys. Chem. A, 112, 8345–8378, https://doi.org/10.1021/jp802310p, 2008.

Surratt, J. D., Chan, A. W. H., Eddingsaas, N. C., Chan, M. N., Loza, C. L., Kwan, A. J., Hersey, S. P., Flagan, R. C., Wennberg, P. O., and Seinfeld, J. H.: Reactive intermediates revealed in secondary organic aerosol formation from isoprene, Proc. Natl. Acad. Sci. U.S.A., 107, 6640–6645, https://doi.org/10.1073/pnas.0911114107, 2010.

Turpin, B. J. and Lim, H.-J.: Species contributions to $pm_{2.5}$ mass concentrations: Revisiting common assumptions for estimating organic mass, Aerosol Sci. Technol., 35, 602–610, https://doi.org/10.1080/02786820119445, 2001.

Vettikkat, L., Miettinen, P., Buchholz, A., Rantala, P., Yu, H., Schallhart, S., Petäjä, T., Seco, R., Männistö, E., Kulmala, M., Tuittila, E.-S., Guenther, A. B., and Schobesberger, S.: High emission rates and strong temperature response make boreal wetlands a large source of isoprene and terpenes, Atmos. Chem. Phys., 23, 2683–2698, https://doi.org/10.5194/acp-23-2683-2023, 2023.

Vodička, P., Kawamura, K., Deshmukh, D. K., Pokorná, P., Schwarz, J., and Ždímal, V.: Anthropogenic and biogenic tracers in fine aerosol based on seasonal distributions of dicarboxylic acids, sugars and related compounds at a rural background site in Central Europe, Atmos. Environ., 299, https://doi.org/10.1016/j.atmosenv.2023.119619, 2023.

Wang, F., Yu, H., Wang, Z., Liang, W., Shi, G., Gao, J., Li, M., and Feng, Y.: Review of online source apportionment research based on observation for ambient particulate matter, Sci Total Environ, 762, 144095, https://doi.org/10.1016/j.scitotenv.2020.144095, 2021a.

Wang, L., Chen, S., Zhu, W., Ren, H., Zhang, L., and Zhu, L.: Spatiotemporal variations of extreme precipitation and its potential driving factors in China's North-South Transition Zone during 1960–2017, Atmos. Res., 252, https://doi.org/10.1016/j.atmosres.2020.105429, 2021b.

Wang, J., Zhang, B., and Yao, Y.: The spatial pattern of the upper limit of montane deciduous broad-leaved forests and its geographical interpretation in the east monsoon realm of China, Forests, 12, https://doi.org/10.3390/f12091225, 2021c.

Wang, J., Ye, J., Zhang, Q., Zhao, J., Wu, Y., Li, J., Liu, D., Li, W., Zhang, Y., Wu, C., Xie, C., Qin, Y., Lei, Y., Huang, X., Guo, J., Liu, P., Fu, P., Li, Y., Lee, H. C., Choi, H., Zhang, J., Liao, H., Chen, M., Sun, Y., Ge, X., Martin, S. T., and Jacob, D. J.: Aqueous production of secondary organic aerosol from fossil-fuel emissions in winter Beijing haze, Proc. Natl. Acad. Sci. U.S.A., 118, https://doi.org/10.1073/pnas.2022179118, 2021d.

Wang, S., Liu, T., Jang, J., Abbatt, J. P. D., and Chan, A. W. H.: Heterogeneous interactions between SO_2 and organic peroxides in submicron aerosol, Atmos. Chem. Phys., 21, 6647–6661, https://doi.org/10.5194/acp-21-6647-2021, 2021e.

Wang, Y., Zhao, Y., Wang, Y., Yu, J.-Z., Shao, J., Liu, P., Zhu, W., Cheng, Z., Li, Z., Yan, N., and Xiao, H.: Organosulfates in atmospheric aerosols in Shanghai, China: Seasonal and interannual variability, origin, and formation mechanisms, Atmos. Chem. Phys., 21, 2959–2980, https://doi.org/10.5194/acp-21-2959-2021, 2021f.

Wang, Y., Hu, M., Wang, Y.-C., Li, X., Fang, X., Tang, R., Lu, S., Wu, Y., Guo, S., Wu, Z., Hallquist, M., and Yu, J. Z.: Comparative study of particulate organosulfates in contrasting atmospheric environments: Field evidence for the

significant influence of anthropogenic sulfate and NOx, Environ. Sci. Technol. Lett., 7, 787–794, https://doi.org/10.1021/acs.estlett.0c00550, 2020.

Wang, L., Lun, X., Wang, Q., and Wu, J.: Biogenic volatile organic compounds emissions, atmospheric chemistry, and environmental implications: a review, Environ. Chem. Lett., 22, 3033–3058, https://doi.org/10.1007/s10311-024-01785-5, 2024a.

Wang, K., Zhang, Y., Tong, H., Han, J., Fu, P., Huang, R.-J., Zhang, H., and Hoffmann, T.: Molecular-level insights into the relationship between volatility of organic aerosol constituents and $PM_{2.5}$ air pollution levels: A study with ultrahigh-resolution mass spectrometry, Environ Sci Technol, 58, 7947–7957, https://doi.org/10.1021/acs.est.3c10662, 2024b.

Wang, X., Hayeck, N., Brüggemann, M., Yao, L., Chen, H., Zhang, C., Emmelin, C., Chen, J., George, C., and Wang, L.: Chemical characteristics of organic aerosols in Shanghai: A study by ultrahigh-performance liquid chromatography coupled with orbitrap mass spectrometry, J. Geophys. Res.-Atmos., 122, 11,703-711,722, https://doi.org/10.1002/2017jd026930, 2017a.

Wang, Y., Hu, M., Lin, P., Guo, Q., Wu, Z., Li, M., Zeng, L., Song, Y., Zeng, L., Wu, Y., Guo, S., Huang, X., and He, L.: Molecular characterization of nitrogen-containing organic compounds in humic-like substances emitted from straw residue burning, Environ. Sci. Technol., 51, 5951–5961, https://doi.org/10.1021/acs.est.7b00248, 2017b.

Wei, J., Li, Z., Wang, J., Li, C., Gupta, P., and Cribb, M.: Ground-level gaseous pollutants (NO_2, SO_2, and CO) in China: daily seamless mapping and spatiotemporal variations, Atmos. Chem. Phys., 23, 1511–1532, https://doi.org/10.5194/acp-23-1511-2023, 2023.

Wu, K., Yang, X. Y., Chen, D., Gu, S., Lu, Y. Q., Jiang, Q., Wang, K., Ou, Y. H., Qian, Y., Shao, P., and Lu, S. H.: Estimation of biogenic VOC emissions and their corresponding impact on ozone and secondary organic aerosol formation in China, Atmos. Res., 231, https://doi.org/10.1016/j.atmosres.2019.104656, 2020.

Xu, L., Kollman, M. S., Song, C., Shilling, J. E., and Ng, N. L.: Effects of NO_x on the volatility of secondary organic aerosol from isoprene photooxidation, Environ. Sci. Technol., 48, 2253–2262, https://doi.org/10.1021/es404842g, 2014.

Xu, L., Guo, H. Y., Boyd, C. M., Klein, M., Bougiatioti, A., Cerully, K. M., Hite, J. R., Isaacman-VanWertz, G., Kreisberg, N. M., Knote, C., Olson, K., Koss, A., Goldstein, A. H., Hering, S. V, de Gouw, J., Baumann, K., Lee, S. H., Nenes, A., Weber, R. J., and Ng, N. L.: Effects of anthropogenic emissions on aerosol formation from isoprene and monoterpenes in the southeastern United States, Proc. Natl. Acad. Sci. U.S.A., 112, 37–42, https://doi.org/10.1073/pnas.1417609112, 2015.

Xu, L., Du, L., Tsona, N. T., and Ge, M.: Anthropogenic effects on biogenic secondary organic aerosol formation, Adv. Atmos. Sci., 38, 1053–1084, https://doi.org/10.1007/s00376-020-0284-3, 2021a.

Xu, L., Yang, Z., Tsona, N. T., Wang, X., George, C., and Du, L.: Anthropogenic-biogenic interactions at night: Enhanced formation of secondary aerosols and particulate nitrogen- and sulfur-containing organics from beta-pinene oxidation, Environ. Sci. Technol., 55, 7794–7807, https://doi.org/10.1021/acs.est.0c07879, 2021b.

Xu, L., Tsona, N. T., and Du, L.: Relative humidity changes the role of SO_2 in biogenic secondary organic aerosol formation, J. Phys. Chem. Lett., 12, 7365–7372, https://doi.org/10.1021/acs.jpclett.1c01550, 2021c.

Xu, Y., Chen, Y. G., Gao, J. S., Zhu, S. Q., Ying, Q., Hu, J. L., Wang, P., Feng, L. G., Kang, H. B., and Wang, D. X.: Contribution of biogenic sources to secondary organic aerosol in the summertime in Shaanxi, China, Chemosphere, 254, https://doi.org/10.1016/j.chemosphere.2020.126815, 2020.

Yan, C., Nie, W., Vogel, A. L., Dada, L., Lehtipalo, K., Stolzenburg, D., Wagner, R., Rissanen, M. P., Xiao, M., Ahonen, L., Fischer, L., Rose, C., Bianchi, F., Gordon, H., Simon, M., Heinritzi, M., Garmash, O., Roldin, P., Dias, A., Ye, P., Hofbauer, V., et al.: Size-dependent influence of NO_x on the growth rates of organic aerosol particles, Sci. Adv., 6, eaay4945, https://doi.org/doi:10.1126/sciadv.aay4945, 2020.

Yang, L., Liu, Z.-L., Li, J., and Dyer, R. J.: Genetic structure of Pinus henryi and Pinus tabuliformis: Natural landscapes as significant barriers to gene flow among populations, Biochem. Syst. Ecol., 61, 124–132, https://doi.org/10.1016/j.bse.2015.06.003, 2015.

860 Yao, Y., Hu, Y., Kou, Z., and Zhang, B.: Spatial patterns of Pinus tabulaeformis and Pinus massoniana forests in Qinling-Daba Mountains and the boundary of subtropical and warm temperate zones, J. Geogr. Sci., 30, 1523–1533, https://doi.org/10.1007/s11442-020-1797-5, 2020.

Yassine, M. M., Harir, M., Dabek-Zlotorzynska, E., and Schmitt-Kopplin, P.: Structural characterization of organic aerosol using Fourier transform ion cyclotron resonance mass spectrometry: aromaticity equivalent approach, Rapid Commun.

865 Mass Spectrom., 28, 2445–2454, https://doi.org/10.1002/rcm.7038, 2014.

Zhang, J., Zhu, L., Li, G., Zhao, F., and Qin, J.: Distribution patterns of SOC/TN content and their relationship with topography, vegetation and climatic factors in China's north-south transitional zone, J. Geogr. Sci., 32, 645–662, https://doi.org/10.1007/s11442-022-1965-x, 2022.

Zhang, M., Cai, D., Lin, J., Liu, Z., Li, M., Wang, Y., and Chen, J.: Molecular characterization of atmospheric organic aerosols

870 in typical megacities in China, NPJ Clim. Atmos. Sci., 7, https://doi.org/10.1038/s41612-024-00784-1, 2024.

Zhang, T., Cao, J. J., Tie, X. X., Shen, Z. X., Liu, S. X., Ding, H., Han, Y. M., Wang, G. H., Ho, K. F., Qiang, J., and Li, W. T.: Water-soluble ions in atmospheric aerosols measured in Xi'an, China: Seasonal variations and sources, Atmos. Res., 102, 110–119, https://doi.org/10.1016/j.atmosres.2011.06.014, 2011.

Zhao, D., Schmitt, S. H., Wang, M., Acir, I.-H., Tillmann, R., Tan, Z., Novelli, A., Fuchs, H., Pullinen, I., Wegener, R., Rohrer,

875 F., Wildt, J., Kiendler-Scharr, A., Wahner, A., and Mentel, T. F.: Effects of NO_x and SO_2 on the secondary organic aerosol formation from photooxidation of alpha-pinene and limonene, Atmos. Chem. Phys., 18, 1611–1628, https://doi.org/10.5194/acp-18-1611-2018, 2018.

Zhao, D. F., Buchholz, A., Kortner, B., Schlag, P., Rubach, F., Fuchs, H., Kiendler-Scharr, A., Tillmann, R., Wahner, A., Watne, A. K., Hallquist, M., Flores, J. M., Rudich, Y., Kristensen, K., Hansen, A. M. K., Glasius, M., Kourtchev, I.,

880 Kalberer, M., and Mentel, T. F.: Cloud condensation nuclei activity, droplet growth kinetics, and hygroscopicity of biogenic and anthropogenic secondary organic aerosol (SOA), Atmos. Chem. Phys., 16, 1105–1121, https://doi.org/10.5194/acp-16-1105-2016, 2016.

Zhao, S. Y., Tie, X. X., Cao, J. J., and Zhang, Q.: Impacts of mountains on black carbon aerosol under different synoptic meteorology conditions in the Guanzhong region, China, Atmos. Res., 164, 286–296,

885 https://doi.org/10.1016/j.atmosres.2015.05.016, 2015.

Zhao, X., Ma, C., and Xiao, L.: The vegetation history of Qinling Mountains, China, Quat. Int., 325, 55–62, https://doi.org/10.1016/j.quaint.2013.10.054, 2014.

Zhong, S., Chen, S., Deng, J., Fan, Y., Zhang, Q., Xie, Q., Qi, Y., Hu, W., Wu, L., Li, X., Pavuluri, C. M., Zhu, J., Wang, X., Liu, D., Pan, X., Sun, Y., Wang, Z., Xu, Y., Tong, H., Su, H., Cheng, Y., Kawamura, K., and Fu, P.: Impact of biogenic

890 secondary organic aerosol (SOA) loading on the molecular composition of wintertime PM2.5 in urban Tianjin: an insight from Fourier transform ion cyclotron resonance mass spectrometry, Atmos. Chem. Phys., 23, 2061–2077, https://doi.org/10.5194/acp-23-2061-2023, 2023.

Zhu, M., Jiang, B., Li, S., Yu, Q., Yu, X., Zhang, Y., Bi, X., Yu, J., George, C., Yu, Z., and Wang, X.: Organosulfur compounds formed from heterogeneous reaction between SO_2 and particulate-bound unsaturated fatty acids in ambient air, Environ.

895 Sci. Technol. Lett., 6, 318–322, https://doi.org/10.1021/acs.estlett.9b00218, 2019.

Zielinski, A. T., Kourtchev, I., Bortolini, C., Fuller, S. J., Giorio, C., Popoola, O. A. M., Bogialli, S., Tapparo, A., Jones, R. L., and Kalberer, M.: A new processing scheme for ultra-high resolution direct infusion mass spectrometry data, Atmos. Environ., 178, 129–139, https://doi.org/10.1016/j.atmosenv.2018.01.034, 2018.

Supplement of

Influence of anthropogenic pollution on the molecular composition of organic aerosols over a forest site in the Qinling Mountains region of central China

Xin Zhang[1,2], Lijuan Li[2], Jianjun Li[2], Yue Lin[2], Yan Cheng[1], Rui Wang[2], Shuyan Xing[2], Chongshu Zhu[2], Junji Cao[2,3,*], and Yuemei Han[2,4,*]

[1]School of Human Settlements and Civil Engineering, Xi'an Jiaotong University, Xi'an 710049, China

[2]Key Laboratory of Aerosol Chemistry and Physics, State Key Laboratory of Loess and Quaternary Geology, Institute of Earth Environment, Chinese Academy of Sciences, Xi'an 710061, China

[3]Institute of Atmospheric Physics, Chinese Academy of Sciences, Beijing 100029, China

[4]National Observation and Research Station of Regional Ecological Environment Change and Comprehensive Management in the Guanzhong Plain, Xi'an 710061, China

Correspondence to: Yuemei Han (yuemei.han@ieecas.cn), Junji Cao (jjcao@mail.iap.ac.cn).

Table S1. Lists of organosulfate (including nitrooxy-organosulfate) compounds derived from biogenic sources and detected in negative ionization mode.

Precursor	Neutral mass	Compound	Reference	Precursor	Neutral mass	Compound	Reference
Glyoxal	140.1152	$C_2H_4O_5S$	1, 2	**Isoprene**	142.1310	$C_2H_6O_5S$	5
	156.1146	$C_2H_4O_6S$	1, 2		154.1417	$C_3H_6O_5S$	1, 6, 7
	200.1241	$C_3H_4O_8S$	3		170.1411	$C_3H_6O_6S$	1, 6, 7
	218.1393	$C_3H_6O_9S$	3		186.1405	$C_3H_6O_7S$	5
	216.1665	$C_4H_8O_8S$	3		172.1570	$C_3H_8O_6S$	5
	230.1931	$C_5H_{10}O_8S$	4		182.1518	$C_4H_6O_6S$	5, 6
Monoterpenes	228.1772	$C_5H_8O_8S$	1, 8		168.1683	$C_4H_8O_5S$	5, 6
	224.2316	$C_7H_{12}O_6S$	1, 8		184.1677	$C_4H_8O_6S$	6,7
	240.2310	$C_7H_{12}O_7S$	1, 8		200.1671	$C_4H_8O_7S$	1, 6, 7
	238.2582	$C_8H_{14}O_6S$	1, 8		166.1955	$C_5H_{10}O_4S$	8, 9
	254.2576	$C_8H_{14}O_7S$	1, 6		182.1949	$C_5H_{10}O_5S$	8, 10
	250.2689	$C_9H_{14}O_6S$	1, 12		198.1943	$C_5H_{10}O_6S$	8, 11
	284.2835	$C_9H_{16}O_8S$	1, 8		214.1937	$C_5H_{10}O_7S$	1, 8
	248.2960	$C_{10}H_{16}O_5S$	1, 8		200.2102	$C_5H_{12}O_6S$	8, 10
	264.2954	$C_{10}H_{16}O_6S$	1, 12		216.2096	$C_5H_{12}O_7S$	1, 6
	330.3089	$C_{10}H_{18}O_{10}S$	1		232.2090	$C_5H_{12}O_8S$	5
	250.3119	$C_{10}H_{18}O_5S$	1, 8		164.1796	$C_5H_8O_4S$	9
	282.3107	$C_{10}H_{18}O_7S$	1, 8		180.1790	$C_5H_8O_5S$	10
	284.3266	$C_{10}H_{20}O_7S$	1, 8		212.1778	$C_5H_8O_7S$	1, 8
	297.2823	$C_9H_{15}NO_8S$	1, 12		244.1766	$C_5H_8O_9S$	5, 8
	313.2817	$C_9H_{15}NO_9S$	1, 12		228.2203	$C_6H_{12}O_7S$	8, 11
	331.2970	$C_9H_{17}NO_{10}S$	1, 12		222.2157	$C_7H_{10}O_6S$	8
	356.3064	$C_{10}H_{16}N_2O_{10}S$	1, 12		238.2151	$C_7H_{10}O_7S$	8
	343.3077	$C_{10}H_{17}NO_{10}S$	1, 12		202.2276	$C_8H_{10}O_4S$	10
	295.3095	$C_{10}H_{17}NO_7S$	1, 12		236.2423	$C_8H_{12}O_6S$	1, 6, 8
	311.3089	$C_{10}H_{17}NO_8S$	1, 12		252.2417	$C_8H_{12}O_7S$	6, 8
	374.3217	$C_{10}H_{18}N_2O_{11}S$	1, 12		302.2558	$C_8H_{14}O_{10}S$	1, 8
	329.3242	$C_{10}H_{19}NO_9S$	1, 12		270.2570	$C_8H_{14}O_8S$	6, 8
	390.3211	$C_{10}H_{18}N_2O_{12}S$	1, 12		332.3248	$C_{10}H_{20}O_{10}S$	1
Sesquiterpenes	334.3853	$C_{14}H_{22}O_7S$	13		334.3407	$C_{10}H_{22}O_{10}S$	1
	350.3847	$C_{14}H_{22}O_8S$	8, 13		322.3315	$C_{12}H_{18}O_8S$	6
	304.4024	$C_{14}H_{24}O_5S$	12, 13		360.2934	$C_{13}H_{12}O_{10}S$	10
	320.4018	$C_{14}H_{24}O_6S$	8, 13		351.2023	$C_5H_9N_3O_{13}S$	5
	352.4006	$C_{14}H_{24}O_8S$	8, 13		275.1907	$C_5H_9NO_{10}S$	5
	348.4119	$C_{15}H_{24}O_7S$	8, 13		229.2083	$C_5H_{11}NO_7S$	12
	364.4113	$C_{15}H_{24}O_8S$	8, 13		245.2077	$C_5H_{11}NO_8S$	1, 5, 12
	318.4289	$C_{15}H_{26}O_5S$	8, 13		261.2071	$C_5H_{11}NO_9S$	1, 12
	334.4283	$C_{15}H_{26}O_6S$	13		306.2047	$C_5H_{10}N_2O_{11}S$	1, 5, 12
	350.4277	$C_{15}H_{26}O_7S$	8, 13				
	364.4543	$C_{16}H_{28}O_7S$	8, 13				
	380.4537	$C_{16}H_{28}O_8S$	8, 13				
	383.4146	$C_{14}H_{25}NO_9S$	12, 13				
	363.4265	$C_{15}H_{25}NO_7S$	12, 13				

The references are listed as follows: [1] Surratt et al., 2008; [2] Lim et al., 2010; [3] Perri et al., 2010; [4] Shalamzari et al., 2016; [5] Bryant et al., 2023; [6] Schindelka et al., 2013; [7] Safi Shalamzari et al., 2013; [8] Wang et al., 2016; [9] Szmigielski, 2016; [10] Riva et al., 2016a; [11] Riva et al., 2016b; [12] Cai et al., 2020; [13] Chan et al., 2011.

Table S2. Lists of organosulfate (including nitrooxy-organosulfate) compounds derived from anthropogenic sources and detected in negative ionization mode.

Precursor	Neutral mass	Compound	Reference	Precursor	Neutral mass	Compound	Reference
Long-chain alkanes	210.2481	$C_7H_{14}O_5S$	11, 12	**Naphthalene**	174.1744	$C_6H_6O_4S$	12, 14
	196.2645	$C_7H_{16}O_4S$	8, 11		186.1851	$C_7H_6O_4S$	12, 14
	210.2911	$C_8H_{18}O_4S$	8, 11		202.1845	$C_7H_6O_5S$	8, 14
	238.3012	$C_9H_{18}O_5S$	8, 11		188.2010	$C_7H_8O_4S$	8, 14
	270.3000	$C_9H_{18}O_7S$	8, 11		230.1946	$C_8H_6O_6S$	8, 14
	286.2994	$C_9H_{18}O_8S$	11, 12		200.2117	$C_8H_8O_4S$	8, 14
	256.3165	$C_9H_{20}O_6S$	11, 12		216.2111	$C_8H_8O_5S$	8, 14
	296.2942	$C_{10}H_{16}O_8S$	11, 12		230.2377	$C_9H_{10}O_5S$	8, 14
	312.2936	$C_{10}H_{16}O_9S$	8, 11		216.2542	$C_9H_{12}O_4S$	12, 14
	252.3278	$C_{10}H_{20}O_5S$	8, 11		232.2536	$C_9H_{12}O_5S$	15
	268.3272	$C_{10}H_{20}O_6S$	8, 11		228.2218	$C_9H_8O_5S$	14
	300.3260	$C_{10}H_{20}O_8S$	11, 12		258.2478	$C_{10}H_{10}O_6S$	8, 14
	308.3480	$C_{12}H_{20}O_7S$	11, 12		274.2472	$C_{10}H_{10}O_7S$	8, 14
	280.3810	$C_{12}H_{24}O_5S$	8, 11		276.2631	$C_{10}H_{12}O_7S$	8, 14
	266.3974	$C_{12}H_{26}O_4S$	8, 11		288.2738	$C_{11}H_{12}O_7S$	8, 14
Diesel	138.1423	$C_3H_6O_4S$	16		290.2897	$C_{11}H_{14}O_7S$	14
	152.1689	$C_4H_8O_4S$	16		219.1720	$C_6H_5NO_6S$	14
	196.1784	$C_5H_8O_6S$	16		321.2606	$C_{10}H_{11}NO_9S$	12, 14
Cyclohexene	166.1524	$C_4H_6O_5S$	17				
	210.2050	$C_6H_{10}O_6S$	17				

The references are listed as follows: [8] Wang et al., 2016; [11] Riva et al., 2016b; [12] Cai et al., 2020; [14] Riva et al., 2015a; [15] Wang et al., 2019; [16] Blair et al., 2017; [17] Liu et al., 2017.

Table S3. Lists of CHO tracer species derived from biogenic/anthropogenic sources and detected in negative ionization mode.

Source	Natural mass	Compound	Potential identity/precursor	Reference
Biogenic	118.0880	$C_4H_6O_4$	Succinic acid	18
	172.1785	$C_8H_{12}O_4$	Terpenylic acid/α-pinene	19
	188.1779	$C_8H_{12}O_5$	Terpenoic acid/α-pinene; β-pinene	20
	204.1773	$C_8H_{12}O_6$	3-methyl-1,2,3-butanetricarboxylic acid/α-pinene	21
	174.1944	$C_8H_{14}O_4$	Suberic acid/unsaturated fatty acids	22
	186.2051	$C_9H_{14}O_4$	Pinic acid/α-pinene; β-pinene	23
	188.2209	$C_9H_{16}O_4$	Azelaic acid/unsaturated fatty acids	22
	232.2304	$C_{10}H_{16}O_6$	Diaterpenylic acid acetate/α-pinene	19
	272.4235	$C_{16}H_{32}O_3$	3-hydroxyhexadecanoic acid/Gram-negative Bacteria	24
	294.3859	$C_{17}H_{26}O_4$	Unknown/β-pinene	25
	300.4766	$C_{18}H_{36}O_3$	3-hydroxyoctadecanoic acid/Gram-negative Bacteria	24
Anthropogenic	90.0779	$C_3H_6O_3$	Unknown/Bonfire	26
	146.1412	$C_6H_{10}O_4$	Adipic acid/Cyclohexene	27, 28
	160.1678	$C_7H_{12}O_4$	Pimelic acid/Cyclohexene	27
	122.1213	$C_7H_6O_2$	Benzoic acid/PAHs	28, 29
	166.1308	$C_8H_6O_4$	Phthalic acid/PAHs	29
	270.4076	$C_{16}H_{30}O_3$	2-Oxo-tetredecanoic acid/Cooking emissions; oils	30

The references are listed as follows: [18] Xu and Zhang, 2012; [19] Claeys et al., 2009; [20] Gómez-González et al., 2012; [21] Szmigielski et al., 2007; [22] Mochida et al., 2003; [23] Ma et al., 2007; [24] Watson and Chow, 2018; [25] Slade et al., 2019; [26] Priestley et al., 2018; [27] Hansen et al., 2014; [28] Riva et al., 2015b; [29] Williams et al., 2010; [30] Qi et al., 2019.

Table S4. Lists of CHO tracer species derived from biogenic sources and detected in positive ionization mode.

Natural mass	Compound	Potential precursor	Reference
128.1690	$C_7H_{12}O_2$	limonene	31
140.1797	$C_8H_{12}O_2$	β-pinene, limonene	31, 32
156.1791	$C_8H_{12}O_3$	α,β-pinene, limonene, sabinene	31, 32, 33
158.1950	$C_8H_{14}O_3$	α-pinene, limonene	31, 33
172.1785	$C_8H_{12}O_4$	α,β-pinene, limonene, Δ3-carene, sabinene	34, 35
154.2063	$C_9H_{14}O_2$	β-pinene, limonene, sabinene	31, 32
156.2221	$C_9H_{16}O_2$	limonene	31
168.1898	$C_9H_{12}O_3$	limonene	31
170.2057	$C_9H_{14}O_3$	α,β-pinene, limonene, Δ3-carene, sabinene	31, 33, 34
184.1892	$C_9H_{12}O_4$	α-pinene, limonene	31, 33
186.2051	$C_9H_{14}O_4$	α,β-pinene, limonene, Δ3-carene, sabinene	34, 36, 37
188.2209	$C_9H_{16}O_4$	α,β-pinene, limonene	34, 38
168.2328	$C_{10}H_{16}O_2$	limonene	31
180.2005	$C_{10}H_{12}O_3$	limonene	31
182.2164	$C_{10}H_{14}O_3$	limonene	31
184.2322	$C_{10}H_{16}O_3$	α,β-pinene, limonene, Δ3-carene	34, 35
186.2481	$C_{10}H_{18}O_3$	α-pinene, limonene	31, 33
198.2158	$C_{10}H_{14}O_4$	α-pinene, limonene	31, 33
200.2316	$C_{10}H_{16}O_4$	α,β-pinene, limonene, sabinene	31, 33
198.2588	$C_{11}H_{18}O_3$	limonene	31
212.2423	$C_{11}H_{16}O_4$	α-pinene, limonene	31, 33
214.2582	$C_{11}H_{18}O_4$	α-pinene, limonene	31, 33
222.2372	$C_{12}H_{14}O_4$	limonene	31
226.2689	$C_{12}H_{18}O_4$	α-pinene, limonene	31, 33
240.2955	$C_{13}H_{20}O_4$	α-pinene, limonene	31, 33
254.3221	$C_{14}H_{22}O_4$	limonene	31
268.3487	$C_{15}H_{24}O_4$	α-pinene, limonene	31, 33

The references are listed as follows: [31] Walser et al., 2008; [32] Yu et al., 1999; [33] Putman et al., 2012; [34] Yasmeen et al., 2011; [35] Kourtchev et al., 2014; [36] Glasius et al., 2000; [37] Camredon et al., 2010; [38] Kourtchev et al., 2015.

Table S5. Lists of CHN tracer species derived from anthropogenic sources and detected in positive ionization mode.[a]

Natural mass	Compound	Natural mass	Compound	Natural mass	Compound
98.1463	$C_5H_{10}N_2$	130.1466	$C_8H_6N_2$	155.1959	$C_{11}H_9N$
100.1622	$C_5H_{12}N_2$	145.1613	$C_8H_7N_3$	183.2093	$C_{11}H_9N_3$
94.1145	$C_5H_6N_2$	132.1625	$C_8H_8N_2$	169.2224	$C_{12}H_{11}N$
96.1304	$C_5H_8N_2$	147.1772	$C_8H_9N_3$	197.2358	$C_{12}H_{11}N_3$
111.1451	$C_5H_9N_3$	146.1891	$C_9H_{10}N_2$	184.2371	$C_{12}H_{12}N_2$
110.1570	$C_6H_{10}N_2$	161.2037	$C_9H_{11}N_3$	199.2517	$C_{12}H_{13}N_3$
112.1729	$C_6H_{12}N_2$	148.2050	$C_9H_{12}N_2$	186.2530	$C_{12}H_{14}N_2$
114.1888	$C_6H_{14}N_2$	157.1720	$C_9H_7N_3$	201.2676	$C_{12}H_{15}N_3$
119.1240	$C_6H_5N_3$	144.1732	$C_9H_8N_2$	203.2835	$C_{12}H_{17}N_3$
108.1411	$C_6H_8N_2$	159.1879	$C_9H_9N_3$	182.2212	$C_{12}H_{10}N_2$
123.1558	$C_6H_9N_3$	158.1998	$C_{10}H_{10}N_2$	180.2053	$C_{12}H_8N_2$
122.1677	$C_7H_{10}N_2$	173.2144	$C_{10}H_{11}N_3$	194.2319	$C_{13}H_{10}N_2$
137.1823	$C_7H_{11}N_3$	160.2157	$C_{10}H_{12}N_2$	181.2331	$C_{13}H_{11}N$
124.1836	$C_7H_{12}N_2$	175.2303	$C_{10}H_{13}N_3$	183.2490	$C_{13}H_{13}N$
126.1995	$C_7H_{14}N_2$	169.1827	$C_{10}H_7N_3$	211.2624	$C_{13}H_{13}N_3$
128.2153	$C_7H_{16}N_2$	156.1839	$C_{10}H_8N_2$	200.2795	$C_{13}H_{16}N_2$
118.1359	$C_7H_6N_2$	171.1986	$C_{10}H_9N_3$	217.3101	$C_{13}H_{19}N_3$
133.1506	$C_7H_7N_3$	170.2105	$C_{11}H_{10}N_2$	196.2478	$C_{13}H_{12}N_2$
120.1518	$C_7H_8N_2$	185.2251	$C_{11}H_{11}N_3$	179.2173	$C_{13}H_9N$
148.1652	$C_7H_8N_4$	172.2264	$C_{11}H_{12}N_2$	223.2731	$C_{14}H_{13}N_3$
135.1665	$C_7H_9N_3$	187.2410	$C_{11}H_{13}N_3$	208.2585	$C_{14}H_{12}N_2$
162.1918	$C_8H_{10}N_4$	189.2569	$C_{11}H_{15}N_3$	237.2997	$C_{15}H_{15}N_3$
149.1930	$C_8H_{11}N_3$	168.1946	$C_{11}H_8N_2$	205.2545	$C_{15}H_{11}N$

[a] These CHN tracer species are mainly derived from anthropogenic sources such as combustion of fossil fuels and biomass according to the following literature: (Jiang et al., 2022; Laskin et al., 2009; Lin et al., 2012; Mao et al., 2022; Song et al., 2022; Wang et al., 2017).
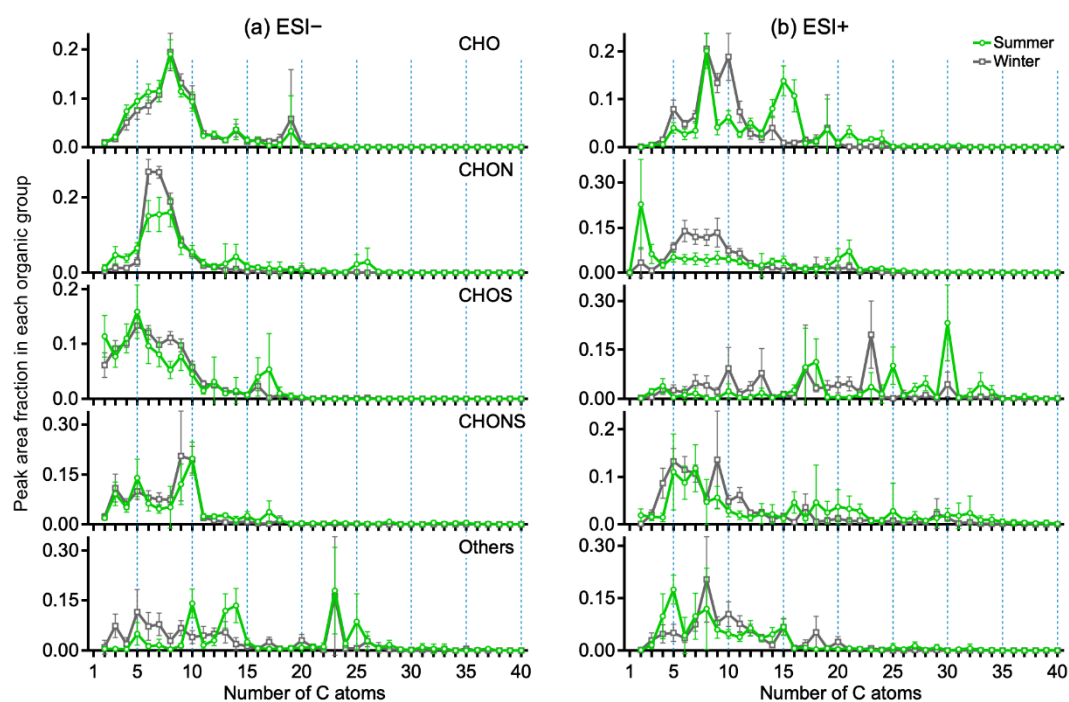
Figure S1. Peak area fractions of organic subgroups sorted by the carbon atoms number in molecular formulas assigned in (a) negative and (b) positive ESI modes for summer and winter samples. The error bars represent 1σ standard deviations for all samples in each season.
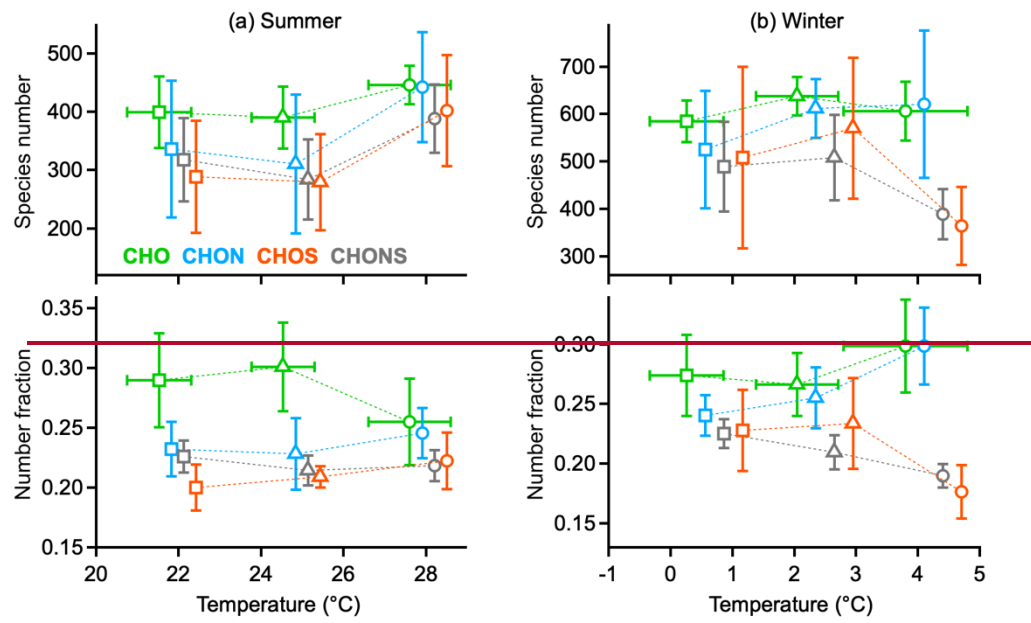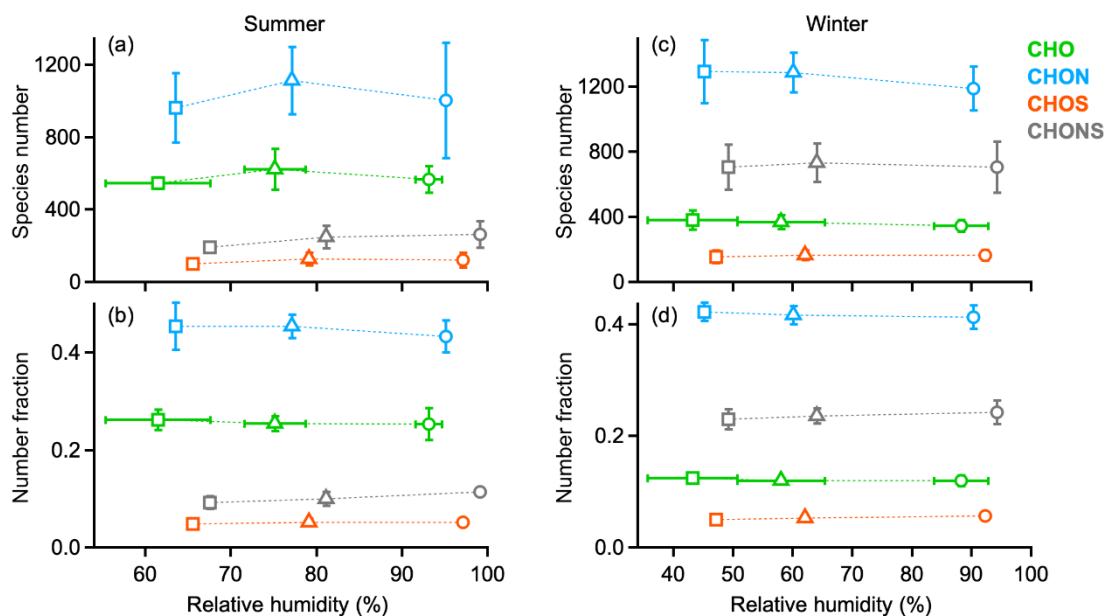
Figure S2.

Figure S2. Species number and the relative fractions of organic molecular subgroups in positive ESI mode under varied relative humidity conditions in (a, b) summer and (c, d) winter periods. The symbols of each type shared the same RH values (that is, 62 ± 6%, 75 ± 4%, 93 ± 2% in summer and 43 ± 8%, 58 ± 7%, 88 ± 5% in winter) but were offset horizontally for a clear vision. The horizontal error bars in the CHO species represent 1σ standard deviations of RH values. The vertical error bars represent 1σ standard deviations for all the samples in each RH condition.
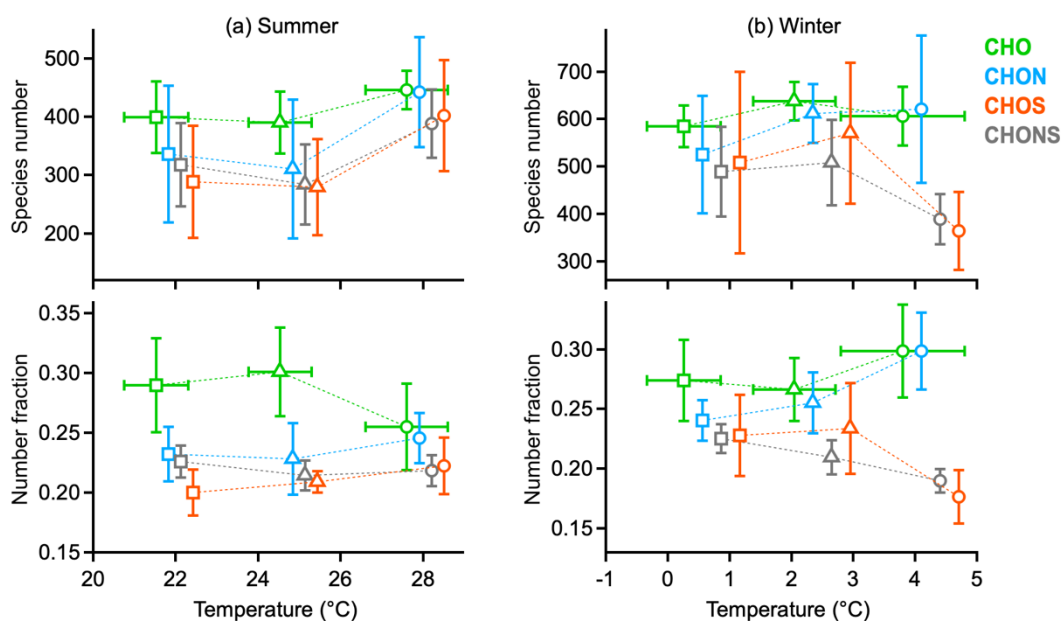
Figure S3. Species number and the relative fractions of organic molecular subgroups in negative ESI mode under varied temperature conditions in (a, ~~b~~) summer and (~~c,~~ ~~d~~b) winter periods. The symbols of each type shared the same temperature values (that is, 21.5 ± 0.8, 24.5 ± 0.8, 27.6 ± 1.0 °C in summer and 0.3 ± 0.6, 2.0 ± 0.7, 3.8 ± 1.0 °C in winter) but were offset horizontally for a clear vision. The horizontal error bars in the CHO species represent 1σ standard deviations of temperature values. The vertical error bars represent 1σ standard deviations for all the samples under each temperature condition.
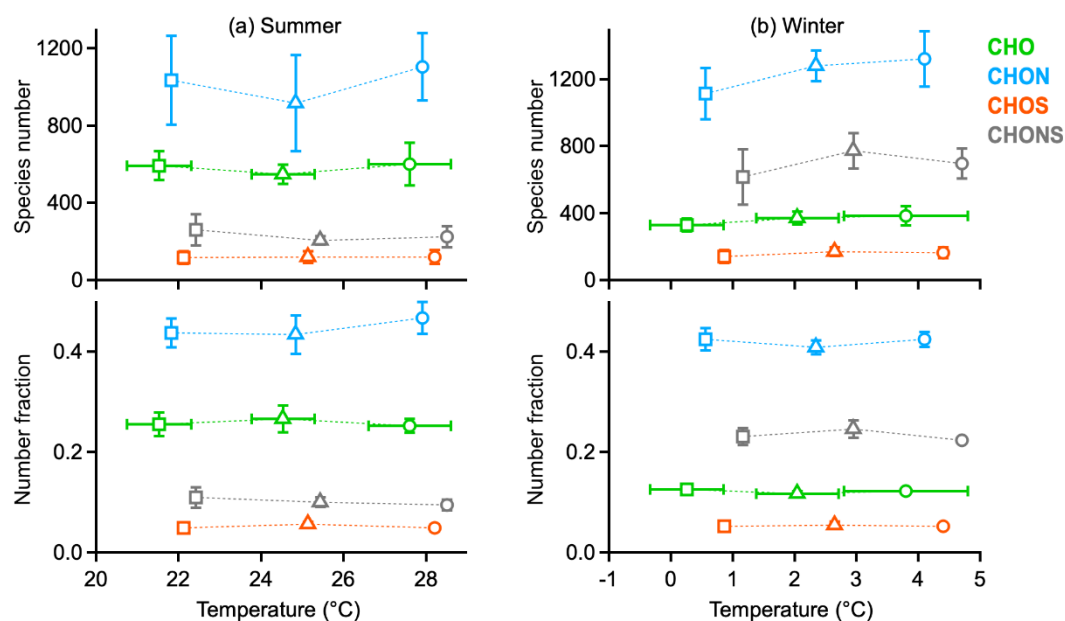
Figure S4. Species number and the relative fractions of organic molecular subgroups in positive ESI mode under varied temperature conditions in (a) summer and (b) winter periods. The symbols of each type shared the same temperature values (that is, 21.5 ± 0.8, 24.5 ± 0.8, 27.6 ± 1.0 °C in summer and 0.3 ± 0.6, 2.0 ± 0.7, 3.8 ± 1.0 °C in winter) but were offset horizontally for a clear vision. The horizontal error bars in the CHO species represent 1σ standard deviations of temperature values. The vertical error bars represent 1σ standard deviations for all the samples under each temperature condition.

References

Blair, S. L., MacMillan, A. C., Drozd, G. T., Goldstein, A. H., Chu, R. K., Pasa-Tolic, L., Shaw, J. B., Tolic, N., Lin, P., Laskin, J., Laskin, A., and Nizkorodov, S. A.: Molecular Characterization of Organosulfur Compounds in Biodiesel and Diesel Fuel Secondary Organic Aerosol, Environ. Sci. Technol., 51, 119–127, https://doi.org/10.1021/acs.est.6b03304, 2017.

Bryant, D. J., Nelson, B. S., Swift, S. J., Budisulistiorini, S. H., Drysdale, W. S., Vaughan, A. R., Newland, M. J., Hopkins, J. R., Cash, J. M., Langford, B., Nemitz, E., Acton, W. J. F., Hewitt, C. N., Mandal, T., Gurjar, B. R., Gadi, R., Lee, J. D., Rickard, A. R., and Hamilton, J. F.: Biogenic and anthropogenic sources of isoprene and monoterpenes and their secondary organic aerosol in Delhi, India, Atmos. Chem. Phys., 23, 61–83, https://doi.org/10.5194/acp-23-61-2023, 2023.

Cai, D., Wang, X., Chen, J., and Li, X.: Molecular Characterization of Organosulfates in Highly Polluted Atmosphere Using Ultra-High-Resolution Mass Spectrometry, J. Geophys. Res.-Atmos., 125, https://doi.org/10.1029/2019jd032253, 2020.

Camredon, M., Hamilton, J. F., Alam, M. S., Wyche, K. P., Carr, T., White, I. R., Monks, P. S., Rickard, A. R., and Bloss, W. J.: Distribution of gaseous and particulate organic composition during dark α-pinene ozonolysis, Atmos. Chem. Phys., 10, 2893–2917, https://doi.org/10.5194/acp-10-2893-2010, 2010.

Chan, M. N., Surratt, J. D., Chan, A. W. H., Schilling, K., Offenberg, J. H., Lewandowski, M., Edney, E. O., Kleindienst, T. E., Jaoui, M., Edgerton, E. S., Tanner, R. L., Shaw, S. L., Zheng, M., Knipping, E. M., and Seinfeld, J. H.: Influence of aerosol acidity on the chemical composition of secondary organic aerosol from β-caryophyllene, Atmos. Chem. Phys., 11, 1735–1751, https://doi.org/10.5194/acp-11-1735-2011, 2011.

Claeys, M., Iinuma, Y., Szmigielski, R., Surratt, J. D., Blockhuys, F., Van Alsenoy, C., Böge, O., Sierau, B., Gómez-González, Y., Vermeylen, R., Van der Veken, P., Shahgholi, M., Chan, A. W. H., Herrmann, H., Seinfeld, J. H., and Maenhaut, W.: Terpenylic Acid and Related Compounds from the Oxidation of α-Pinene: Implications for New Particle Formation and Growth above Forests, Environ. Sci. Technol., 43, 6976–6982, https://doi.org/10.1021/es9007596, 2009.

Glasius, M., Lahaniati, M., Calogirou, A., Di Bella, D., Jensen, N. R., Hjorth, J., Kotzias, D., and Larsen, B. R.: Carboxylic acids in secondary aerosols from oxidation of cyclic monoterpenes by ozone, Environ. Sci. Technol., 34, 1001–1010, https://doi.org/10.1021/es990445r, 2000.

Gómez-González, Y., Wang, W., Vermeylen, R., Chi, X., Neirynck, J., Janssens, I. A., Maenhaut, W., and Claeys, M.: Chemical characterisation of atmospheric aerosols during a 2007 summer field campaign at Brasschaat, Belgium: sources and source processes of biogenic secondary organic aerosol, Atmos. Chem. Phys., 12, 125–138, https://doi.org/10.5194/acp-12-125-2012, 2012.

Hansen, A. M. K., Kristensen, K., Nguyen, Q. T., Zare, A., Cozzi, F., Nøjgaard, J. K., Skov, H., Brandt, J., Christensen, J. H., Ström, J., Tunved, P., Krejci, R., and Glasius, M.: Organosulfates and organic acids in Arctic aerosols: speciation, annual variation and concentration levels, Atmos. Chem. Phys., 14, 7807–7823, https://doi.org/10.5194/acp-14-7807-2014, 2014.

Jiang, H., Li, J., Tang, J., Zhao, S., Chen, Y., Tian, C., Zhang, X., Jiang, B., Liao, Y., and Zhang, G.: Factors Influencing the Molecular Compositions and Distributions of Atmospheric Nitrogen-Containing Compounds, J. Geophys. Res.-Atmos., 127, https://doi.org/10.1029/2021jd036284, 2022.

Kourtchev, I., Fuller, S. J., Giorio, C., Healy, R. M., Wilson, E., O'Connor, I., Wenger, J. C., McLeod, M., Aalto, J., Ruuskanen, T. M., Maenhaut, W., Jones, R., Venables, D. S., Sodeau, J. R., Kulmala, M., and Kalberer, M.: Molecular composition of biogenic secondary organic aerosols using ultrahigh-resolution mass spectrometry: comparing laboratory and field studies, Atmos. Chem. Phys., 14, 2155–2167, https://doi.org/10.5194/acp-14-2155-2014, 2014.

Kourtchev, I., Doussin, J. F., Giorio, C., Mahon, B., Wilson, E. M., Maurin, N., Pangui, E., Venables, D. S., Wenger, J. C., and Kalberer, M.: Molecular composition of fresh and aged secondary organic aerosol from a mixture of biogenic volatile compounds: a high-resolution mass spectrometry study, Atmos. Chem. Phys., 15, 5683–5695, https://doi.org/10.5194/acp-15-5683-2015, 2015.

Laskin, A., Smith, J. S., and Laskin, J.: Molecular Characterization of Nitrogen-Containing Organic Compounds in Biomass Burning Aerosols Using High-Resolution Mass Spectrometry, Environ. Sci. Technol., 43, 3764–3771, https://doi.org/10.1021/es803456n, 2009.

Lim, Y. B., Tan, Y., Perri, M. J., Seitzinger, S. P., and Turpin, B. J.: Aqueous chemistry and its role in secondary organic aerosol (SOA) formation, Atmos. Chem. Phys., 10, 10521–10539, https://doi.org/10.5194/acp-10-10521-2010, 2010.

Lin, P., Rincon, A. G., Kalberer, M., and Yu, J. Z.: Elemental composition of HULIS in the Pearl River Delta Region, China: results inferred from positive and negative electrospray high resolution mass spectrometric data, Environ. Sci. Technol., 46, 7454–7462, https://doi.org/10.1021/es300285d, 2012.

Liu, S. J., Jia, L., Xu, Y. F., Tsona, N. T., Ge, S. S., and Du, L.: Photooxidation of cyclohexene in the presence of SO2: SOA yield and chemical composition, Atmos. Chem. Phys., 17, 13329–13343, https://doi.org/10.5194/acp-17-13329-2017, 2017.

Ma, Y., Willcox, T. R., Russell, A. T., and Marston, G.: Pinic and pinonic acid formation in the reaction of ozone with α-pinene, Chem. Commun., 1328–1330, https://doi.org/10.1039/b617130c, 2007.

Mao, J., Cheng, Y., Bai, Z., Zhang, W., Zhang, L., Chen, H., Wang, L., Li, L., and Chen, J.: Molecular characterization of nitrogen-containing organic compounds in the winter North China Plain, Sci. Total Environ., 838, https://doi.org/10.1016/j.scitotenv.2022.156189, 2022.

Mochida, M., Kawabata, A., Kawamura, K., Hatsushika, H., and Yamazaki, K.: Seasonal variation and origins of dicarboxylic acids in the marine atmosphere over the western North Pacific, J. Geophys. Res.-Atmos., 108, https://doi.org/10.1029/2002jd002355, 2003.

Perri, M. J., Lim, Y. B., Seitzinger, S. P., and Turpin, B. J.: Organosulfates from glycolaldehyde in aqueous aerosols and clouds: Laboratory studies, Atmos. Environ., 44, 2658–2664, https://doi.org/10.1016/j.atmosenv.2010.03.031, 2010.

Priestley, M., Le Breton, M., Bannan, T. J., Leather, K. E., Bacak, A., Reyes-Villegas, E., De Vocht, F., Shallcross, B. M. A., Brazier, T., Anwar Khan, M., Allan, J., Shallcross, D. E., Coe, H., and Percival, C. J.: Observations of Isocyanate, Amide, Nitrate, and Nitro Compounds From an Anthropogenic Biomass Burning Event Using a ToF-CIMS, J. Geophys. Res.-Atmos., 123, 7687–7704, https://doi.org/10.1002/2017jd027316, 2018.

Putman, A. L., Offenberg, J. H., Fisseha, R., Kundu, S., Rahn, T. A., and Mazzoleni, L. R.: Ultrahigh-resolution FT-ICR mass spectrometry characterization of α-pinene ozonolysis SOA, Atmos. Environ., 46, 164–172, https://doi.org/10.1016/j.atmosenv.2011.10.003, 2012.

Qi, L., Chen, M., Stefenelli, G., Pospisilova, V., Tong, Y., Bertrand, A., Hueglin, C., Ge, X., Baltensperger, U., Prévôt, A. S. H., and Slowik, J. G.: Organic aerosol source apportionment in Zurich using an extractive electrospray ionization time-of-flight mass spectrometer (EESI-TOF-MS) – Part 2: Biomass burning influences in winter, Atmos. Chem. Phys., 19, 8037–8062, https://doi.org/10.5194/acp-19-8037-2019, 2019.

Riva, M., Tomaz, S., Cui, T., Lin, Y. H., Perraudin, E., Gold, A., Stone, E. A., Villenave, E., and Surratt, J. D.: Evidence for an unrecognized secondary anthropogenic source of organosulfates and sulfonates: gas-phase oxidation of polycyclic aromatic hydrocarbons in the presence of sulfate aerosol, Environ. Sci. Technol., 49, 6654–6664, https://doi.org/10.1021/acs.est.5b00836, 2015a.

Riva, M., Robinson, E. S., Perraudin, E., Donahue, N. M., and Villenave, E.: Photochemical Aging of Secondary Organic Aerosols Generated from the Photooxidation of Polycyclic Aromatic Hydrocarbons in the Gas-Phase, Environ. Sci. Technol., 49, 5407–5416, https://doi.org/10.1021/acs.est.5b00442, 2015b.

Riva, M., Budisulistiorini, S. H., Zhang, Z. F., Gold, A., and Surratt, J. D.: Chemical characterization of secondary organic aerosol constituents from isoprene ozonolysis in the presence of acidic aerosol, Atmos. Environ., 130, 5–13, https://doi.org/10.1016/j.atmosenv.2015.06.027, 2016a.

Riva, M., Budisulistiorini, S. H., Chen, Y. Z., Zhang, Z. F., D'Ambro, E. L., Zhang, X., Gold, A., Turpin, B. J., Thornton, J. A., Canagaratna, M. R., and Surratt, J. D.: Chemical Characterization of Secondary Organic Aerosol from Oxidation of Isoprene Hydroxyhydroperoxides, Environ. Sci. Technol., 50, 9889–9899, https://doi.org/10.1021/acs.est.6b02511, 2016b.

Shalamzari, M. S., Ryabtsova, O., Kahnt, A., Vermeylen, R., Hérent, M., Quetin-Leclercq, J., Van der Veken, P., Maenhaut, W., and Claeys, M.: Mass spectrometric characterization of organosulfates related to secondary organic aerosol from isoprene, Rapid Commun. Mass Spectrom., 27, 784–794, https://doi.org/10.1002/rcm.6511, 2013.

Schindelka, J., Iinuma, Y., Hoffmann, D., and Herrmann, H.: Sulfate radical-initiated formation of isoprene-derived organosulfates in atmospheric aerosols, Faraday Discuss., 165, https://doi.org/10.1039/c3fd00042g, 2013.

Shalamzari, M. S., Vermeylen, R., Blockhuys, F., Kleindienst, T. E., Lewandowski, M., Szmigielski, R., Rudzinski, K. J., Spólnik, G., Danikiewicz, W., Maenhaut, W., and Claeys, M.: Characterization of polar organosulfates in secondary organic aerosol from the unsaturated aldehydes 2-E-pentenal, 2-E-hexenal, and 3-Z-hexenal, Atmos. Chem. Phys., 16, 7135–7148, https://doi.org/10.5194/acp-16-7135-2016, 2016.

Slade, J. H., Ault, A. P., Bui, A. T., Ditto, J. C., Lei, Z. Y., Bondy, A. L., Olson, N. E., Cook, R. D., Desrochers, S. J., Harvey, R. M., Erickson, M. H., Wallace, H. W., Alvarez, S. L., Flynn, J. H., Boor, B. E., Petrucci, G. A., Gentner, D. R., Griffin, R. J., and Shepson, P. B.: Bouncier Particles at Night: Biogenic Secondary Organic Aerosol Chemistry and Sulfate Drive Diel Variations in the Aerosol Phase in a Mixed Forest, Environ. Sci. Technol., 53, 4977–4987, https://doi.org/10.1021/acs.est.8b07319, 2019.

Song, J., Li, M., Zou, C., Cao, T., Fan, X., Jiang, B., Yu, Z., Jia, W., and Peng, P.: Molecular Characterization of Nitrogen-Containing Compounds in Humic-like Substances Emitted from Biomass Burning and Coal Combustion, Environ. Sci. Technol., 56, 119–130, https://doi.org/10.1021/acs.est.1c04451, 2022.

Surratt, J. D., Gomez-Gonzalez, Y., Chan, A. W. H., Vermeylen, R., Shahgholi, M., Kleindienst, T. E., Edney, E. O., Offenberg, J. H., Lewandowski, M., Jaoui, M., Maenhaut, W., Claeys, M., Flagan, R. C., and Seinfeld, J. H.: Organosulfate formation in biogenic secondary organic aerosol, J. Phys. Chem. A, 112, 8345–8378, https://doi.org/10.1021/jp802310p, 2008.

Szmigielski, R.: Evidence for C5 organosulfur secondary organic aerosol components from in-cloud processing of isoprene: Role of reactive SO4 and SO3 radicals, Atmos. Environ., 130, 14–22, https://doi.org/10.1016/j.atmosenv.2015.10.072, 2016.

Szmigielski, R., Surratt, J. D., Gómez-González, Y., Van der Veken, P., Kourtchev, I., Vermeylen, R., Blockhuys, F., Jaoui, M., Kleindienst, T. E., Lewandowski, M., Offenberg, J. H., Edney, E. O., Seinfeld, J. H., Maenhaut, W., and Claeys, M.: 3-methyl-1,2,3-butanetricarboxylic acid: An atmospheric tracer for terpene secondary organic aerosol, Geophys. Res. Lett., 34, https://doi.org/10.1029/2007gl031338, 2007.

Walser, M. L., Desyaterik, Y., Laskin, J., Laskin, A., and Nizkorodov, S. A.: High-resolution mass spectrometric analysis of secondary organic aerosol produced by ozonation of limonene, Phys. Chem. Chem. Phys., 10, 1009–1022, https://doi.org/10.1039/b712620d, 2008.

Wang, K., Zhang, Y., Huang, R.-J., Wang, M., Ni, H., Kampf, C. J., Cheng, Y., Bilde, M., Glasius, M., and Hoffmann, T.: Molecular Characterization and Source Identification of Atmospheric Particulate Organosulfates Using Ultrahigh Resolution Mass Spectrometry, Environ. Sci. Technol., 53, 6192–6202, https://doi.org/10.1021/acs.est.9b02628, 2019.

Wang, X. K., Rossignol, S., Ma, Y., Yao, L., Wang, M. Y., Chen, J. M., George, C., and Wang, L.: Molecular characterization of atmospheric particulate organosulfates in three megacities at the middle and lower reaches of the Yangtze River, Atmos. Chem. Phys., 16, 2285–2298, https://doi.org/10.5194/acp-16-2285-2016, 2016.

Wang, Y., Hu, M., Lin, P., Guo, Q., Wu, Z., Li, M., Zeng, L., Song, Y., Zeng, L., Wu, Y., Guo, S., Huang, X., and He, L.: Molecular Characterization of Nitrogen-Containing Organic Compounds in Humic-like Substances Emitted from Straw Residue Burning, Environ. Sci. Technol., 51, 5951–5961, https://doi.org/10.1021/acs.est.7b00248, 2017.

Watson, J. G. and Chow, J. C.: Protocol for Applying and Validating Receptor Model Source Apportionment in PMEH Study Areas, Pollution Management and Environmental Health (PMEH) Program The World Bank, 5–24, 2018.

Williams, B. J., Goldstein, A. H., Kreisberg, N. M., and Hering, S. V: In situ measurements of gas/particle-phase transitions for atmospheric semivolatile organic compounds, Proc. Natl. Acad. Sci., 107, 6676–6681, https://doi.org/10.1073/pnas.0911858107, 2010.

Xu, W. and Zhang, R.: Theoretical Investigation of Interaction of Dicarboxylic Acids with Common Aerosol Nucleation Precursors, J. Phys. Chem. A, 116, 4539–4550, https://doi.org/10.1021/jp301964u, 2012.

Yasmeen, F., Szmigielski, R., Vermeylen, R., Gómez-González, Y., Surratt, J. D., Chan, A. W. H., Seinfeld, J. H., Maenhaut, W., and Claeys, M.: Mass spectrometric characterization of isomeric terpenoic acids from the oxidation of α-pinene, β-pinene, d-limonene, and Δ3-carene in fine forest aerosol, J. Mass Spectrom., 46, 425–442, https://doi.org/10.1002/jms.1911, 2011.

Yu, J. Z., Cocker, D. R., Griffin, R. J., Flagan, R. C., and Seinfeld, J. H.: Gas-phase ozone oxidation of monoterpenes: Gaseous and particulate products, J. Atmos. Chem., 34, 207–258, https://doi.org/10.1023/a:1006254930583, 1999.